A STUDY ON METAL ION COMPLEXATION WITH A MACROCYCLIC LIGAND

(A Thermodynamic, Kinetic, and Mechanistic Investigation)

A Thesis Presented for the Degree of
Master of Science
in the University of Adelaide.
by

Benu Kumar Dey
B.Sc.(Hons.), University of Chittagong
M.Sc., University of Chittagong

The Department of Physical and Inorganic Chemistry,
The University of Adelaide, Adelaide, SA 5001, Australia.

October, 1991.

TO

MY PARENTS

Contents

Page No.

Contents .....(iii)

Abstract .....(vii)

Acknowledgements .....(x)

Declaration .....(xi)

Glossary of Abbreviations for Ligands, Solvents etc. .....(xii)

CHAPTER 1 Literature Review and Objectives.....1

1.1 Introduction 1

1.2 Thermodynamic Stability 3

1.2.1 Macrocyclic Effect 3

1.2.1(a) The Enthalpic Origin of the Macrocyclic Effect 5

1.2.1(b) The Entropic Origin of the Macrocyclic Effect 6

1.2.1(c) The Ring Size of Ligands and the Macrocyclic Effect 7

1.2.1(d) The Kinetic Origin of the Macrocyclic Effect 8

1.3 The Kinetics of Metal Ion Complexation 9

1.4 The Kinetics of Decomplexation of Metal Complexes 15

1.5 The Mechanistic Terminology of Kinetic Studies 17

1.5.1 Introduction 17

1.5.2 The Hydrated Metal ion in Aqueous Solution 18

1.5.3 Typical Reactions of Metal Complexes in Aqueous Solution 20

1.5.4 General Mechanisms Involved in Substitution Reactions of Metal Complexes in Solution 23

1.5.4(a) The Associative Mechanism 24
1.5.4(b) The Dissociative Mechanism 25
1.5.4(c) The Interchange Mechanisms 26
1.6 Objectives of the Present Work 33

CHAPTER 2 Experimental 35

2.1 Reagents and Materials 35
2.2 Preparation of Experimental Solutions 35
2.2.1 Stock Solutions 35
2.2.2 Solutions for Potentiometric Titrations 36
2.2.3 Solutions for Complexation Kinetic Studies 36
2.2.4 Solutions for Decomplexation Kinetic Studies 37
2.2.5 Degassing of Experimental Solutions 37
2.3 Measurement of pH of Experimental Solutions 37
2.4 Measurement of Visible Spectra 38
2.5 Potentiometric Titrations 38
2.6 Kinetic Measurements 40
2.6.1 Introduction 40
2.6.2 The Principle of Stopped-flow Spectrophotometry 41
2.6.3 The Stopped-flow Apparatus 45
2.6.4 Data Storage and Analysis 49

CHAPTER 3 Determination of Stability Constants 50

3.1 Introduction 50
3.2 Results and Discussion 52

3.2.1 Acid Dissociation Constants of THEC 52
3.2.2 Stability Constants of Metal Complexes of THEC 54
3.2.3 Speciation Diagrams for THEC and its Metal Complexes ...62

CHAPTER 4 Kinetic Studies on the Complexation of Metal Ions 68

4.1 Introduction 68
4.2 Results 69
4.2.1 Visible Spectra of Metal Complexes of THEC in Buffered Aqueous Solution 69
4.2.2 The Kinetics of Complexation 73
4.2.3 Data Analyses and Discussion 77

CHAPTER 5 Kinetic Studies on the Decomplexation of metal complexes 101

5.1 Introduction 101
5.2 Results 102
5.2.1 Visible Spectra of Metal Complexes of THEC in Unbuffered Aqueous Solution 102
5.2.2 The Kinetics of Decomplexation 107
5.2.3 Data Analyses and Discussion 111

CHAPTER 6 General Conclusions 134

6.1 Introduction 134

6.2 The pK_a values of THEC 135

6.3 The Stabilities of Complex Species in Solution 135

6.4 The Kinetics of Complexation of Metal Ions with THEC ..136

6.5 The Decomplexation Kinetics 137

6.6 The Decomplexation Kinetics ..... .139

6.7 The Proposed Mechanism 139

REFERENCES 143

ABSTRACT

The values of the acid dissociation constants (K_a) of the ligand, 1, 4, 8, 11-tetrakis(2-hydroxyethyl)-1, 4, 8, 11-tetraazacyclotetradecane (THEC), have been determined at 298.2 (±0.2) K and ionic strength of 1.50 mol dm^{-3} adjusted with $NaNO_3$, using the potentiometric titration technique in combination with a pH electrode. The concentration stability constants for the formation of different complex species of Cu^{2+}, Ni^{2+}, and Co^{2+} with THEC have also been determined under identical conditions using the same technique.

The kinetics of complexation of metal ions, Ni^{2+} and Co^{2+}, with THEC have been studied at pH 6.8, 298.2 (±0.2) K and ionic strength of 1.50 mol dm^{-3} $NaNO_3$ in aqueous solution under pseudo first-order conditions (more than 10 fold excess concentration of metal ions compared to the concentration of the ligand) using the stopped-flow spectrophotometric technique. The variation of the observed pseudo first-order rate constant $k_{obs.}(s^{-1})$ against excess metal ion, $[M^{2+}]_{ex.}$, is consistent with the following equation,

$$k_{obs.} = k_d + k_c [M^{2+}]_{ex.}$$

where k_d (s^{-1}) and k_c (dm^3 mol^{-1} s^{-1}) are the rate constants for decomplexation and complexation respectively.

The kinetics of complexation of Ni^{2+} ion with THEC have also been studied at various pH values, at the same temperature and ionic strength under pseudo first-order conditions, and the variation of $k_{obs.}(s^{-1})$ against

hydrogen ion concentration, $[H^+]$ (mol dm^{-3}), is consistent with the following equation:

$$k_{obs.} = \frac{k'_{(L)} K_{a1} K_{a2} + k'_{(LH^+)} K_{a2} [H^+] + k'_{(LH_2{}^{2+})} [H^+]^2}{K_{a1} K_{a2} + K_{a2} [H^+] + [H^+]^2}$$

where K_{a1} and K_{a2} are the first and second acid dissociation constants for THEC; and $k'_{(L)}$, $k'_{(LH^+)}$, and $k'_{(LH_2{}^{2+})}$ are the first order (s^{-1}) rate constants for the complexation of Ni^{2+} with zero-, mono-, and di-protonated species of THEC respectively. The analyses of the results indicate that the mono-protonated species of the ligand is the only reacting species at pH 6.8, and the values of the second order rate constant, $k_{(LH^+)}$ (dm^3 mol^{-1} s^{-1}), for the complexation of Ni^{2+} and Co^{2+} ions with the mono-protonated species of THEC have been evaluated.

The kinetics of acid catalysed decomplexation of the Cu^{2+}-, Ni^{2+}-, and Co^{2+}- complexes of THEC have been studied at various temperatures and at a constant ionic strength of 1.50 mol dm^{-3} $NaNO_3$ in aqueous solution under pseudo first-order conditions (more than 10 fold excess of acid concentration compared to the total concentration complex species) using the same stopped-flow spectrophotometric technique. The variation of the observed rate constant, $k_{obs.}$(s^{-1}), against excess acid concentration, $[H^+]_{ex.}$(mol dm^{-3}), can be represented by a general relationship of the form:

$$k_{obs.} = \frac{k_o + k_1 K_1 [H^+]_{ex.} + k_2 K_1 K_2 ([H^+]_{ex.})^2}{1 + K_1 [H^+]_{ex.} + K_1 K_2 ([H^+]_{ex.})^2}$$

where k_o, k_1 and k_2 are the first-order rate constants (s^{-1}) characterising the decomplexation of zero-, mono-, and di- protonated species of metal complexes of THEC ($[M(THECH_n)]^{(n+2)+}$) respectively, and K_1 and K_2 are the corresponding protonation constants ($dm^3\ mol^{-1}$).

The activation parameters, $\Delta H^{\#}$ (enthalpy of activation) and $\Delta S^{\#}$ (entropy of activation), for the kinetic parameter, $k_1(s^{-1})$, have been evaluated for all the metal-THEC systems studied.

The mechanistic implications of the observed rate laws have been discussed, and the values of the resolved kinetic parameters have been compared with related macrocyclic systems published in the literature. A mechanism for the complexation of metal ions with the mono-protonated species of the ligand, $THECH^+$, has been proposed on the basis of observed rate laws.

ACKNOWLEDGEMENTS

I would sincerely like to extend my gratitude and thanks to my supervisors Stephen Lincoln and John Coates for their keen interest, diligent guidance and criticisms throughout the course of this research.

Special thanks also go to Kevin Wainwright for the preparation of the ligand and Paul Duckworth for his assistance in using the program MINIQUAD to evaluate the formation constants from potentiometric titration data and invaluable discussion on it.

I thank all academic staff of this Department for their encouragement.

I would also like to thank my many co-workers for their encouragement, and especially I like to acknowledge Sue Brown, Philip Clarke, Ashley Stephens and Sonya Whitbread for their assistance with computing and in proof reading this thesis.

I am also thankful for the help from the workshop personnel of this Department towards maintenance of apparatus, especially to John Netting for designing and making the water labyrinth around the reaction chamber of the stopped-flow apparatus.

I gratefully acknowledge the financial assistance provided by the Australian International Development Assistance Bureau (AIDAB), and the University of Chittagong for granting me study leave.

I am indebted to my mother and my brothers for their moral support and inspiration during these years which made this work possible.

Finally, I am thankful to all of my friends and well-wishers in Adelaide who affectionately encouraged me to carry out my study in Australia.

DECLARATION

To the best of my knowledge and belief, this thesis contains no material which has been submitted for any other degree or diploma in any University, nor any material previously published or written by another author except where due reference is made in the text.

Upon being accepted for the award of the degree consent is given for this thesis being made available for photocopying and loan if applicable.

Benu Kumar Dey

This thesis was produced in October 1991, on an Apple-Macintosh computer using MS-Word 4.0, in 8,9,10,12,14,18, and 24 point Times/Symbol font.

Glossary of Abbreviations for Ligands, Solvents etc.

$12aneN_4$	1,4,7,10-tetraazacyclododecane
$13aneN_4$	1,4,7,10-tetraazacyclotridecane
$14aneN_4$	1,4,8,11-tetraazacyclotetradecane
$15aneN_4$	1,4,8,12-tetraazacyclopentadecane
$16aneN_4$	1,5,9,13-tetraazacyclohexadecane
14aneNSNS	1,8-dithio-4,11-diazacyclotetradecane
14aneNSSN	1,11-dithio-4,8-diazacyclotetradecane
$14aneN_2S_2$	1,4-dithio-8,11-diazacyclotetradecane
cyclam	1,4,8,11-tetraazacyclotetradecane
cyclen	1,4,7,10-tetraazacyclododecane
DMF	N,N-dimethylformamide
DMSO	dimethylsulphoxide
E	observed potential
E_o	standard electrode potential
Et_2-2,3,2-tet	3,6,10,13-tetraazapentadecane
F	Faraday's constant (9.6485×10^4 C mol^{-1})
h	Planck's constant (6.62618×10^{-34} J s)
K	Kelvin (absolute temperature scale)
K_a	acid dissociation constant (dm^3 mol^{-1})
k_B	Boltzmann's constant (1.38066×10^{-23} J K^{-1})

kJ	kilo Joule
K_w	ionisation constant for water ($dm^3\ mol^{-1}$)
log	logarithm to base 10
ln	logarithm to base e
MBPC	1-(2,2'-bipyridyl-6yl-methyl)-1,4,8,11-tetraazacyclotetradecane
Me	methyl moiety, $-CH_3$
Me-cyclam	1-methyl-1,4,8,11-tetraazacyclotetradecane
Me_2-cyclam	1,5-dimethyl-1,5,8,12-tetraazacyclotetradecane
Me_4-cyclam	1,4,8,11-tetramethyl-1,4,8,11-tetraazacyclotetradecane
Me_4trien	1,1,10,10-tetramethyl-1,4,7,10-tetraazadecane
Me_6trien	1,1,4,7,10,10-hexamethyl-1,4,7,10-tetraazadecane
PIPES	monohydrate sodium salt of [Piperazine-N,N'-bis-(2-ethane-sulphonic acid]
pH	negative logarithm (to base 10) of hydrogen ion concentration ($-\log_{10}[H^+]$)
pOH	negative logarithm (to base 10) of hydroxide ion concentration ($-\log_{10}[OH^-]$)
pK_a	negative logarithm (to base 10) of acid dissociation constant ($-\log_{10}K_a$)
pK_w	negative logarithm (to base 10) of ionisation constant for water ($-\log_{10}K_w$)
R	gas constant (8.31441 $J\ K^{-1}\ mol^{-1}$)

T	absolute temperature (Kelvin)
TCEC	1,4,8,11-tetrakis(2-cyanoethyl)-1,4,8,11-tetraazacyclotetradecane
TETA	1,4,8,11-tetraazacyclotetradecane-1,4,8,11-tetraacetate
2,3,2-tet	1,4,8,11-tetraazaundecane
tet-a	meso-5,7,7,12,14,14-hexamethyl-1,4,8,11-tetraazacyclotetradecane
tet-b	racemic-5,7,7,12,14,14-hexamethyl-1,4,8,11-tetraazacyclotetradecane
THEC-12	1,4,7,10-tetrakis(2-hydroxyethyl)-1,4,7,10-tetraazacyclododecane
THEC	1,4,8,11-tetrakis(2-hydroxyethyl)-1,4,8,11-tetraazacyclotetradecane
$THECH^{+}$	mono-protonated form of THEC
$THECH_2^{2+}$	di-protonated form of THEC
$THECH_3^{3+}$	tri-protonated form of THEC
$THECH_4^{4+}$	tetra-protonated form of THEC
$THEC\text{-}H^{-}$	mono-deprotonated form of THEC
$THEC\text{-}H_2^{2-}$	di-deprotonated form of THEC
TMC	1,4,8,11-tetramethyl-1,4,8,11-tetraazacyclotetradecane
trien	1,4,7,10-tetraazadecane

CHAPTER 1

LITERATURE REVIEW AND OBJECTIVES

1.1 Introduction

Since 1960, macrocyclic ligands have attracted considerable attention due to their metal ion selectivity and the unusual properties of their metal complexes, particularly their very high thermodynamic stability, their kinetic inertness, and also their occurrence in biological systems. There are many excellent texts[1-3] and review articles[4-18] in which different aspects of macrocyclic ligands and their metal complexes have been discussed. Various terms such as "macrocyclic effect", "macrobicyclic effect", "cryptate effect", "ring size effect", "multiple desolvation", "ligand conformation change", and "multiple juxtapositional fixedness", have been used by different authors to describe the unusual behaviour associated with these complexes.

Some of these synthetic complexes are found to be useful in different fields,[2,3,6] for example, metal ion transport through the cellular membrane, metal ion separation, industrial scavenging, and as antibiotics. The important roles which metal complexes of macrocyclic ligands play in many naturally occuring biological systems have been well known for a long time,[1] for example, the porphyrin ring in haem protein, the chlorin ring in chlorophyll and the corrin ring in vitamin B_{12}.

Tetraaza macrocyclic ligands, for example, cyclam (Figure 1.1) and its cyclic analogues, may be considered as a "prototype family of macrocyclic ligands"[12] or "model-system" devised[2,3] to study natural complexation reactions in biological systems, and for practical applications. However, their metal complexes are insufficiently labile for practical uses. For an example, when cyclam is attached to polystyrene beads so as to produce ion exchange resin it is capable of metal ion selective extraction from a solution but due to kinetic inertness reasonable rates of extraction can only be obtained at a very high temperature.[19]

For practical application of these ligands, in metal ion transport or industrial scavenging processes or in understanding complexation reactions in biological systems, the principal conditions[1] to be met are: (i) their metal complexes should be optimally stable, and (ii) both complexation of metal ions with these ligands and decomplexation of their metal complexes should be fast.

Figure 1.1 Some typical tetraaza macrocyclic ligands :
(a) cyclam
(b) N-functionalised cyclam derivatives
(i) TMC, when R = $-CH_3$;
(ii) THEC, when R = $-CH_2-CH_2-OH$;
(iii) TCEC, when R = CH_2-CH_2-CN;
(iv) TETA, when R = $-CH_2-COOH$.

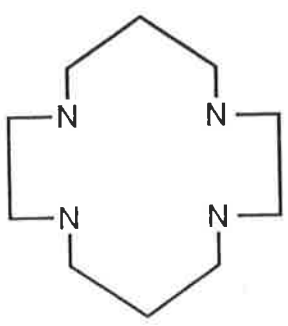

(a)

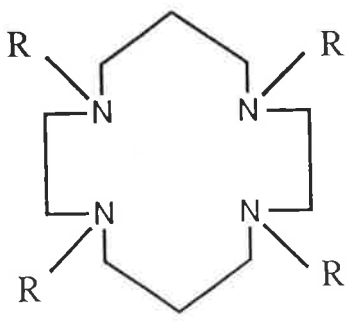

(b)

The attachment of N-functionalised pendant arm donor groups, for example, $-CH_2-CH_2-OH$, $-CH_2-COOH$, $-CH_2-CH_2-CN$, and $-CH_2-CH_2-NH_2$, to the parent tetraaza macrocyclic ligand, cyclam, produces complexes of moderately high stability as well as greater lability.[19-23]

Moreover, the majority of transition metal ions, most having a coordination number of at least six, cannot be enclosed completely by the tetraaza macrocyclic ligands. This however can be brought about by the attachment of coordinating groups on the periphery of the macrocycles.[4] Accordingly, this study is concerned with the investigation of the effect of pendant 2-hydroxyethyl arms on the stability and lability of metal complexes of THEC. It is therefore pertinent to review previous work done involving thermodynamic and kinetic studies of tetraaza macrocyclic ligands, their C- and N-functionalised derivatives, their linear analogues, and cyclic analogues containing different donor atoms.

1.2 Thermodynamic Stability

1.2.1 Macrocyclic Effect

Cabbiness and Margerum[25] first introduced the term "Macrocyclic Effect" to highlight the enhanced stability of a Cu^{2+}-complex formed with the reduced Curtis macrocyclic ligand (tet-a) compared to that formed with its open chain analogue (2,3,2 tet) the stability of which could be characterised by the well known chelate effect. Similarly, an increased stability was also observed in many metal complexes of optimally fitting macrocyclic ligands. Examples of those are cyclic tetraaza,[26-38] cyclic polythioethers,[39-42] cyclic polyethers,[43-46]

cryptands,[47-49] and cyclic ligands containing mixed donors,[50-53] compared to their open chain analogues. This phenomenon was found to an even greater extent in the case of cryptands where *Lehn et al.*[13,48] used the term "Macrobicyclic Cryptate Effect" or "Cryptate Effect". However, the discussion here will be limited mainly to tetraaza macrocyclic ligands, and their cyclic and linear analogues.

In principle, the macrocyclic effect refers to the decrease in the standard Gibbs free energy, ΔG^o, for the metathetical reaction (1.1).

$$[ML_1]^{n+} + L_2 \rightleftharpoons [ML_2]^{n+} + L_1 \qquad (1.1)$$

where M^{n+} = metal ion,
L_1 = noncyclic ligand (analogue of L_2), and
L_2 = macrocyclic ligand

A great deal of interest has been shown in separating ΔG^o into its entropic and enthalpic components to explain the macrocyclic effect.[33-35,54-62] It has been established that the chelate effect is of largely entropic origin,[60,64-65] but controversy has arisen over the specific thermodynamic origin of the macrocyclic effect.

The contributions of the enthalpy and entropy terms to the stabilisation of macrocyclic complexes differ substantially from system to system. It is evident from the study of various systems reported in the literature that the increased stability is a result of either wholly entropy factors[26-31,54-55] or wholly enthalpy factors,[33-35,55-58] or a combination of both entropy and enthalpy factors.[55, 59-62]

1.2.1(a) The Enthalpic Origin of the Macrocyclic Effect

Margerum et al.[25,33,34] have reported that the solvation of free macrocyclic ligands compared to noncyclic analogues is the primary contributor to the macrocyclic effect in the case of polyamines in aqueous solution. Similarly, the important role of free ligand solvation enthalpy has been mentioned by *Dei et al.*[56] and *Clay et al.*[58] in the case of Cu^{2+}- and Ni^{2+}- complexes of tetraaza macrocyclic ligands, and by *Izatt et al.*[44] in the case of polyethers.

With reference to the thermochemical cycle shown in Figure 1.2, the release of solvent molecules from the metal ion (step 2) and from the ligand (step 3) results in positive ΔH and ΔS changes.

Figure 1.2 A typical thermochemical cycle representing the desolvation steps for the complex formation between a solvated metal ion ($M^{2+}_{(solv.)}$) and a solvated ligand ($L_{(solv.)}$).

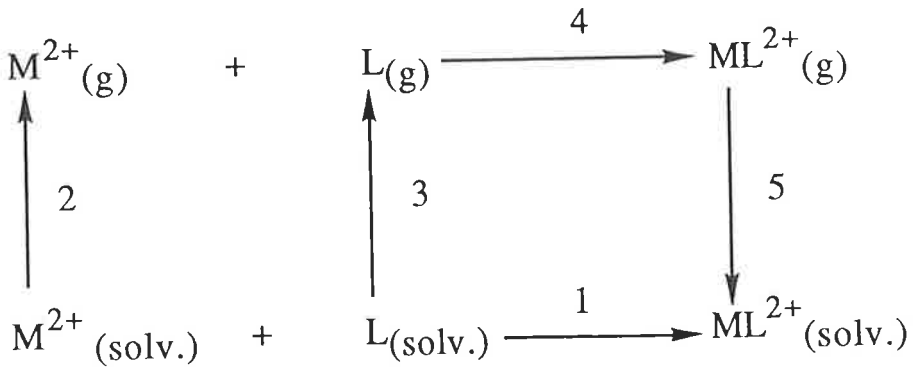

If the desolvation of the metal ion is identical in the reactions with both macrocyclic and linear ligands, then the desolvation of the ligand is the important step when the complexation of metal ions with

different ligands is compared in a given solvent. *Hinz et al.*[33,34] assumed that the macrocyclic ligand, cyclam, should be less solvated than its linear analogue, 2,3,2-tet, since the much more compact cyclic nature of cyclam physically prohibited it from being hydrated by the same number of hydrogen bonded water molecules as 2,3,2-tet. Consequently, less energy is required for desolvation of cyclic ligands resulting in increased stability for complexes containing the cyclic ligand.

Paoletti et al.[57-62] emphasised the importance of configurational enthalpies of the macrocyclic ligands. According to their assumptions, during the synthesis of cyclic ligands a certain amount of conformational strain is built into the macrocycle. That is, the synthetically pre-oriented macro-cyclic ligand already has its donor atoms in a favourable position for binding to a particular metal ion. On the other hand, the open chain ligands must expend extra energy in arranging their donor atoms around the metal ion relative to cyclic ligands (in which donor atoms are already arranged). *Haymore et al.*[45] also mentioned that favourable configurational enthalpy changes for macrocyclic polyethers are an important contributor to the macrocyclic effect. Hence, according to these two groups of authors, either favourable ligand desolvation enthalpy or configurational enthalpy of the macrocyclic ligand is the enthalpic origin of the macrocyclic effect.

1.2.1(b) The Entropic Origin of the Macrocyclic Effect

Hinz et al.[34] have suggested that unfavourable configurational entropy changes for the macrocyclic ligands make a small but important contribution to the macrocyclic effect in the Ni^{2+} complex of cyclam compared to its linear analogue, 2,3,2-tet. *Smith et al.*[39] have also found

that configurational entropy effects are the primary cause for the smaller macrocyclic effect observed in the case of Ni^{2+}-tetrathioether systems studied in nitromethane. It has also been suggested by *Paoletti et al.*[61a,62] that the favourable configurational entropy changes in the macrocyclic ligand upon complexation are the primary contribution to the entropic origin of the macrocyclic effect. An open chain ligand is more flexible compared to its cyclic analogue, and is expected to have a considerable configurational component to its internal entropy. On complexation the flexible open chain ligand tends to undergo much more geometrical change relative to its cyclic analogue. Thus, an open chain ligand loses a significant proportion of its internal entropy component on complexation. Hence, the less flexible macrocyclic ligands are accompanied with a more favourable configurational entropy which is responsible for the increased stability of their complexes.

1.2.1(c) The Ring Size of Ligands and the Macrocyclic Effect

It might be expected that the best match of the metal ion size to the macrocyclic cavity size would result in complexes of high stability. Although some correlation between the stability of complexes and the ring size[1] of ligands is observed for cryptands[13] and polyethers,[15,63,63a] such a correlation is not possible in the case of tetraaza ligands. This is probably due to their greater flexibility providing various conformations.[7, 19a] It has been observed from the stability of metal complexes of tetraaza macrocyclic ligands that the smaller metal ion, Cu^{2+}, prefers the larger macrocyclic ring 13aneN$_4$ or 14aneN$_4$ whereas the larger ions, Pb^{2+} and Cd^{2+}, prefer the smaller macrocyclic ring 12aneN$_4$. This is

due to the fact that tetraaza macrocyclic ligands exhibit two or more conformers, each with different metal ion preferences, and are able to change their conformation to accommodate too-large metal ions which are coordinated lying out of the plane of the donor atoms of the ligand.[7,19a]

1.2.1(d) The Kinetic Origin of the Macrocyclic Effect

Busch et al.[66] have introduced the term "multiple juxtapositional fixedness", which involves a kinetic model,[66a] to describe the macrocyclic effect The enhanced stabilities of metal complexes of macrocyclic ligands are due to their very slow rates of decomplexation. It is assumed that open chain ligands can undergo successive S_N1 replacement steps of the nitrogen donors by the solvent molecules commencing at one end of the ligand, in the presence of acid the ligand is quickly protonated and thus the metal ion is decomplexed. Such a simple mechanism is not possible in the case of macrocyclic complexes because the macrocyclic ring has no free end. A mechanism resembling S_N2 is proposed, whence one coordination bond is significantly weakened and finally broken. The thermodynamic consequences of this mechanistic constraint on the dissociation accounts for the enhanced stability of macrocyclic complexes.[2,66]

Kodama et al.[26,28] have also mentioned that the increased stability constants of the macrocyclic ligand complexes are reflected mostly in the decomplexation rate constant. Similarly, *Jones et al.*[40] have also supported this kinetic approach in understanding the macrocyclic effect. According to their assumptions, the slow decomplexation step of

the cyclic thioether complex is responsible for its extra stability over the complexes of linear analogues. Thus, systematic studies on the rates of complexation of metal ions with macrocyclic ligands, the rates of decomplexation of their metal complexes, and the thermodynamic stability constants of these complexes would explore the kinetic origin of the macrocyclic effect.

1.3 The Kinetics of Metal Ion Complexation

The simple monodentate amines react with metal ion in aqueous solution as fast as the water exchange rate,[67] and the unsubstituted linear polyamines react with metal ions at a rate even faster than that of water exchange.[67a] In the former case, dissociation of the first coordinated water molecule has been considered as the rate determining step, and in the latter case an internal conjugate base mechanism has been suggested. In contrast, the polyaza macrocyclic ligands in their protonated form react with metal ions at a slower rate than the corresponding open chain polyamines.[68-74] Several reasons for this have been put forward by different authors and are discussed below.

In 1970, *Kaden*[68] reported that the rate of formation of $[Ni(cyclam)]^{2+}$ was 30,000 times slower than that of $[Ni(trien)]^{2+}$.[75] It was assumed that the rate determining step for the complexation with cyclam could not be the dissociation of the first coordinated water molecule, which is the common feature of complexation with simple linear amines, but it might be the formation of the second coordinative metal-nitrogen bond. The slowness of formation rate was considered to be due to the more rigid structure of cyclam in comparison with trien, since

the former was associated with a potential energy barrier for internal rotation.

Meanwhile, *Cabbiness et al.*[69] independently published that C-alkylated derivatives of cyclam (tet-a and tet-b) in alkali medium reacted with $Cu(OH)_x^{(2-x)+}$ species with rates 10^3 - 10^4 times more slowly than the open chain analogue, 2,3,2-tet. They suggested that the multiple desolvation of the metal ion and the formation of intermediate structural isomers might be responsible for the slowness of the complexation. They also studied the complexation of $[Cu(H_2O)_6]^{2+}$ with tet-a in acid medium. They pointed out that compared to the open chain amine molecule, the two protons in $H_2(tet\text{-}a)^{2+}$ are nearer to one another and electrostatic repulsion and hydrogen bonding of the nitrogen atoms might be responsible for the slower rate of complexation of the macrocyclic ligand compared to its linear analogue.

In 1973, *Barefield et al.*[76] mentioned that metal complexes of TMC were labile compared to those of cyclam.

However, in 1974, *Kaden et al.*[70,71] studied the rate of complexation of metal ions, Zn^{2+}, Cu^{2+}, Ni^{2+}, and Co^{2+} with N-methylated derivatives of cyclam (Me-cyclam, Me_2-cyclam and Me_4-cyclam (TMC)), and found that the methyl group had a small effect on the rates of complexation. Moreover, the observed rates were slower than the normal complexation (with linear analogues) by a factor 10^3-10^4, and closely followed the water exchange rate order of

$$Cu^{2+} > Zn^{2+} > Co^{2+} > Ni^{2+}.$$

From this, they concluded that beside the dissociation of the first water molecule another constant factor played an important role in the rate determining step. They also pointed out that the rate of complexation was increased with the increase of pH, and although the di-protonated form of the ligands was the predominant species (in the pH range studied), the mono-protonated species was the reacting species. They suggested that the probable reason for slow complexation could be a conformational change which might either occur in a rapid pre-equilibrium before the complexation step or in an intermediate in which the metal ion is already coordinated to one or more nitrogen atoms of the ligand.

In 1975, *Lin et al.*,[77] in an extension of the earlier work,[69] employed a highly basic medium to avoid the affect of ligand protonation in the complexation kinetics, and found that the unprotonated form of cyclam reacted with the $Cu(OH)_3^-$ species as fast as its linear analogue (Et_2-2, 3, 2-tet). This implied that the electrostatic interaction between the positive metal ion and the protonated ligand was mainly responsible for the slow rate of complexation with macrocyclic ligands in aqueous medium (at lower pH). They also pointed out that the cyclisation was not the only factor affecting the slowness of complexation of metal ions with C-methylated cyclam[69]. Other factors present were (i) the steric effect resulting from the six methyl groups on tet-a and tet-b, and (ii) the greater reactivity of the primary nitrogen donor atoms in 2,3,2-tet relative to secondary nitrogen donor atoms as found in the cyclic ligands.

In 1978, *Kaden et al.*[74] studied the rates of complexation of metal ions, Zn^{2+}, Cu^{2+}, Ni^{2+}, and Co^{2+} with various cyclic analogues of cyclam (12aneN_4(cyclen), 13aneN_4, 14aneN_4 (cyclam), 15aneN_4, and

16aneN$_4$). They found that the rates of complexation with the similarly protonated species of the ligands were slower than that with the corresponding linear tetraamine analogues. They did not find any linear relationship between the rate constants and the ring size of the ligands, and concluded that electrostatic factors and conformational effects might play important roles in the complexation with di-protonated species and mono-protonated species of the ligands respectively. *Kodama et al.*[31] also studied the complexation of metal ions Pb^{2+}, Cd^{2+}, and Zn^{2+} with tetraaza macrocyclic ligands of different ring size using a polarographic technique. They reported that the slower rates of complexation with tetraaza macrocyclic ligands were due to the protonation of the ligands. Moreover, the mono-protonated and unprotonated species of the ligands were the main reacting species, and the contribution of di-protonated species to the net formation rate could be ignored.

In 1980, *Hay et al.*[78] reported that the bimolecular rate constants for the complexation of Ni^{2+} with cyclam, with N-methylated derivatives of cyclam and with their linear analogues in acetonitrile (as solvent) were essentially identical within the experimental error at *ca* 900 $dm^3\ mol^{-1}\ s^{-1}$ at 298.2 K. This also supported the view that the electrostatic factor was responsible for the slowness of metal ion complexation rates with macrocyclic ligands in an aqueous medium.[68-74] They also observed that the rates of complexation of Ni^{2+} with cyclam in dipolar hydrogen bonded solvents such as methanol, and mixtures of methanol and water were markedly decreased, which might be partly due to the protonation and also due to the solvation of the ligand (because of hydrogen bonding). *Hertli et al.*[79] also studied the complexation of Ni^{2+} ion with cyclam and its linear analogue (2,3,2-tet) in the nonaqueous

solvents, DMF and DMSO. They found that the values of the bimolecular complexation rate constants were similar for both the ligands in a given solvent. This indicated that the protonation of ligands in an aqueous medium is responsible for the slowness of Ni^{2+} ion complexation with cyclam in water. On the other hand, the rate of metal ion complexation with TMC in a given solvent was slower than that with cyclam, indicating the steric effect of the methyl groups.

In 1982, *Kasprzyk et al.*[20] published that the rate constants for the complexation of various metal ions with the mono-protonated species of TETA, $TETAH^{3-}$ (TETA is a derivative of cyclam with N-functionalised tetraacetate pendant arms), were 10^3-10^4 times larger than those for the mono-protonated species of cyclam, $cyclamH^+$, which apparently implied that the acetate pendant arms could capture the metal ion outside of the macrocyclic ring. This could qualitatively be understood by the different charges of the ligands, where the former bears a charge of 3- and the latter one has 1+, and/or the acetate group could also modify the mechanism by forming an adduct.

In 1986, *Drumhiller et al.*[80] studied the kinetics of complexation of Cu^{2+} ion with TMC and its linear analogues (Me_4-trien, Me_6-trien) in a strongly basic medium in which the ligands existed predominantly (>99.6%) in the unprotonated form. They found that the the constant, k_c ($dm^3\ mol^{-1}\ s^{-1}$), decreased with increasing hydroxide ion concentration due to lower reactivity of the $Cu(OH)_4^{2-}$ species relative to $Cu(OH)_3^-$ species and the rate of complexation decreased in the following order

cyclam > Me_2-cyclam > Me_4-cyclam (TMC).

Moreover, the second Cu^{2+}-N bond formation or multiple desolvation was proposed as the rate determining step for the complexation of TMC with the $Cu(OH)_3^-$ and $Cu(OH)_4^{2-}$ species.

In 1989, *McLaren et al.*[81] reported that the complexation of metal ions by a mono-N-functionalised cyclam derivative, MBPC (cyclam with one pendant 2,2′-bipyridyl-6-yl-methyl arm), in DMSO involved two steps in the overall reaction :

$$[M(DMSO)_6]^{2+} + L \underset{k_2}{\overset{k_1}{\rightleftharpoons}} \text{Intermediate} \xrightarrow{k_3} \text{Products} \qquad (1.2)$$

They evaluated the values of k_1 ($dm^3\ mol^{-1}\ s^{-1}$), k_2 (s^{-1}), and k_3 (s^{-1}), and found that the value of the rate constant, k_1, was similar to the rate constant for the complexation of the metal ion with a free bipyridyl ligand. From this fact they concluded that the pendant bipyridyl arm captured metal ions rapidly, and that the rate determining step in the overall formation process was the coordination of the captured metal ion to the macrocyclic ring.

Although it has been reported that the metal complexes of THEC are labile,[22] and that THEC equilibrates quickly with metal ions[20] due to its pendant 2-hydroxyethyl arms, systematic and quantitative information about the metal ion complexation with THEC is not known in the literature. Thus the present study is intended to elucidate the role of pendant 2-hydroxyethyl arms on the rate of complexation of metal ions with THEC.

1.4 The Kinetics of Decomplexation of Metal Complexes

The free decomplexation (solvolytic decomplexation) of metal complexes of polyamines in aqueous solution is a very slow reaction provided that no scavenging reagent is present. For example, the half-life for free decomplexation of $[Ni(trien)]^{2+}$ in water is about 16 years.[82] However, most metal complexes of open chain polyamines are rapidly decomplexed by strong aqueous acid, yielding the aquated metal ion and protonated amine.[83-90] In contrast, the metal complexes of tetraaza macrocyclic ligands are found to decomplex very slowly even under extreme conditions.[69,91-93]

In 1964, *Curtis*[91] reported that the complexes of Ni^{2+} with tet-a and tet-b were stable to acid, alkali, and ammoniacal dimethylglyoxime. In 1965, *Bosnich et al.*[92] found that a hydrochloric acid solution of Ni^{2+}-cyclam complex could be boiled for several minutes without any noticeable colour change. In 1970, *Cabbiness et al.*[69] reported that the half life of $[Cu(tet\text{-}a)]^{2+}$ (red isomer) in 6 mol dm^{-3} HCl was about 22 days. In 1984, *Billo*[93] reported that the estimated half-life for the decomplexation of planar $[Ni(cyclam)]^{2+}$ in acid medium was about 30 years. Due to such extreme inertness of the metal complexes of tetraaza macrocyclic ligands, substantial attention has been focused on more labile systems including, for example, N_2O_2-systems,[1] N-functionalised derivatives of cyclam,[20-24,72,76] S_4,[40,41] N_xS_{4-x} (x=1,2,3),[53] N_3 and N_5[94-97] macrocyclic systems. However, the discussion here will be limited mainly to N-functionalised cyclam derivatives.

In 1973, *Barefield et al.*[76] qualitatively mentioned that the Ni^{2+}-complex of TMC was kinetically labile. In 1974, *Hertli et al.*[72] studied quantitatively the rate of decomplexation of various metal complexes of TMC in aqueous acid solution. They found that the rates of decomplexation were much faster than those of metal cyclam complexes. The bimolecular rate constants for $[Cu(TMC)]^{2+}$, $[Ni(TMC)]^{2+}$, and $[Co(TMC)]^{2+}$ were 6.7×10^{-3} dm^3 mol^{-1} s^{-1}, 2.9×10^{-2} dm^3 mol^{-1} s^{-1}, and 2.5 dm^3 mol^{-1} s^{-1}, respectively. Thus the rate of decomplexation was found to be dramatically increased with the N-alkylation of cyclam whereas it did not affect the rate of complex formation.[71,72] In 1975, *Jones et al.*[40] studied the rates of decomplexation of tetrathioethers of different ring size (cyclic analogues of cyclam). They also found that the rate of decomplexation was markedly affected by ring size whereas it did not affect the rate of complex formation. In the case of other cyclic analogues of cyclam, for example, *Westerby et al.*[53] qualitatively observed that Cu^{2+}-complexes of $14aneN_xS_{4-x}$(x=1,2,3) were rapidly decomplexed in strong aqueous acid solution with the exception of N_2S_2, the latter needing several weeks for complete decomplexation. Similarly, metal complexes of triaza and pentaaza macrocyclic ligands were found to be very labile compared to those of tetraaza macrocyclic ligands.[94-97]

In 1982, *Hay and Bembi*[21] reported that the attachment of 2-cyanoethyl pendant arms to the N-atoms of cyclam (TCEC) lead to increased lability. They found that the half-life of $[Cu(TCEC)]^{2+}$ in 0.5 mol dm^{-3} aqueous acid solution was about 0.03 s whereas in the complex formation reaction with metal ion, equilibrium was attained very slowly.[23] In 1984, *Hancock et al.*[23] and *Hay et al.*[22] qualitatively

reported that metal complexes of THEC were labile in aqueous acid solution. In 1987, *Hay et al.*[24] studied acid catalysed decomplexation of $[Cu(THEC)]^{2+}$ quantitatively. They found that the observed pseudo first-order rate constant was linearly dependant on the excess acid concentration up to 0.5 mol dm^{-3} and the half-life for the decomplexation of $[Cu(THEC)]^{2+}$ in aqueous solution of 0.05 mol dm^{-3} $HClO_4$ at 298.2 K was 3.5 s. However, they did not study the decomplexation of other metal complexes. Thus, the present study is intended to investigate the effect of pendant 2-hydroxyethyl arms on the relative lability of metal complexes of THEC and also to investigate the mechanistic pathways in collaboration with the kinetic results of complex formation.

1.5 The Mechanistic Terminology of Kinetic Studies

1.5.1 Introduction

The systematic study of the rates of reactions is known as reaction kinetics, and there are two main reasons[98] for studying the rates of reactions as discussed below.

The first reason is to predict how fast a reaction mixture will move to its equilibrium state under the given conditions (temperature, pressure, catalyst, etc.), and what factors determine how rapidly a given reaction will proceed at an optimum rate as required for practical applications.

The second reason is to establish the mechanism by which the reaction takes place. All chemical reactions take place by sequences of one or more elementary steps. An elementary step is the simplest process by which stable species are converted into another stable species. The

mechanism of the reaction is the description of the sequences of all elementary steps by which a complex reaction takes place. Generally, the mechanism is elucidated from the rate law (interpreted from kinetic data) using some working rules.[99,100] However, such an assumed mechanism may be one of several possible mechanisms. It might even turn out to be incorrect.[101]

1.5.2 The Hydrated Metal Ion in Aqueous Solution

In water, a metal ion is surrounded by a definite number of water molecules[102] which is termed a hydrated metal ion or aquo-metal ion complex, $[M(H_2O)_x]^{n+}$. In the case of other solvents it is called a solvated metal ion or solvento-metal ion complex. Thus in order to evaluate the mechanism for a reaction at the metal ion centres, it is necessary to consider the environmental features of the solvated metal ion which is often the precursor of inorganic reaction mechanisms involving metal ions.

A model of a hydrated metal ion[103] can be illustrated by Figure 1.3. In this model, the metal ion is at the centre of a series of four concentric regions of water. In the innermost region, A, the water molecules are directly bonded with metal ion through oxygen atoms by electrostatic attraction. In this region water molecules are highly ordered, since they have lost their translational degrees of freedom and move as one entity with the metal ion in solution. This region is known as the first coordination sphere or primary solvation shell of the metal ion.

The region, B, is called the secondary coordination sphere or secondary solvation shell, where water molecules still have some order in

orientation due to electrostatic influence of metal ion as well as enhanced hydrogen bonding with polarised water molecules in the primary solvation shell. The boundary between these coordination spheres (A and B) is well defined for most ions in aqueous solution.

Figure 1.3 A model for the hydrated metal ion.

(i) Region, A, the primary hydration shell where water molecules are highly ordered.

(ii) Region, B, the secondary hydration shell where water molecules still have some order in orientation.

(iii) Region, C, the third hydration shell where water molecules are disordered.

(iv) Region, D, the bulk solvent.

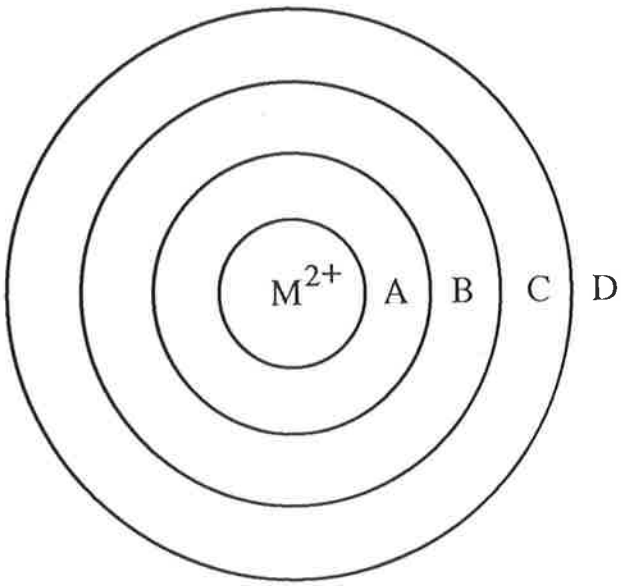

The electrostatic influence of a metal ion on the water molecules in the third region, C, is negligible and thus the water molecules are disordered in orientation due to competitive influences between C and D

(the bulk water) where the orientations of water molecules are influenced by neighbouring water molecules. The boundaries among the regions B, C, and D are indistinguishable, and kinetically there are only two water environments distinguishable, region A, and the rest of the regions (B, C, and D).

The rate of exchange of solvent molecules between the first coordination sphere of the metal ion and the bulk of the solvent has been determined for most metal ions in different solvents.[101,103] These solvent exchange studies play a key role in understanding the mechanisms involved in typical reactions of metal complexes in solution.

1.5.3 Typical Reactions of Metal Complexes in Aqueous Solution

The types of reactions of interest in this study are the complexation of metal ions with THEC and the acid catalysed decomplexation of metal complexes of THEC. Thus in order to evaluate the mechanisms involved in these reactions, the following typical reactions of metal complexes must be considered.

For simplicity, consider a divalent metal ion of coordination number six which exists in a solvent, S, as a solvento-metal ion complex, $[M(S)_6]^{2+}$. In solution, the solvent molecules, S, from the first coordination sphere of the metal ion may be displaced by identical solvent molecules from the bulk, S*, in the following manner,

$$[M(S)_6]^{2+} + S^* \rightleftharpoons [M(S)_5(S^*)]^{2+} + S \qquad (1.3)$$

where the asterisk is merely a typographical distinction. This process (equation 1.3) is termed solvent exchange and no net chemical change occurs as a result of that exchange.

The solvent molecules from the first coordination sphere can also be displaced by other ligands. For example, in the case of a neutral mono-dentate ligand, L (occupying one coordination site on the metal ion), displacing the solvent molecules, S,

$$[M(S)_6]^{2+} + L \rightleftharpoons [M(S)_5(L)]^{2+} + S$$

leading eventually to

$$[M(S)(L)_5]^{2+} + L \rightleftharpoons [M(L)_6]^{2+} + S \qquad (1.4)$$

(Note that for simplicity a solvation sphere around L has been omitted although it exists). The forward reaction is a complex formation reaction, and the reverse reaction is a solvolysis or more specifically a solvolytic decomplexation reaction. When L is a multidentate ligand (occupying more than one coordination site of the metal ion), solvent molecules are displaced sequentially.

The difference between the solvent exchange (equation 1.3) and complex formation reaction (equation 1.4) is due to the different entering group and a net chemical change does occur in the latter case. On the other hand, in both the cases the leaving groups from the first coordination sphere of the metal ion are the solvent molecules, and hence

the mode of metal-solvent bond breaking is used as "finger print" to evaluate the mechanisms of simple complex formation reactions with metal ions.

Generally the solvolytic decomplexation reaction is very slow particularly for metal complexes of polyamines in aqueous solution (see section 1.4). However, for simple amine ligands in the presence of strong aqueous acid, amine groups are protonated in a succession of protonation steps and are rapidly decomplexed from the central metal ion, finally all the amine groups are displaced from the first coordination sphere of the metal ion by water molecules as shown in equation 1.5 (L is a mono-amine ligand)

$$[M(L)_6]^{2+} + 6(H_3O)^+ \rightleftharpoons [M(H_2O)_6]^{2+} + 6LH^+ \qquad (1.5)$$

This scavenging process is called acid-catalysed hydrolysis or acid catalysed decomplexation. Such a reaction is helpful in evaluating the reaction mechanism because, from the principle of microscopic reversibility, at equilibrium the transition probabilities for a given step for the forward and reverse direction are equal. That is, the postulated mechanism should serve for both forward and reverse direction of that step.[99]

The replacement of one ligand from the first coordination sphere of the metal ion by another free ligand in solution is a fundamental process which permeates all aspects of reaction kinetics in coordination chemistry. Since the solvent molecule can also be considered as a ligand or a Lewis base, and the metal ion as a Lewis acid, in order to evaluate

the mechanism, solvent exchange and complex formation reactions can be considered as special cases of ligand substitution (or nucleophilic substitution) reactions[103-106] in which one Lewis base (L) displaces another (S) from a Lewis acid, $[M(S)_n]^{2+}$, i.e., the entering group, (L), displaces the leaving group, S, from the first coordination sphere of the metal ion :

$$[M(S)_n]^{2+} + L \rightleftharpoons [M(S)_{n-1}(L)]^{2+} + S \qquad (1.6)$$

the charges of S and L, and the solvent phase are omitted for simplicity.

(i) When S = L = H_2O, then equation 1.6 describes the water exchange process. (ii) When S = H_2O, L = a ligand, then equation 1.6 describes a typical complex formation reaction in aqueous solution (it also may be called substitution of a water molecule, H_2O, by the ligand molecule, L). (iii) When S = a ligand, L = a ligand, and S ≠ L, then equation 1.6 may be considered as a typical ligand substitution reaction in aqueous solution.

1.5.4 General Mechanisms Involved in Substitution Reactions of Metal Complexes in Solution

The possible mechanistic pathways of substitution reactions of metal complexes in solution can be classified mainly into three categories:[106]

(i) associative mechanism, A,

(ii) dissociative mechanism, D,

(iii) interchange mechanisms, I_a and I_d.

These mechanisms can be illustrated by the following flow diagram:

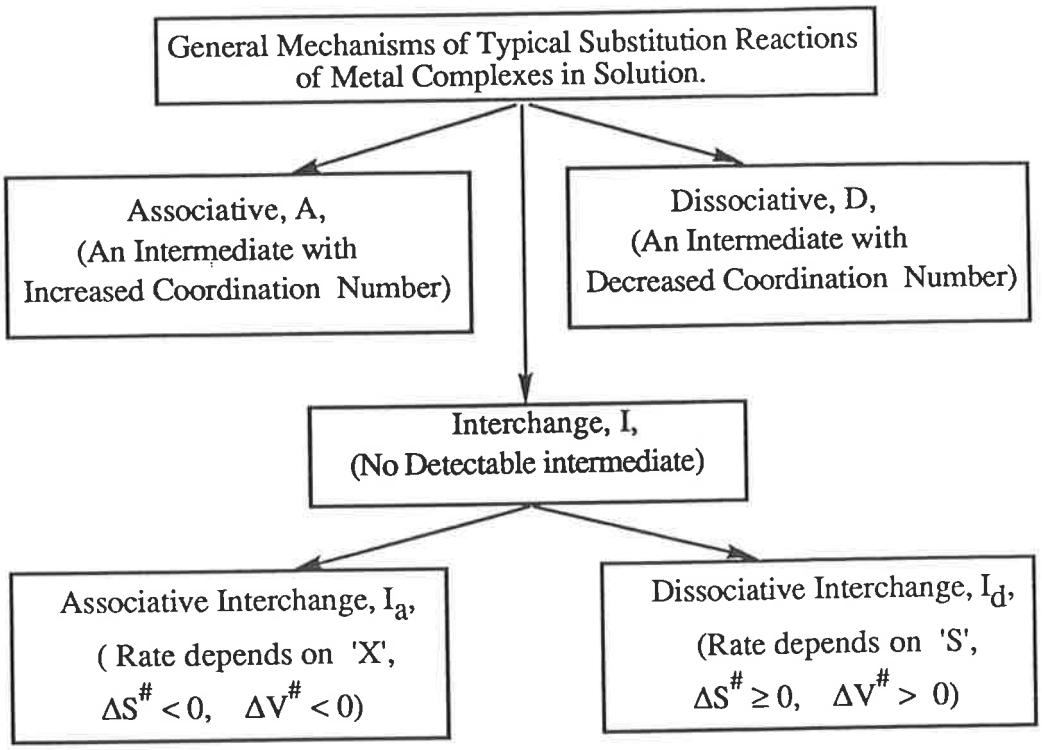

For the purposes of illustration the examples of reacting species will be a solvated metal ion, MS_6 (S is the solvent or a leaving ligand), and a solvated ligand X (an entering ligand).

1.5.4a The Associative Mechanism

This mechanism is characterised by the formation of an intermediate with increased coordination number while a new bond between metal ion and entering ligand is formed:

$$MS_6 + X \xrightarrow[\text{r.d.s.}]{\text{slow}} \underset{\text{t.s.}_{(1)}}{S_6M\cdots X} \xrightarrow[\text{intermediate}]{\text{fast}} S_6MX \xrightarrow[\text{t.s.}_{(2)}]{\text{fast}} S_5XM\cdots S \xrightarrow{\text{fast}} MS_5X + S \qquad (1.7)$$

For the forward reaction, the rate determining step (r.d.s.) is the formation of transition state, t.s.$_{(1)}$, and for the reverse reaction the rate determining step is the formation of transition state, t.s.$_{(2)}$. In this mechanism the entering group is actively involved in the r.d.s. during the formation of the reactive intermediate and hence the rate of an associative reaction is dependant on the nature of the entering group, X.

1.5.4b The Dissociative Mechanism

This mechanism is characterised by the formation of an intermediate with decreased coordination number while a bond between the metal ion and the leaving ligand is broken.

$$MS_6 + X \xrightarrow[\text{r.d.s.}]{\text{slow}} \underset{\text{t.s.}_{(1)}}{S_5M\cdots S + X} \xrightarrow{\text{fast}} \underset{\text{intermediate}}{S_5M + S + X} \xrightarrow{\text{fast}} \underset{\text{t.s.}_{(2)}}{S_5M\cdots X + S} \xrightarrow{\text{fast}} MS_5X + S \qquad (1.8)$$

For the forward reaction, the rate determining step (r.d.s.) is the formation of the transition state, t.s.$_{(1)}$, and for the backward reaction the r.d.s. is the formation of transition state, t.s.$_{(2)}$. In this mechanism the entering group is not involved in the r.d.s. for the generation of the reactive intermediate and thus the rate of the reaction is expected to be independent of the nature of the incoming group, X because in the r.d.s., a bond between M and S is virtually broken leading to the formation of the reactive intermediate, MS_5. Thus, the rate of the reaction depends upon the rate at which the leaving ligand dissociates from the first

coordination sphere of the metal ion, and here this may be equated to the rate of solvent exchange.

1.5.4c The Interchange Mechanisms

The concept of interchange mechanisms is more sophisticated than the simple dissociative or associative mechanism outlined above. The interchange mechanisms involve the formation of an activated complex in a single step where the leaving and entering groups interchange their positions in the first and second coordination sphere of the metal ion synchronously, leading to the product without the formation of any detectable intermediate. Before exchange occurs, the incoming ligand is suitably placed to enter the primary coordination sphere of the metal ion as soon as leaving group has left. Thus, it is assumed that the starting complex (e.g., solvated metal ion) and the incoming ligand form an outer sphere association or encounter complex (of ion pair or ion-dipole nature and which occurs at a diffusion controlled rate) followed by the rate determining step while interchange occurs.

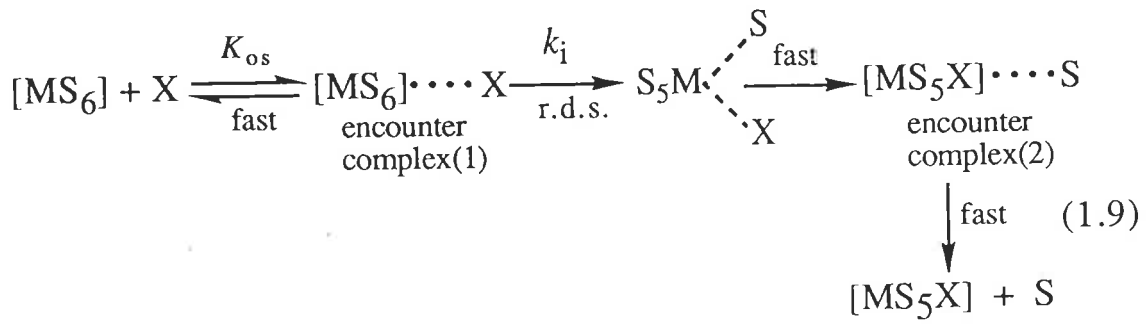

(1.9)

For the forward reaction, interchange (the rate determining step) occurs through the encounter complex(1), and for the reverse reaction it occurs through encounter complex(2).

Although no detectable intermediate exists in interchange mechanisms, it is the degree of bond making and bond breaking in the rate determining step (r.d.s.) that determines the classification of the process which may, in principle, continuously span the conceptual "gap" that exists between that observed for the D mechanism and that observed for the A mechanism. When bond breaking is predominant in the r.d.s., that is, when it involves the elongation of a M-S bond followed by the interchange with X in the encounter complex then it is termed a dissociative interchange mechanism (I_d), and k_i is independent of the nature of the entering group. Due to bond breaking, the number of total particles in the transition state should be greater compared to the initial state, and hence both entropy of activation ($\Delta S^{\#}$) and volume of activation ($\Delta V^{\#}$) should be positive (i.e., $\Delta S^{\#} > 0$, and $\Delta V^{\#} > 0$). On the other hand, when bond making between the metal ion and entering ligand is predominant in the r.d.s. it is called an associative interchange mechanism (I_a), and thus k_i should show a dependence on the nature of the entering group, and both $\Delta S^{\#}$ and $\Delta V^{\#}$ should be negative (i.e., $\Delta S^{\#} < 0$, and $\Delta V^{\#} < 0$). However, it should be noted that if any solvation or desolvation or a change in charge numbers occurs in the transition state in addition to bond making or bond breaking then the sign of $\Delta S^{\#}$ and $\Delta V^{\#}$ for the prediction of I mechanism is unreliable.

To derive the rate law for interchange mechanisms, for simplicity, equation 1.9 can be written as follows :

$$[MS_6] + X \underset{\text{fast}}{\overset{K_{os}}{\rightleftharpoons}} \underset{\text{encounter complex}}{[MS_6]\cdots X} \xrightarrow[\text{r.d.s.}]{k_i} S_5M\begin{matrix} \diagup S \\ \diagdown X \end{matrix} \qquad (1.10)$$

for which,

$$\text{rate} = k_i\,[[MS_6]\cdots X]$$
$$= k_i K_{os}\,[MS_6]\,[X] \qquad (1.11)$$

where k_i is the forward rate constant, and K_{os} is the formation constant for the encounter complex, can be expressed as follows :

$$K_{os} = \frac{[[MS_6]\cdots X]}{[MS_6]\,[X]} \qquad (1.12)$$

In practice, under pseudo first-order conditions, either of the reactants are used in excess. Thus, if [X] is in large excess then the rate can be expressed as follows,

$$\text{rate} = k_{obs.}\,[MS_6]_T \qquad (1.13)$$

where $k_{obs.}$ = the observed pseudo first-order rate constant

$[MS_6]_T = [MS_6] + [[MS_6]\cdots X]$

Therefore, from equations 1.11 and 1.13, the rate law is,

$$k_{obs.} = \frac{k_i K_{os}\,[X]}{1 + K_{os}\,[X]} \qquad (1.14)$$

When the reverse reaction is considered in the r.d.s.,

$$[MS_6] + X \underset{\text{fast}}{\overset{K_{os}}{\rightleftharpoons}} \underset{\text{encounter complex}}{[MS_6]\cdots X} \underset{k_{-i}\ \text{(r.d.s.)}}{\overset{k_i}{\rightleftharpoons}} S_5M\begin{matrix} \diagup S \\ \diagdown X \end{matrix} \qquad (1.15)$$

(A) (B) (C) (D)

then the rate law (for reaction 1.15) can be expressed by equation 1.16

$$k_{obs.} = k_{-i} + \frac{k_i K_{os} [X]}{1 + K_{os} [X]} \qquad (1.16)$$

where k_{-i} is the rate constant for backward reaction.

This rate law (equation 1.16) can be deduced as follows,

$$\text{rate} = \frac{d[D]}{dt} = k_i [C] - k_{-i} [D]$$
$$= k_i K_{os} [A] [B] - k_{-i} [D] \qquad (1.16a)$$

where [ ] represents the concentration of the enclosed species (also see the notations shown in equation 1.15). Under pseudo first-order conditions,

$$\text{rate} = k_{obs.} [MS_6]_T$$
$$= k_{obs.} ([MS_6] + [[MS_6]\cdots X])$$
$$= k_{obs.} ([A] + [C]) \qquad (1.16b)$$

Thus, from equation 1.16a and 1.16b,

$$k_{obs.} ([A] + [C]) = k_i K_{os} [A] [B] - k_{-i} [D]$$

or, $$d\{k_{obs.} ([A] + [C])\} = d\{k_i K_{os} [A] [B] - k_{-i} [D]\}$$

or, $$k_{obs.}(d[A] + d[C]) = k_i K_{os} d\{[A] [B]\} - k_{-i} d[D] \qquad (1.16c)$$

If B is used in excess (at least 10 fold), then d[B] ~0 (since B is invariant). Therefore, equation 1.16c reduces to equation 1.16d

$$k_{obs.} (d[A] + d[C]) = k_i K_{os} [B] d[A] - d\{k_{-i} [D]\} \qquad (1.16d)$$

From mass balance,

$$[A]_{total} = [A] + [C] + [D]$$

or, $d[A]_{total} = d[A] + d[C] + d[D] = 0$

or, $d[D] = -d[A] - d[C]$ (1.16e)

Therefore, from equations 1.16d and 1.16e,

$$k_{obs.}(d[A] + d[C]) = k_i K_{os}\, d\{[A][B]\} + k_{-i}\{d[A] + d[C]\} \quad (1.16f)$$

Again, from equations 1.12 one can write,

$$[C] = K_{os}[A][B]$$

or, $$d[C] = K_{os}[B]\, d[A] + K_{os}[A]\, d[B]$$

$$= K_{os}[B]\, d[A] \quad \text{(since } d[B]=0\text{)} \quad (1.16g)$$

Therefore from equations 1.16f and 1.16g,

$$k_{obs.} = k_{-i} + \frac{k_i K_{os}[B]}{1 + K_{os}[B]} \quad (1.16h)$$

Thus, equations 1.16 and 1.16h are similar in form.

Under limiting conditions, (i) when [X] = 0, equation 1.16 reduces to $k_{obs.} = k_{-i}$, representing the rate constant for a solvolytic decomplexation, (ii) when $K_{os}[X] << 1$, the equation 1.16 reduces to $k_{obs.} = k_{-i} + k_i K_{os}[X]$, where $k_{obs.}$ has a linear dependence on [X] with a slope of $k_i K_{os}$ and an intercept at k_{-i}; and (iii) when $K_{os}[X] >> 1$ (at large excess of [X] and/or the pre-equilibrium step (K_{os}) forming the encounter complex lies completely to the right),equation 1.16 reduces to $k_{obs.} = k_{-i} + k_i$, with the rate being independent of [X]. A typical curve representing the variation of the observed pseudo first-order rate constant, $k_{obs.}(s^{-1})$, with excess concentration of the entering ligand, [X] (mol dm^{-3}), for a substitution

reaction occuring through an interchange mechanism is shown in Figure-1.4.

Figure 1.4 A typical curve representing the variation of the pseudo first-order rate constant, $k_{obs.}$ (s^{-1}) with excess concentration of the entering ligand, [X] (mol dm^{-3}), for a substitution reaction occuring through an interchange mechanism :

(i) when [X] = 0, then $k_{obs.} = k_{-i}$;

(ii) when K_{os} [X] << 1, then $k_{obs.} = k_{-i} + k_i K_{os}$ [X], slope = $k_i K_{os}$;

(iii) when K_{os} [X] >> 1, then $k_{obs.} = k_{-i} + k_i$.

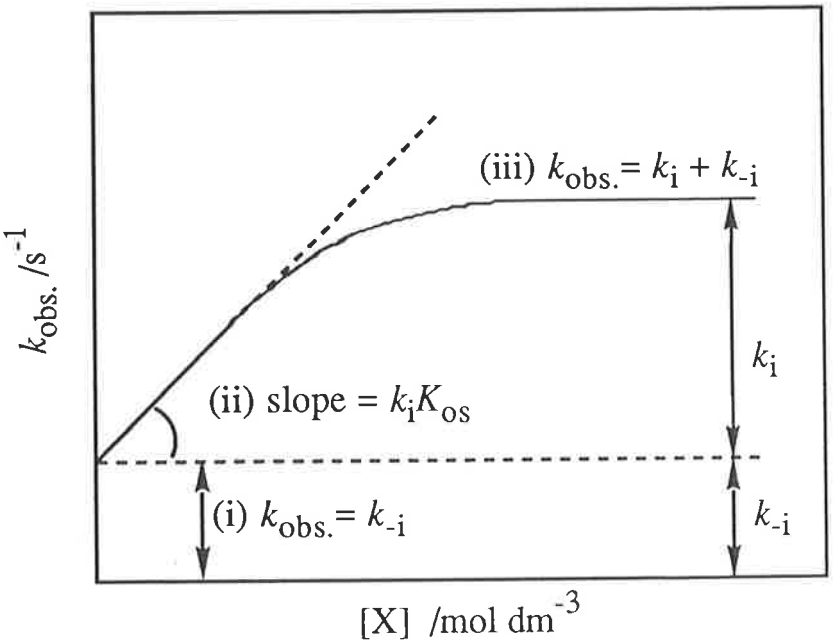

For a rapidly reacting system, K_{os} can be determined by using ultrasonic or temperature-jump relaxation techniques. However, the values of K_{os} can also be approximately estimated using the Fuoss equation[107] (equation 1.17),

$$K_{os} = \frac{4\pi Na^3}{3000} \exp - \{ \frac{U(a)}{k_B T} \} \qquad (1.17)$$

where $U(a)$ = the Debye-Hückel interionic potential,

that is, $U(a) = \frac{Z_1 Z_2 e^2}{aD} - \frac{Z_1 Z_2 e^2 k}{D(1+ka)}$,

$k^2 = \frac{8\pi Ne^2 I}{1000 D k_B T}$,

N = Avogadro's number,

a = centre to centre distance of closest approach of the solvated metal ion and the reacting site of the ligand (in cm),

k_B = Boltzmann's constant (in ergs),

e = charge of an electron (in e.s.u.),

D = bulk dielectric constant (of solvent),

I = ionic strength,

Z_n = charges on reactants, and

T = absolute temperature.

Although the calculation has been applied for the association of solvated cation with

(i) uncharged ligand;[108,109]

(ii) negatively charged ligand;[110]

(iii) positively charged ligand;[111,112]

the applicability of this equation is questionable, involving uncertainties and dubious assumptions, particularly for an incoming ligand of complicated stereochemistry.[113] However, the Fuoss equation may be useful in some cases as a first approximation.

This is, of course, a very simplistic overview of substitution reactions of metal complexes in aqueous solution and mechanistic pathways therein. In practice, particularly those reactions with macrocyclic ligands, it is difficult to evaluate the rate determining step accurately, and sometimes it becomes controversial.[41,68,114,115]

1.6 Objectives of The Present Work

The aim of the present work is (i) the kinetic investigation of the role of the 2-hydroxyethyl pendant arms on the rate of complexation of metal ions with THEC, and the acid catalysed decomplexation of the metal complexes of THEC at same temperature and ionic strength, and hence the evaluation of the mechanistic pathways therein; (ii) to make a comparison of the kinetic results of these systems with those obtained for the related macrocyclic systems; and (iii) to analyse the formation constants of the metal complexes in terms of rate constants for the complexation and for the decomplexation.

It should be noted here that the values of the acid dissociation constants (K_a) of THEC and the formation constants (K_{ML}) for the complexation of Cu^{2+}, Ni^{2+}, and Co^{2+} with THEC in the literature have been determined[23,24] at an ionic strength different from that maintained in the present kinetic studies. For the present kinetic studies, it is required to evaluate thc speciation of various protonated species of THEC and its metal complexes in different pH regions which needs the values of pK_a and K_{ML}, determined at the same temperature and ionic strength. Moreover, to analyse the formation constants (K_{ML}) in terms of rate constants and to verify with the values determined by other methods, the

values of K_{ML} should be determined under identical conditions of temperature and ionic strength using, for instance, the potentiometric titration method.

Therefore, the objectives of this project include :

(i) determination of the pK_a values of THEC at 298.2 K and ionic strength[a] of 1.5 mol dm^{-3} using the potentiometric titration method;
(ii) determination of the formation constants for the complexation of metal ions, Cu^{2+}, Ni^{2+}, and Co^{2+} with THEC at the same temperature and ionic strength using the potentiometric titration method;
(iii) kinetic studies on the complexation of the metal ions with THEC at the same temperature and ionic strength using the stopped-flow spectrophotometric technique;
(iv) kinetic studies on the decomplexation of metal complexes of THEC in excess strong aqueous acid solutions at the same temperature and ionic strength using the same technique;
(iv) kinetic studies of the decomplexation of metal complexes of THEC in strong (and excess) aqueous acid solution at different temperatures, at the same ionic strength, in order to determine the activation parameters (enthalpy of activation and entropy of activation).

[a] It should be noted that the molar absorptivity, $\varepsilon_{max.}$ (dm^3 mol^{-1} cm^{-1}) for Co^{2+}- and Ni^{2+}-complexes of THEC are very low. To obtain a measurable absorbance change upon complexation, for example, with Co^{2+}, the concentration of THEC needed to be 0.005 mol dm^{-3} (before mixing). To control the pH of the metal solution, the concentration of the buffer (PIPES) needed to be 0.6 mol dm^{-3} (before mixing). To observe the variation of the pseudo first-order rate constant against excess metal ion concentration, at least 10-60 fold excess was needed, and the maximum metal ion concentration used was 0.3 mol dm^{-3} (before mixing). Thus due to all these experimental constraints, a constant ionic strength was maintained at very high value, viz., 1.5 mol dm^{-3}.

CHAPTER 2

EXPERIMENTAL

2.1 Reagents and Materials

All solutions were prepared in Milli-Q® water (deionized water ultrapurified with a Milli-Q system to produce water with specific resistance of >12 M Ω cm). All volumetric glassware used was A-grade. $Cu(II)(NO_3)_2.6H_2O$ (AJAX), $Ni(II)(NO3)2.6H_2O$, $Co(II)(NO_3)_2.6H_2O$, $NaNO_3$, NaOH, HNO_3 (BDH), and PIPES (Calbiochem) were AR grade chemicals and used without further purification. The ligand, THEC, was prepared and purified by Kevin Wainwright[116] according to a literature method.[23]

2.2 Preparation of Experimental Solutions

2.2.1 Stock Solutions

The stock solutions of metal ions were prepared by dissolving the required weight of $M(II)(NO_3)_2.6H_2O$ (M = Cu, Ni, and Co) in water and standardised by EDTA titrations[117,118] and by cation exchange chromatography.[118] The HNO_3 stock solutions were prepared by diluting 70% AR grade HNO_3 in water and standardised by titration against NaOH solution using bromothymol blue as an indicator. Stock solutions of 0.60 mol dm^{-3} PIPES were used to control pH and ionic

strength was adjusted using a 3.00 mol dm^{-3} solution of $NaNO_3$. All standard solutions of NaOH were prepared by diluting the contents of BDH ampoules.

2.2.2 Solutions for Potentiometric Titrations

Solution (A), a stock solution of HNO_3 (4.0×10^{-3} mol dm^{-3}, adjusted to ionic strength of 1.50 mol dm^{-3} $NaNO_3$) was prepared from 0.10 mol dm^{-3} HNO_3 and 3.0 mol dm^{-3} $NaNO_3$. Solution (B), a stock solution of THEC (1.00×10^{-3} mol dm^{-3}) was prepared by dissolving 0.1888 g. of THEC in 500 cm^3 of solution (A). 10 cm^3 of solution (A) was used in each calibration titration and 10 cm^3 of solution (B) was used in each pK_a determination titration. Solution (C) was prepared by adding an exactly known quantity of the respective aqueous metal ion solution by means of a micropipette (Microman G10338K, Gilson) to 10 cm^3 of solution (B) and was used in each potentiometric titration for the determination of stability constants of metal complexes (see section 2.5).

2.2.3 Solutions for Complexation Kinetic Studies

The pH values of all experimental solutions used in the study of formation kinetics were maintained[119,120] to a precision of ±0.02 pH units using the zwitterion buffer PIPES, with the addition of either NaOH or HNO_3. All solutions of metal ions, Ni^{2+} and Co^{2+}, and of the ligand (THEC) were prepared by volumetric dilution of the respective stock solutions into 25 cm^3 flasks containing 12.5 cm^3 of 0.60 mol dm^{-3} PIPES and ionic strength was adjusted to 1.50 mol dm^{-3} using 3.00 mol dm^{-3} $NaNO_3$.

2.2.4 Solutions for Decomplexation Kinetic Studies

The solutions of metal complexes ($[M(THEC)]^{2+}$ (M = Cu, Ni, and Co), were prepared by dissolving an accurately weighed amount of THEC into water contained in 200 cm^3 flasks followed by the addition of an exact volume of standard metal ion stock solution by means of a micropipette (so that the molar ratio of metal:ligand was 1:1), and the requisite volume of 3.00 mol dm^{-3} $NaNO_3$ solution was added to maintain ionic strengths at 1.50 mol dm^{-3}. The sample solutions of HNO_3 of different concentrations were prepared by volumetric dilution of standard stock solutions into 50 cm^3 flasks followed by the adjustment of ionic strength to 1.50 mol dm^{-3} using 3.00 mol dm^{-3} $NaNO_3$ solution.

2.2.5 Degassing of Experimental Solutions

To avoid the formation of air bubbles in the stopped-flow experiments all sample solutions were degassed in a vacuum desiccator using a magnetic stirrer and a water pump. The degassed solutions were then transferred into air-tight plastic reservoir syringes (see section 2.5.3) as quickly as possible.

2.3 Measurement of pH of Experimental Solutions

The pH of the experimental solutions for complexation kinetic studies was measured using an Orion Research potentiometer (model SA 720) and a glass electrode (Orion, 8103 Ross Combination Electrode). Standard buffer solutions,[118,119] of potassium hydrogen phthalate (pH 4.01 at 298.2 K), and Na_2HPO_4/KH_2PO_4 (pH 6.86 at 298.2 K) were used to calibrate the electrode.

2.4 Measurement of Visible Spectra

Electronic spectra (visible) of experimental solutions were measured on a Zeiss DMR10 double beam spectrophotometer using identical cells of 1 cm path length kept at 298.2 (±0.2) K by circulating water from a constant temperature water bath. The wavelength for each metal ion monitored in stopped-flow kinetic measurements was chosen from the region of the spectrum where the difference between the molar absorptivity of the metal-complex ($[M(THEC)]^{2+}$) and that of the free aquo-metal ion ($[M(H_2O)_6]^{2+}$) was a maximum.

2.5 Potentiometric Titrations

The acid dissociation constants of THEC and the stability constants of its metal complexes were measured by potentiometric titrations performed with a Metrohm E665 Dosimat autoburette using an Orion Ross sureflow combination electrode connected to an Orion SA 720 pH meter interfaced to an IBM personal computer. All titrations were carried out at 298.2 (±0.2) K (the temperature was kept constant by circulating water through the outer compartment of the titrating vessel from a constant temperature water bath using a thermostat, Julabo Paratherm IM). The ionic strengths of all sample solutions were adjusted to 1.50 mol dm^{-3} using 3.00 mol dm^{-3} $NaNO_3$ solution. The solution in the titrating vessel was stirred constantly throughout the titration using a magnetic stirrer, and a constant steam of dry nitrogen gas was bubbled through the solution to remove any CO_2 which might be present initially and to prevent CO_2 absorption.

Calibration preceded every three titrations. For a calibration run, 10 cm^3 of HNO_3 (4.0×10^{-3} mol dm^{-3}) was titrated with 1 cm^3 of standard NaOH solution (0.10 mol dm^{-3}) while measuring the E.M.F (mV) of the pH electrode as a function of volume of NaOH added. The values of E_o and pK_w were evaluated by fitting the data from the calibration titration to equations 2.1a and 2.1b

$$E = E_o - \frac{2.303\,RT}{F} \log [H^+] \qquad (2.1a)$$

$$pK_w = pH + pOH \qquad (2.1b)$$

where the symbols have their usual significance.

To determine the acid dissociation constants (pK_a) of THEC, 10 cm^3 of a solution of THEC (1.00×10^{-3} mol dm^{-3}) in HNO_3 (4.0×10^{-3} mol dm^{-3}) was titrated with 1 cm^3 of standard NaOH solution (0.10 mol dm^{-3}). The E.M.F. (mV) was recorded as a function of volume of NaOH added.

For the determination of stability constants of the complex species, a solution containing 10 cm^3 of THEC solution (1.00×10^{-3} mol dm^{-3}) in HNO_3 (4.0×10^{-3} mol dm^{-3}) and 0.09 cm^3 (90 microlitre) of standard solution of respective metal ion was titrated with 1 cm^3 standard NaOH solution (0.10 mol dm^{-3}). The same titration was repeated for 0.050 cm^3, 0.070 cm^3, and 0.20 cm^3 solutions of each metal ion. The concentrations of standard solutions of metal ions were 0.1021 mol dm^{-3}, 0.1022 mol dm^{-3}, and 0.1011 mol dm^{-3}, for $[Co(H_2O)_6]^{2+}$, $[Ni(H_2O)_6]^{2+}$, and $[Cu(H_2O)_6]^{2+}$, respectively.

The acid dissociation constants of THEC and stability constants of the metal complexes of THEC were determined separately using MINIQUAD.[121]

2.6 Kinetic Measurements

2.6.1 Introduction

A wide variety of techniques for studying different types of chemical reactions have been discussed in several texts.[122-124] Reactions having half-lives greater than 10 s can be studied by conventional methods, reactions having half-lives between 10 s and a few milliseconds can be studied by flow methods, reactions having half-lives within the range of 10^{-2} s to 10^{-7} s can be studied by relaxation techniques e.g., pressure jump, temperature jump, and by flash photolysis, and half-lives $<10^{-9}$ s have been measured by ultrasonic, fluorescence and other spectroscopic techniques.[123,125]

The half-lives of the reactions in the present investigation were found to be within the range of flow methods. Due to the simplicity of apparatus operation and reagent economy, the stopped-flow spectrophotometric technique was used. An existing stopped flow apparatus was modified for variable temperature operation and was suitable for reaction half-lives from a few milliseconds up to seconds or even minutes (see section 2.6.3).

2.6.2 The Principles of Stopped-flow Spectrophotometry

In this technique, the two reactant solutions are forced into a mixing chamber where they are rapidly mixed and reaction commences. The mixed solution passes swiftly into an observation cell, the flow is abruptly stopped, and simultaneously a trigger switch activates the spectrophotometric observation and recording units as the reaction proceeds in the observation cell.

The light from a stable source is passed in at the one end of the observation cell, and at the other end a photomultiplier tube is placed to record the intensity of light transmitted from the observation cell during the course of a reaction. The electrical signal from the photomultiplier tube is fed into a transient digital recorder connected to an oscilloscope.

As the reaction proceeds, there is a change in concentration of the absorbing species being monitored, which causes a change in the intensity of the light transmitted, and consequently there is an equivalent change in the photomultiplier voltage. A reaction which causes an increase in concentration of absorbing species is accompanied by a drop in voltage (corresponding to less light transmitted), whereas a reaction which causes a decrease in concentration of the absorbing species is accompanied by a rise in voltage (corresponding to more light transmitted). The variation of photomultiplier voltage with time during the course of reaction is subsequently analysed to determine the rate constant of the reaction under investigation.

A typical curve for a reaction involving an increase in concentration of absorbing species is shown in figure 2.1. Under pseudo first-order conditions (10 fold excess of one reactant), the evaluation[126] of the pseudo first-order rate constant is made as follows. The voltage output from the photomultiplier tube, V_t, at any time t, is proportional to the intensity of light transmitted from the solution (in the observation cell), I_t, thus one can write:

$$V_t = C\, I_t \tag{2.2}$$

where C is a constant for a fixed photomultiplier voltage.

If V'_o is the voltage and I'_o is the intensity of transmitted light with solvent alone in the observation cell (the case corresponding in spectrophotometry to 100% transmission), then

$$V'_o = C I'_o. \tag{2.2a}$$

The absorbance, A_t, at any time t, may be defined as follows:

$$A_t = \log \frac{I'_o}{I_t} \tag{2.3}$$

Therefore, from equations 2.2a and 2.3

$$A_t = \log \frac{V'_o}{V_t} \tag{2.4}$$

Figure 2.1 Typical stopped-flow trace for a reaction involving an increase in absorbance, i.e., $A_\infty > A_t$, $V_\infty < V_t$ (not to scale).

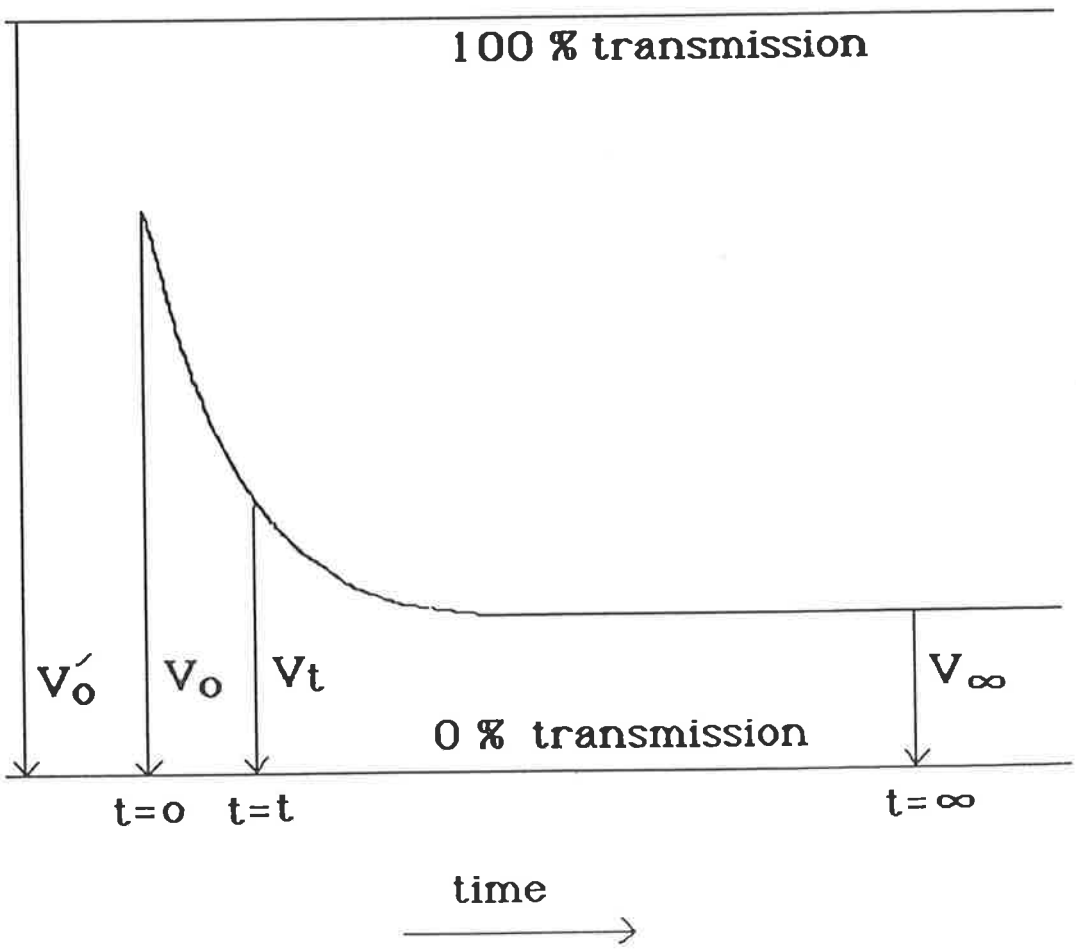

An estimation of the pseudo-first-order rate constant, k, characterizing the reaction trace may be expressed[127,128] by equation (2.5),

$$\ln \frac{A_\infty - A_t}{A_\infty - A_o} = -k\,t \qquad (2.5)$$

where A_∞ is the absorbance at infinite time (more than seven half-lives), A_t is the absorbance at time t, and A_o is the absorbance at time, t = 0.

Using equation (2.4) one can derive equations (2.6) and (2.7),

$$A_\infty - A_t = \log \frac{V_t}{V_\infty} \qquad (2.6)$$

$$A_\infty - A_o = \log \frac{V_o}{V_\infty} \qquad (2.7)$$

Substituting equations (2.6) and (2.7) in equation (2.5),

$$\ln \frac{\log \frac{V_t}{V_\infty}}{\log \frac{V_o}{V_\infty}} = -kt \qquad (2.8)$$

Since $\ln \{ \log \frac{V_o}{V_\infty} \}$ is a constant term thus one can write,

$$\ln \{\log \frac{V_t}{V_\infty}\} = \text{constant} - k\,t \qquad (2.9)$$

in exponential form,

$$\log \frac{V_t}{V_\infty} = B_1\, e^{-kt} \qquad (2.10)$$

where B_1 is a constant, equal to $\log \frac{V_o}{V_\infty}$.

Equation 2.9 indicates that a plot of $\ln \{\log \frac{V_t}{V_\infty}\}$ against the corresponding values of t will give a straight line, the slope of which will give an estimate of the pseudo first-order rate constant, *k*. The value of *k* can also be evaluated by fitting the observed data to equation 2.10 using an appropriate computer program (see section 2.6.4). It should be noted that to obtain *k* using this treatment, it is not required to know the value of V_O, and the reaction should be followed for at least ten half-lives to be sure that the reaction is close to completion and that the final voltage is steady at the end of each run.

2.6.3 The Stopped-flow Apparatus

The existing apparatus[128-130] was a modified form of the Gibson apparatus.[123] It was further upgraded for variable temperature work involving a large range of reaction half-lives (from several minutes to milliseconds), by extending the time range of the digital transient recorder, and improving the temperature control of the block containing the reaction chamber.

The apparatus is shown schematically in figure 2.2 and is described below.

The degassed reactant solutions were stored in two plastic gas-tight reservoir syringes (F). The two Hamilton gas-tight drive syringes (H) with teflon plungers and luer-tips, were filled with reactant solutions from the reservoir syringes by means of two three-way Hamilton valves.

The reactant solutions in the drive syringes were rapidly pushed into the mixing chamber (R) and then into the observation chamber (E) by means of a piston (G) thrust forward by nitrogen gas pressure (7 p.s.i.),
from a high pressure gas cylinder fitted with a regulator. The piston (G) was mounted with a threaded cylindrical mechanical stop which was wound (7 revolutions) back prior to each push, so that typically 0.2 cm^3 of solution from each of the drive syringes entered the observation chamber when the motion of the drive syringe plunges ceased.

The mixing chamber was an eight jet tangential mixer designed to minimize the mixing time.[128] The mixed solution reacted in the observation cell (E) of path length 2.0 cm which was contained between two well-sealed conical quartz windows so that the light beam passed along the direction of solution in the reaction observation cell. The observation cell was located very close to the mixing chamber to minimize dead time.

For low temperature work, a constant flow of dry nitrogen was maintained around the observation cell to prevent condensation of water vapour on the quartz windows. The drive syringes, mixing chamber, and reaction chamber were thermostted by circulating water (S) through the surrounding brass jacket from a constant temperature water bath. A constant temperature (±0.2 K) was maintained in the water bath using a digital thermostat (Julabo pc), and a refrigeration unit (Frigowatt Sarl). The temperature of the drive syringes was checked by a thermocouple (Fluke 51 K/J Thermometer).

Figure 2.2 Schematic diagram for the stopped-flow apparatus.

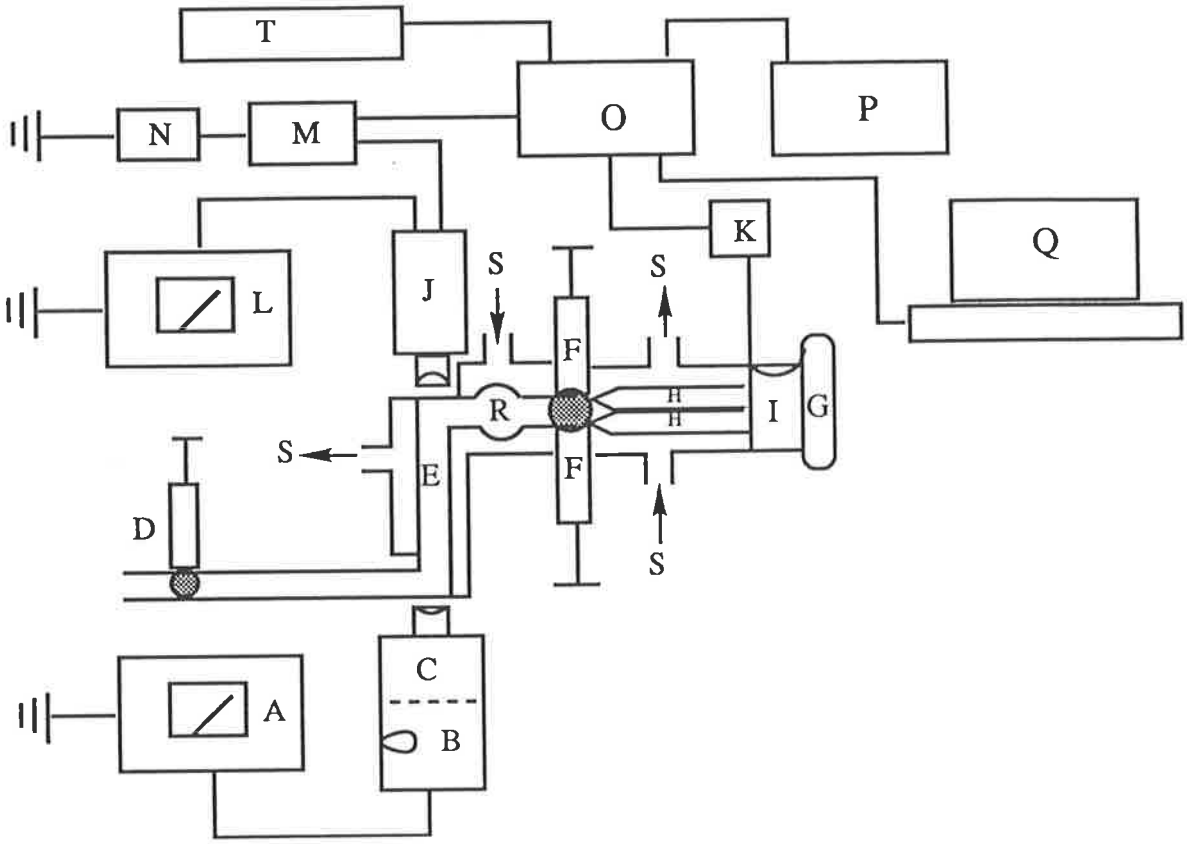

A = power supply to light source

B = light source

C = monochromator

D = syringe for waste solution

E = observation cell

F = reservoir syringes

G = nitrogen pressure push

H = drive syringes

I = trigger microswitch

J = photomultiplier tube

K = trigger voltage source

L = high tension power supply

M = back-off voltage supply and pre-amplifier

N = digital voltmeter

O = Datalab DL905

P = oscilloscope

Q = IBM personal computer

R = mixing chamber

S = water circulation

T = sweep time expander

The light from a stable D.C. light source (B), a tungsten lamp (Philips FCR A1/215), was passed through a high intensity (Bausch and Lomb) mono-chromator (C), grating 1350 Grooves/mm, with adjustable slits and iris, and finally through the reacting solution in the observation cell. The transmitted light from the solution entered an EMI 6256S photomultiplier tube (J) using only 7 dynodes, the anode voltage of which varied with the change of intensity of transmitted light during the course of the reaction. The entire mechanical components of the apparatus (including light source and photomultiplier tube) were constructed on a vibrationally insulated aluminium base plate.

Before each push, while retaining spent solution (from the previous experiment) in the observation cell, the voltage of the photomultiplier tube was backed-off using a back off voltage supply (M) and a voltmeter (N), usually to -3.50 volts for Ni^{2+}- and Cu^{2+}-systems, and -4.50 volts for Co^{2+}-system. The voltage from the high tension (L) power supply to the photomultiplier tube was usually within the range of 400 to 500 volts.

As each run was initiated, the piston (G) forced reactant solutions into the observation cell (via the mixing chamber) and the spent solution into the waste syringe (D), and the mechanical stop abruptly terminated the flow and simultaneously activated the microswitch (I) which triggered the data acquisition facilities. The signal output from the photomultiplier tube was fed into a pre-amplifier and then into the voltage input of a Datalab transient recorder, DL905 (O). The recorder was connected to a timer, a sweep time expander (T), to allow the collection of data up to a period of 9.99×10^3 s, and to an oscilloscope (P,

Telequipment S61) to view the reaction trace in order to assess the suitability of data for storage and analysis using an IBM personal computer (Q).

2.6.4 Data Storage and Analysis

Acceptable exponential reaction voltage traces with minimum noise (free from any effect due to air bubbles in the reaction chamber or other interferences), as viewed on the oscilloscope screen, were transferred from the transient recorder memory into the IBM personal computer. Typically seven to twelve reproducible traces for each sample solution were computer averaged to improve the signal to noise ratio. The computer averaged reaction traces (catted traces) were fitted to the first-order rate equation (2.11), using a nonlinear least square fitting subroutine[131] modified for a SUN 3/60 workstation[132] to give the value of the first-order rate constant.

$$y = B_1 \exp(-B_2 t) \qquad (2.11)$$

where

$$y = \log \frac{V_t}{V_\infty} ,$$

$$B_1 = \log \frac{V_0}{V_\infty} , \text{ and}$$

B_2 = the first-order rate constant.

Finally, the observed first-order rate constants for different concentrations of reacting species were fitted to appropriate models of reaction schemes using the least square best fit program.[133-135]

CHAPTER 3

DETERMINATION OF STABILITY CONSTANTS

3.1 Introduction

The thermodynamic aspects of the interaction of metal ions with tetraaza macrocyclic ligands have been studied extensively [see section 1.2], especially to investigate the origin of the macrocyclic effect and also to compare the relative stabilities of metal complexes of related macrocyclic ligands. A variety of methods[10] has been used to determine the stability constants of macrocyclic complexes.

The formation of a simple 1:1 complex of a divalent metal ion (M^{2+}) with a macrocyclic ligand (L) can be illustrated by equation 3.1 (charges and protons are omitted for simplicity),

$$M + L \underset{}{\overset{K_{ML}}{\rightleftharpoons}} ML \qquad (3.1)$$

and the concentration stability constant (K_{ML}) for the reaction 3.1 is given by equation 3.2,

$$K_{ML} = \frac{[ML]}{[M]\,[L]} \qquad (3.2)$$

where [ ] indicates the equilibrium concentration of the enclosed species.

The tetraaza macrocyclic ligands have four protonatable nitrogen atoms. Thus the potentiometric titration method using a pH electrode has been chosen for the determination of stability constants of metal-THEC complexes.

The determination of stability constants of metal complexes by potentiometric titration using a pH electrode is based on the competition of protons and metal ions for the ligand donor atoms. Initially the value of the standard electrode potential (E_o) of the pH electrode, and the pK_w value of water are determined by the titration of a solution of strong acid with a solution of strong base (without adding metal or ligand) while measuring E.M.F of the pH electrode.

The determination of pK_a values for the ligand involves the titration, under identical conditions to the above titration, of a solution of protonated ligand with a solution of strong base while measuring the E.M.F. of the pH electrode. The pK_a values of the ligand can be evaluated from the titration data, known values of E_o and pK_w, using the program MINIQUAD.[121]

Similarly, in the determination of stability constants of metal complexes, an acidic solution of the ligand containing an approximately equal amount of the metal ion is titrated with a solution of strong base. The stability constants are then evaluated from the titration data, known values of E_o, pK_w, and pK_a, using the same program MINIQUAD.

3.2 Results and Discussion

3.2.1 Acid Dissociation Constants of THEC

When an acidic solution of THEC is titrated with a solution of strong base, the pH is increased and the ligand is gradually deprotonated. The equilibria among the protonated species of THEC can be illustrated by equations 3.3a to 3.3d (where L= THEC),

$$LH_4^{4+} \overset{K_{a4}}{\rightleftharpoons} LH_3^{3+} + H^+ \qquad (3.3a)$$

$$LH_3^{3+} \overset{K_{a3}}{\rightleftharpoons} LH_2^{2+} + H^+ \qquad (3.3b)$$

$$LH_2^{2+} \overset{K_{a2}}{\rightleftharpoons} LH^+ + H^+ \qquad (3.3c)$$

$$LH^+ \overset{K_{a1}}{\rightleftharpoons} L + H^+ \qquad (3.3d)$$

where the equilibrium constants K_{a1}, K_{a2}, K_{a3}, and K_{a4} are the first, second, third, and fourth acid dissociation constants of THEC, and can be defined by a general equation 3.4.

$$K_{an} = \frac{[LH_{n-1}^{(n-1)+}]\,[H^+]}{[LH_n^{n+}]} \qquad (3.4)$$

At the pH when the concentrations of the two species $[LH_n^{n+}]$ and $[LH_{n-1}^{(n-1)+}]$ in the n^{th} equilibrium step are equal, the pK_{an} for the n^{th} equilibrium step is equal to that pH. The titration curve for the

determination of pK_a of THEC is shown in Figure 3.1 and the pK_a values evaluated from the titration data are shown in Table 3.1. For comparison, the pK_a values of cyclam, TMC, and THEC at various ionic strengths collected from the literature are also shown in Table 3.1.

Table 3.1 The pK_a values of THEC, TMC, and cyclam at 298.2 K and various ionic strengths.

Ligand	pK_{a1}	pK_{a2}	pK_{a3}	pK_{a4}
THEC[a]	9.25 (±0.02)	8.79 (±0.03)	3.31 (±0.06)	2.88 (±0.03)
THEC[b]	8.80	8.24	2.69	~1.20
THEC[c]	8.83	8.30	2.65	< 2.0
TMC[d]	9.70	9.31	3.09	2.64
cyclam[d]	11.59	10.62	1.61	2.42

[a] I = 1.50 mol dm^{-3} $NaNO_3$.[present work] Values in parentheses are standard errors in log units determined from four independent titrations

[b] I = 0.1 mol dm^{-3} $NaNO_3$.[23]

[c] I = 0.1 mol dm^{-3} $NaClO_4$.[24]

[d] I = 0.5 mol dm^{-3} KNO_3.[32]

From Table 3.1, it is evident that the protonation constants of THEC are increased with the increase in concentration of inert electrolyte, and it also indicates that the increased concentration of inert

electrolyte stabilizes the higher charged species compared to lower charged ones.

3.2.2 Stability Constants of Metal Complexes of THEC

The potentiometric titration curves for the determination of stability constants of metal-THEC complexes ($[M(THEC)]^{2+}$ and $[M(THEC-H)]^{+}$) are shown in Figures 3.2, 3.3, and 3.4 for Cu^{2+}, Ni^{2+}, and Co^{2+}, respectively, and each overlayed on the pK_a curve of THEC. From these titration data, the stability constants, $\log\beta_{110}$ and $\log\beta_{11\text{-}1}$, respectively for the reactions 3.5 and 3.6 (where M = Cu^{2+}, Ni^{2+}, and Co^{2+}), have been evaluated and are shown in Table 3.2.

$$M^{2+} + THEC \overset{\beta_{110}}{\rightleftharpoons} [M(THEC)]^{2+} \qquad (3.5)$$

$$\text{where} \quad \beta_{110} = \frac{[M(THEC)^{2+}]}{[M^{2+}]\,[THEC]} \qquad (3.5a)$$

$$M^{2+} + THEC \overset{\beta_{11\text{-}1}}{\rightleftharpoons} [M(THEC\text{-}H)]^{+} + H^{+} \qquad (3.6)$$

$$\text{where} \quad \beta_{11\text{-}1} = \frac{[M(THEC\text{-}H)^{+}]\,[H^{+}]}{[M^{2+}]\,[THEC]} \qquad (3.6a)$$

Four titrations for each system were carried out with varying concentration of metal ions to check the stoichiometry of the complexes. In all cases, experimental data were found to be consistent with 1:1 complex formation and the evaluated stability constants were reproducible between repeat experiments within the experimental error.

Figure 3.1 Potentiometric equilibrium curve for the titration of an acidic solution (10 cm^3) of THEC with NaOH at 298.2(±0.2) K and ionic strength 1.50 mol dm^{-3} $NaNO_3$.

[THEC] = 1.00 x 10^{-3} mol dm^{-3}.

[H^+] = 4.0 x 10^{-3} mol dm^{-3}.

[NaOH] = 0.10 mol dm^{-3}.

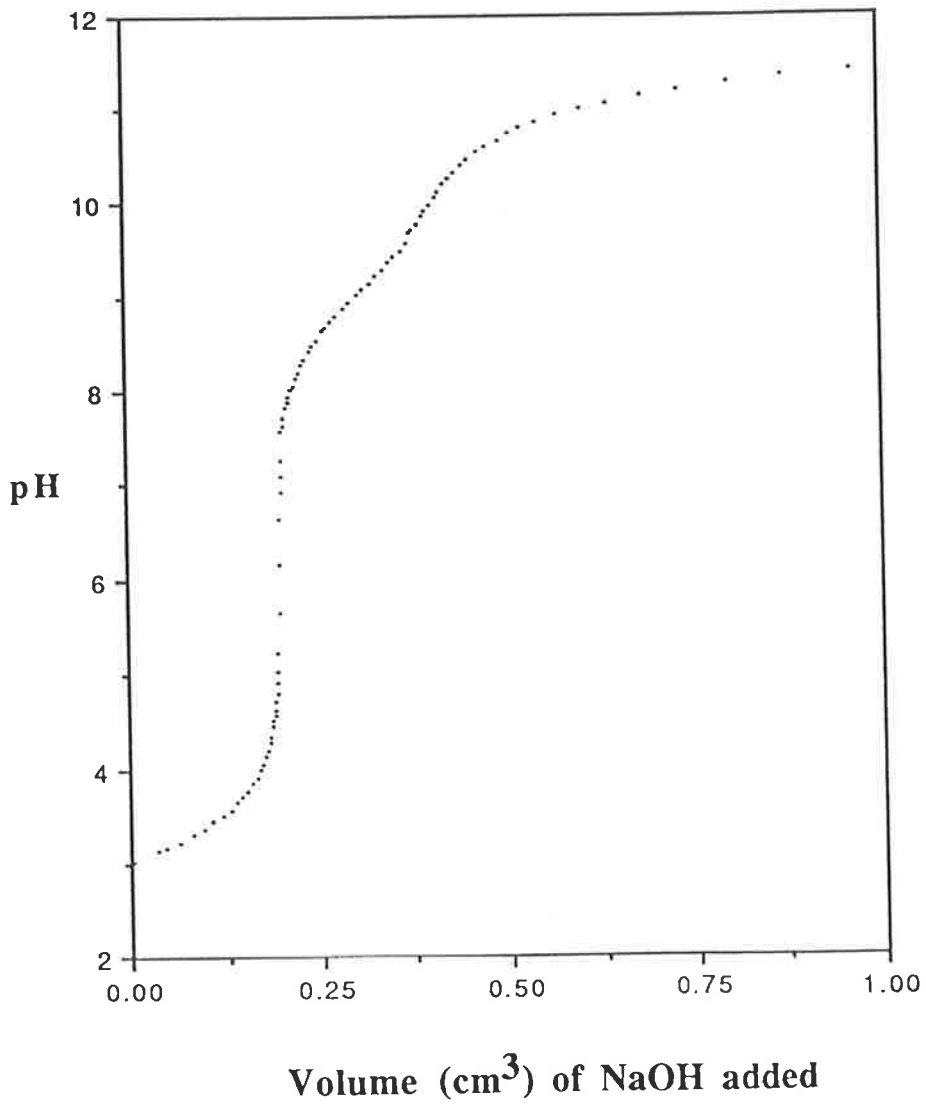

Figure 3.2 Potentiometric equilibrium curves for the titration of acidic solutions containing:

(a) 10 cm^3 of THEC (1.00 x 10^{-3} mol dm^{-3}, $[H^+]$ = 4.0 x 10^{-3} mol dm^{-3}), and

(b) 0.090 cm^3 of $[Cu(H_2O)_6]^{2+}$ (0.1011 mol dm^{-3}) and 10 cm^3 of THEC (1.00 x 10^{-3} mol dm^{-3}, $[H^+]$ = 4.0 x 10^{-3} mol dm^{-3}), with NaOH (0.10 mol dm^{-3}) at 298.2(±0.2) K and ionic strength 1.50 mol dm^{-3} $NaNO_3$.

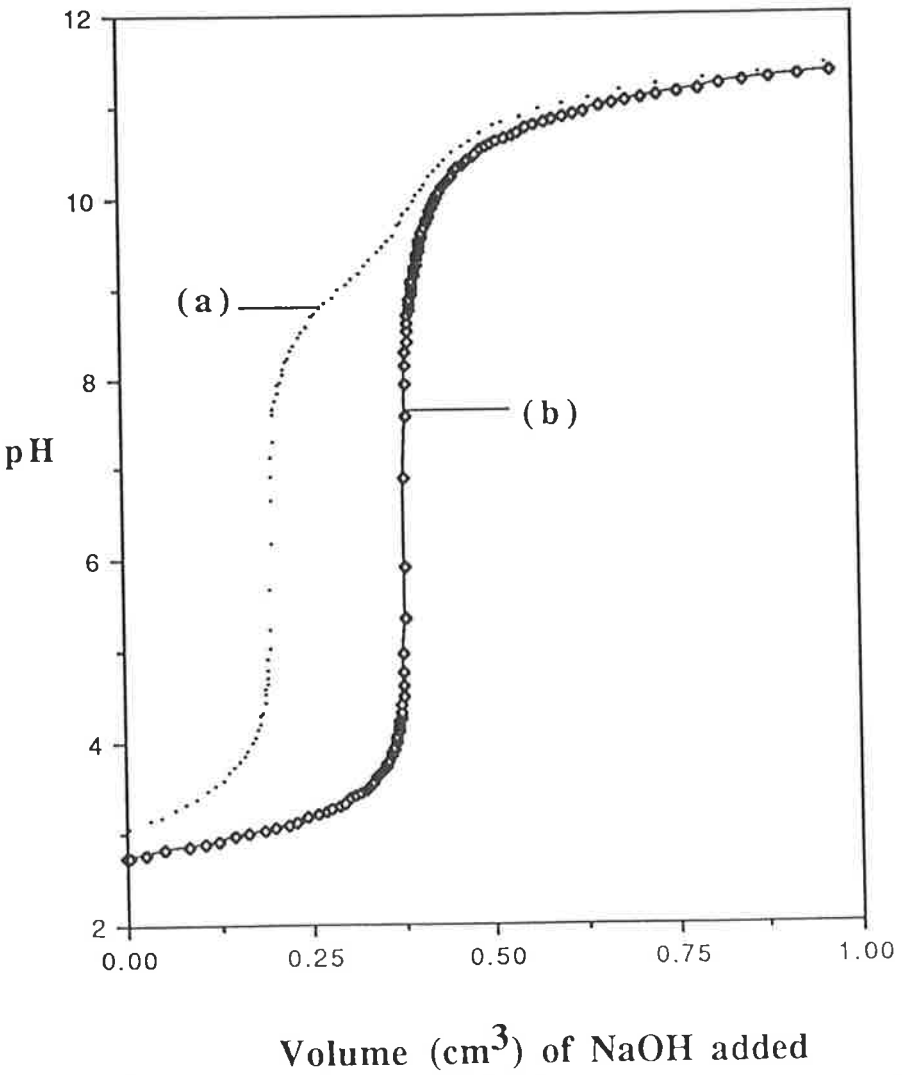

Figure 3.3 Potentiometric equilibrium curves for the titration of acidic solutions containing:

(a) 10 cm^3 of THEC (1.00 x 10^{-3} mol dm^{-3}, $[H^+]$ = 4.0 x 10^{-3} mol dm^{-3}), and

(b) 0.090 cm^3 of $[Ni(H_2O)_6]^{2+}$ (0.1022 mol dm^{-3}) and 10 cm^3 of THEC (1.00 x 10^{-3} mol dm^{-3}, $[H^+]$ = 4.0 x 10^{-3} mol dm^{-3}), with NaOH (0.10 mol dm^{-3}) at 298.2(±0.2) K and ionic strength 1.50 mol dm^{-3} $NaNO_3$.

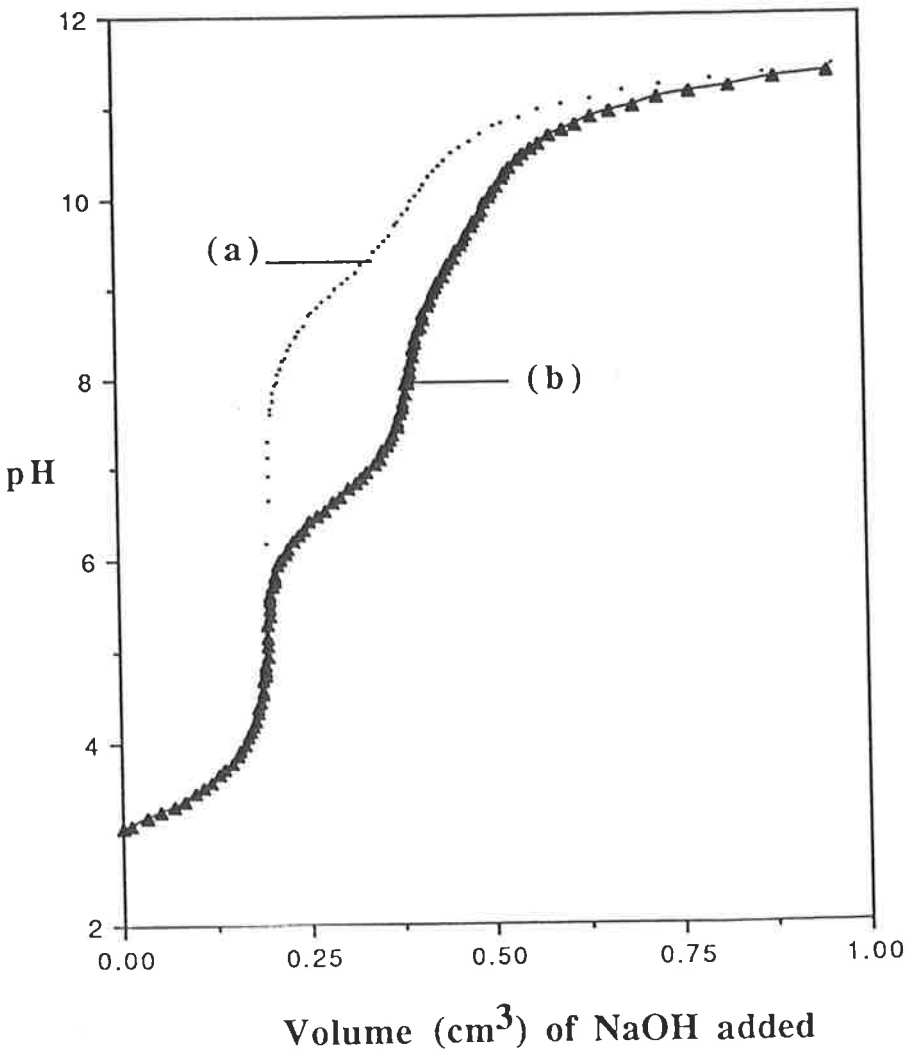

Figure 3.4 Potentiometric equilibrium curves for the titration of acidic solutions containing:

(a) 10 cm^3 of THEC (1.00 x 10^{-3} mol dm^{-3}, $[H^+]$ = 4.0 x 10^{-3} mol dm^{-3}), and

(b) 0.090 cm^3 of $[Co(H_2O)_6]^{2+}$ (0.1021 mol dm^{-3}) and 10 cm^3 of THEC (1.00 x 10^{-3} mol dm^{-3}, $[H^+]$ = 4.0 x 10^{-3} mol dm^{-3}), with NaOH (0.10 mol dm^{-3}) at 298.2(±0.2) K and ionic strength 1.50 mol dm^{-3} $NaNO_3$.

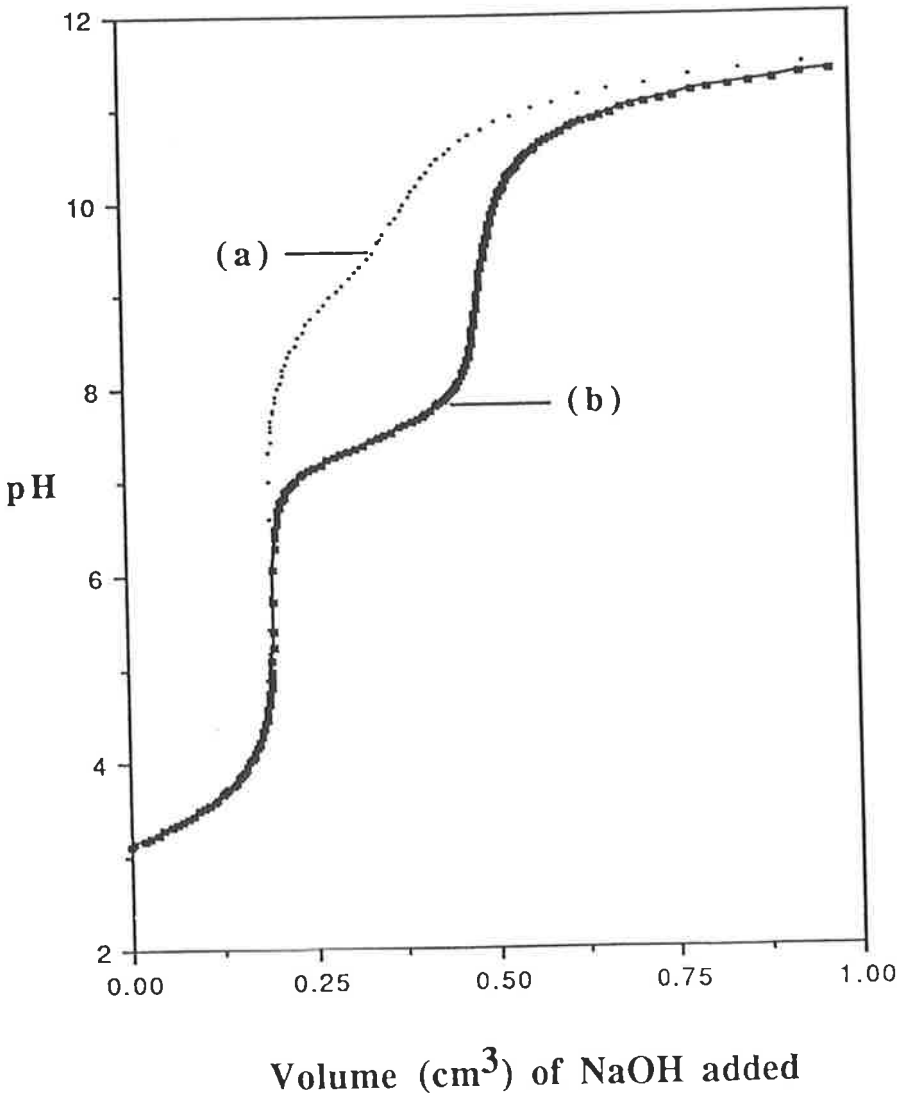

For comparison with the literature values[24] (see Table 3.2), the $pK_{a(ML)}$ values for the reaction 3.7,

$$[M(THEC)]^{2+} \overset{K_{a(ML)}}{\rightleftharpoons} [M(THEC\text{-}H)]^{+} + H^{+} \qquad (3.7)$$

$$\text{where } K_{a(ML)} = \frac{[M(THEC\text{-}H)^{+}]\,[H^{+}]}{[M(THEC)^{2+}]} \qquad (3.7a)$$

have been calculated for all three systems simply by subtracting equation 3.5 from equation 3.6, that is, by equation 3.8a.

$$\log K_{a(ML)} = \log\beta_{11\text{-}1} - \log\beta_{110} \qquad (3.8)$$

or,
$$pK_{a(ML)} = -(\log\beta_{11\text{-}1} - \log\beta_{110}) \qquad (3.8a)$$

The value of pK_W at 298.2 K and ionic strength 1.50 mol dm^{-3} $NaNO_3$ evaluated from calibration titrations is 13.7(±0.05). This observed value is not equal to the standard pK_W value(14.0) for pure water at 298.2 K. This discrepancy is probably due to the ion associations, e.g., NO_3^- with H^+, and Na^+ with OH^- since the experimental ionic strength is very high.

For comparison with the literature values[23] (see Table 3.2), the values of $\log K_{(MLOH)}$ for the reactions 3.9a,

$$[M(THEC)]^{2+} + OH^{-} \overset{K_{(MLOH)}}{\rightleftharpoons} [M(THEC\text{-}H)]^{+} + H_2O \qquad (3.9a)$$

$$\text{where} \qquad K_{(MLOH)} = \frac{[M(THEC\text{-}H^{+})]}{[M(THEC)^{2+}]\,[OH^{-}]} \qquad (3.9b)$$

have been calculated by subtracting $pK_{a(ML)}$ values from the determined pK_W value (13.7). That is, by equation 3.10 (since both the terms, $[M(LOH)^+]$ used by *Hancock et al.*[23]*a* and $[M(L\text{-}H)^+]$ used in equation 3.9b, represent the same mono-deprotonated complex species, and the term $[H_2O]$ is omitted from equation 3.9b as it remains constant).

$$\begin{aligned} \log K_{(MLOH)} &= pK_W - pK_{a(ML)} \\ &= 13.7 - pK_{a(ML)} \end{aligned} \qquad (3.10)$$

The values of $pK_{a(ML)}$ and $\log K_{(MLOH)}$ are also shown in the Table 3.2. From the comparison of the values of stability constants of different complex species in different ionic strengths (Table 3.2), it is difficult to interpret the effect of ionic strength on the stability constants of metal-THEC complexes. For example, the values of $\log\beta_{110}$ for $[Cu(THEC)]^{2+}$ and $[Ni(THEC)]^{2+}$ are increased by 0.5 compared to the literature[24] values whereas in the case of $[Co(THEC)]^{2+}$ it is decreased by 0.23 compared to the literature values.[23] Such differences may arise either from the effect of ionic strength (the effect of ionic strength on different systems are not always consistent [147]) or from experimental errors.

a Although *Hancock et al.* have used the equation, $ML + OH^- = [M(LOH)]^+$, they have mentioned that the species, $[MLOH]^+$, is formed, in fact, not by the addition of a -OH group but by the removal of a proton from the OH group bonded to the metal ion.

Table 3.2 The values of $\log\beta_{110}$, $\log\beta_{11\text{-}1}$, $pK_{a(ML)}$, and $\log K_{(MLOH)}$ of the metal-THEC complexes at 298.2 K and various ionic strengths.

M^{2+}	$\log\beta_{110}$	$\log\beta_{11\text{-}1}$	$pK_{a(ML)}$	$\log K_{(MLOH)}$
Cu^{2+}	16.7[a] (±0.1) 16.2[b] 15.7[c]	6.60[a] (±0.1)	10.1[a]	3.6[a]
Ni^{2+}	7.96[a] (±0.06) 7.45[b] 7.31[c]	-1.26[a] (±0.07) -1.42[b]	9.22[a] 8.87[b]	4.48[a] 5.01[c]
Co^{2+}	5.87[a] (±0.08) 6.10[c]	-0.945[a] (±0.06)	6.82[a]	6.88[a] 6.85[c]

[a] I = 1.50 mol dm^{-3} $NaNO_3$.[present work] Values in parentheses are standard errors in log units determined from four independent titrations

[b] I = 0.1 mol dm^{-3} $NaNO_3$.[24]

[c] I = 0.1 mol dm^{-3} $NaNO_3$.[23]

3.2.3 Speciation Diagrams for THEC and its Metal Complexes

The variations in percentage composition of different species of THEC and its metal complexes in solution with pH have been illustrated by speciation diagrams in Figures 3.5, 3.6, 3.7, and 3.8, respectively for THEC, and its complexes of Cu^{2+}, Ni^{2+}, and Co^{2+}. The data points shown for the various species are calculated from the values of equilibrium constants (Table 3.2) using a Macintosh version of the program SPE.[136] The concentration of THEC used in the species calculation is 1.00×10^{-3} mol dm^{-3}. For metal-THEC complexes (molar ratio of metal and ligand is 1:1), the concentrations of metal ions (and those of THEC) used in the species calculations are 1.00×10^{-3} mol dm^{-3}, 3.00×10^{-3} mol dm^{-3}, and 5.00×10^{-3} mol dm^{-3} respectively for Cu^{2+}, Ni^{2+}, and Co^{2+} systems. The concentrations were chosen to be similar to those used in the stopped flow kinetics experiments.

Figure 3.5 indicates that at low pH values both $THECH_4^{4+}$ and $THECH_3^{3+}$ are the predominant species and that their concentrations are equal at pH 2.88 which represents the value of pK_{a4}. As the pH increases, the concentration of $[THECH_2^{2+}]$ also gradually increases. At pH 3.31, the concentrations of both $[THECH_3^{3+}]$ and $[THECH_2^{2+}]$ are equal, corresponding to pK_{a3}. In the pH range of 4 to 7, $THECH_2^{2+}$ is the predominant species. The formation of $THECH^+$ starts at about pH 6, and the concentrations of both $[THECH_2^{2+}]$ and $[THECH^+]$ species are equal at pH 8.79 which is the value of pK_{a2}. The free ligand, THEC, is predominant in the pH range above 11 and the concentrations of both $[THECH^+]$ and [THEC] are equal at pH 9.25, corresponding to pK_{a1}.

On the other hand from Figures 3.6 to 3.8, it is evident that depending on the magnitude of the stability constants of the metal complexes, formation of $[M(THEC)]^{2+}$ species starts at various pH values. Formation of $[Cu(THEC)]^{2+}$ starts at very low pH and reaches a maximum at pH 6.1, $[Ni(THEC)]^{2+}$ starts at about pH 4.5, and reaches a maximum at pH 7.8, and $[Co(THEC)]^{2+}$ starts at about pH 5.5 and reaches a maximum at pH 7.2.

The formation of $[M(THEC\text{-}H)]^{+}$ species starts at higher pH, viz., $[Cu(THEC\text{-}H)]^{+}$ at pH~6.8, $[Ni(THEC\text{-}H)]^{+}$ at pH~6.5, and $[Co(THEC\text{-}H)]^{+}$ at pH~6.0. The concentrations of the complex species, $[M(THEC)^{2+}]$ and $[M(THEC\text{-}H)^{+}]$, are equal at pHs 10.1, 9.22, and 6.82 respectively for Cu^{2+}, Ni^{2+}, and Co^{2+} corresponding to the respective $pK_{a(ML)}$ values shown in table 3.2.

The concentrations of different species of THEC and its metal complexes have been considered to select the pH range and the appropriate buffers for the determination of the formation rate constants of particular metal complexes (see chapter 4).

Figure 3.5 Distribution plots for different species of THEC (as a percentage of total concentration of THEC) at 298.2 (±0.2) K and ionic strength 1.50 mol dm^{-3} $NaNO_3$ as a function of pH.

Total [THEC] = 1.00 x 10^{-3} mol dm^{-3}.

(A) $THECH_4^{4+}$, (B) $THECH_3^{3+}$,
(C) $THECH_2^{2+}$, (D) $THECH^{+}$, and
(E) THEC.

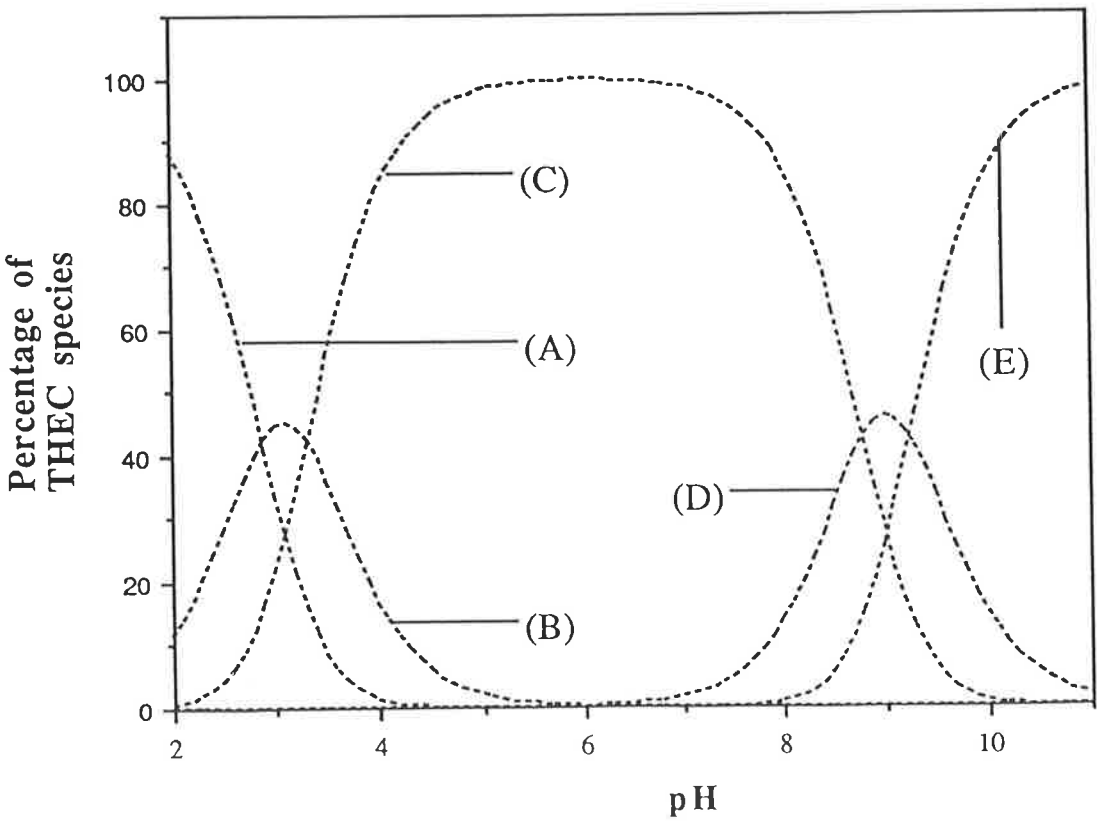

Figure 3.6 Distribution plots for different species of complexes (as a percentage of total concentration of metal ion) formed from $[Cu(H_2O)_6]^{2+}$ and THEC at 298.2 (±0.2) K and ionic strength 1.50 mol dm^{-3} $NaNO_3$, as a function of pH.

Total $[Cu(H_2O)_6^{2+}] = 1.00 \times 10^{-3}$ mol dm^{-3}.

Total [THEC] = 1.00×10^{-3} mol dm^{-3}.

(A) $[Cu(H_2O)_6]^{2+}$,

(B) $[Cu(THEC)]^{2+}$, and

(C) $[Cu(THEC\text{-}H)]^{+}$.

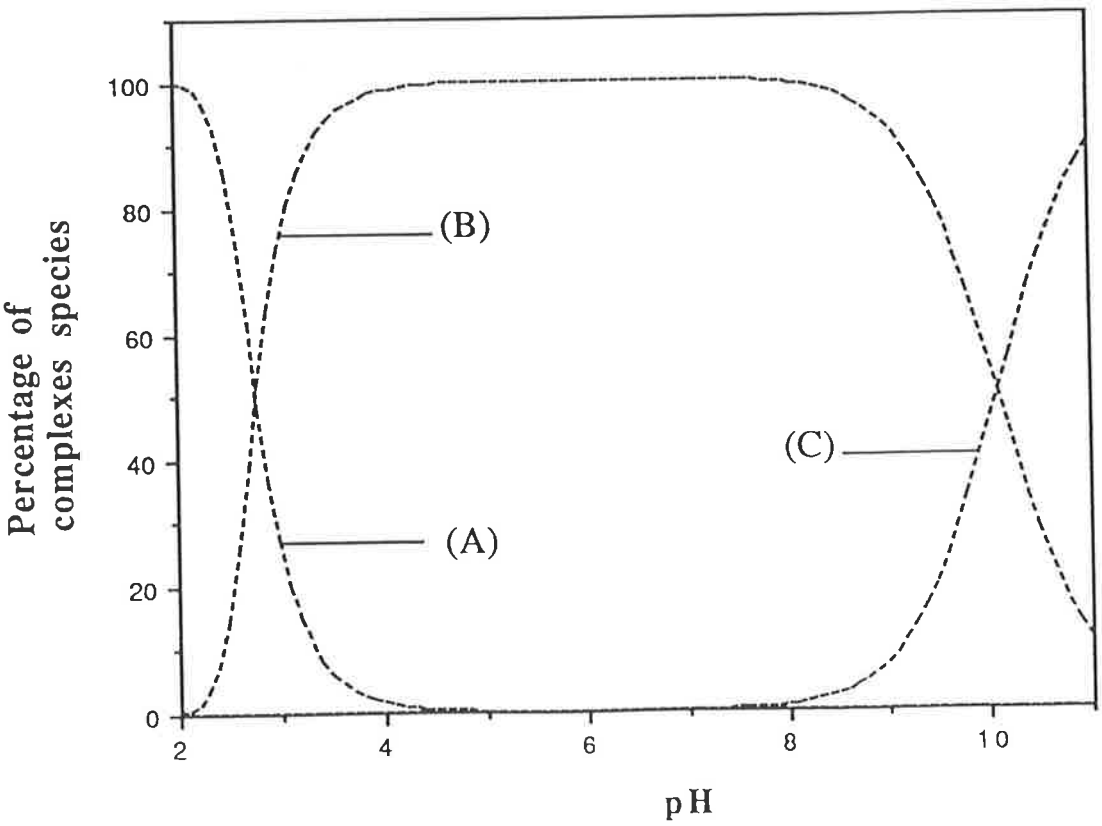

Figure 3.7 Distribution plots for different species of complexes (as a percentage of total concentration of metal ion) formed from $[Ni(H_2O)_6]^{2+}$ and THEC at 298.2 (±0.2) K and ionic strength 1.50 mol dm^{-3} $NaNO_3$, as a function of pH.

Total $[Ni(H_2O)_6^{2+}] = 3.00 \times 10^{-3}$ mol dm^{-3} .

Total [THEC] = 3.00×10^{-3} mol dm^{-3}.

(A) $[Ni(H_2O)_6]^{2+}$,

(B) $[Ni(THEC)]^{2+}$, and

(C) $[Ni(THEC\text{-}H)]^{+}$.

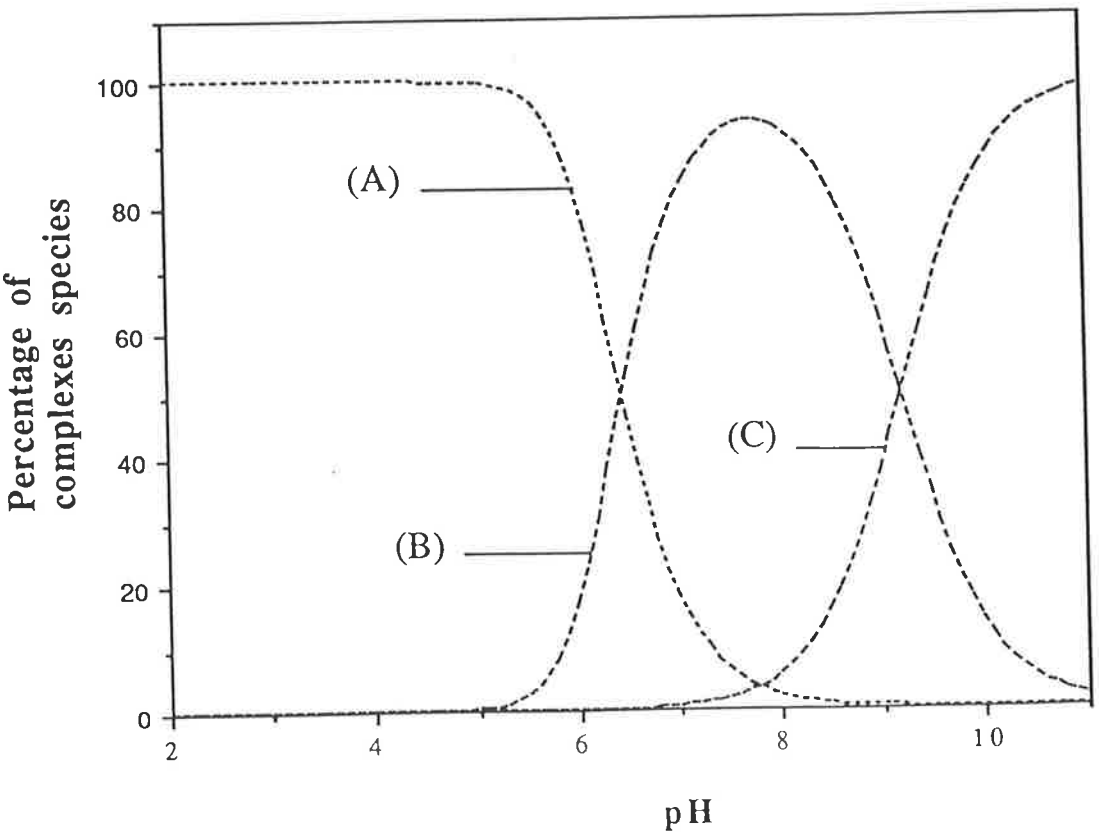

Figure 3.8 Distribution plots for different species of complexes (as a percentage of total concentration of metal ion) formed from $[Co(H_2O)_6]^{2+}$ and THEC at 298.2 (±0.2) K and ionic strength 1.50 mol dm^{-3} $NaNO_3$, as a function of pH.

Total $[Co(H_2O)_6^{2+}] = 5.00 \times 10^{-3}$ mol dm^{-3}.

Total [THEC] = 5.00×10^{-3} mol dm^{-3}.

(A) $[Co(H_2O)_6]^{2+}$,

(B) $[Co(THEC)]^{2+}$, and

(C) $[Co(THEC\text{-}H)]^{+}$.

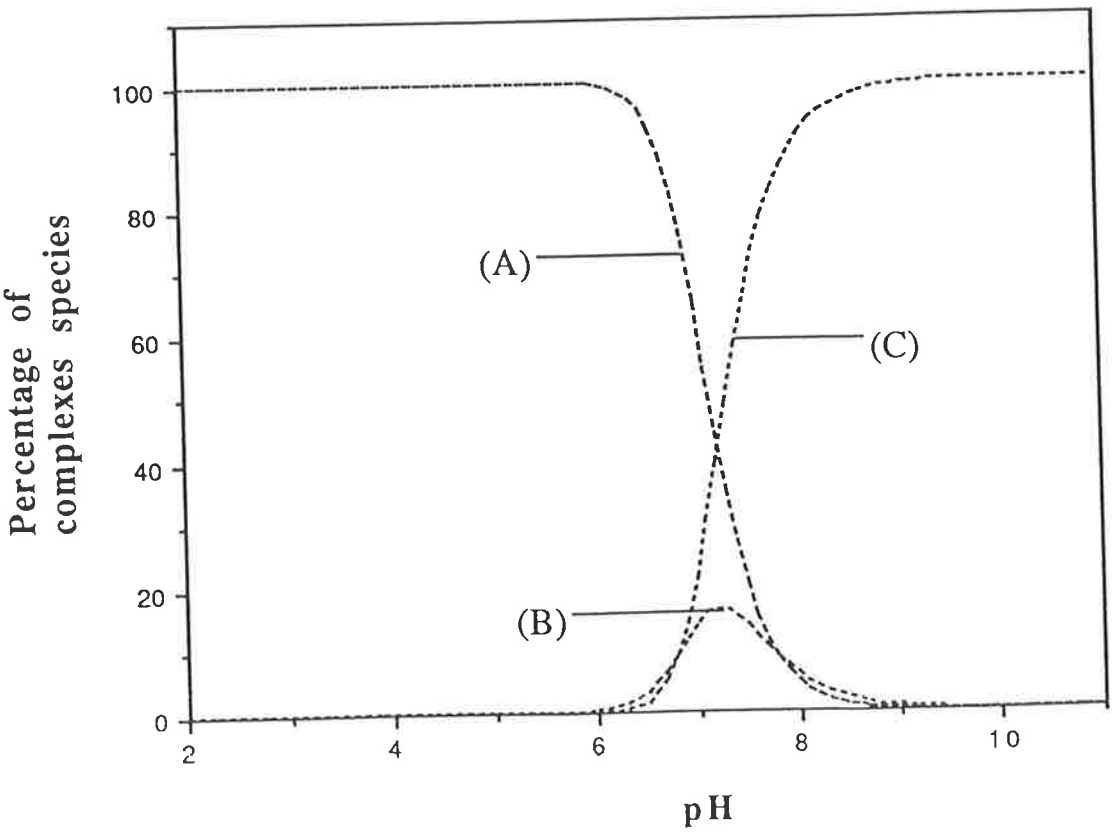

CHAPTER 4

KINETIC STUDIES ON THE COMPLEXATION OF METAL IONS

4.1 Introduction

A typical complexation reaction of a divalent metal ion, $[M(H_2O)_6]^{2+}$, with a monodentate ligand, L (equation 4.1), can be compared with a typical ligand substitution reaction (equation 4.2),[105]

$$[M(H_2O)_6]^{2+} + L \longrightarrow [M(H_2O)_5L]^{2+} + H_2O \quad (4.1)$$

$$M\text{-}X + Y \longrightarrow M\text{-}Y + X \quad (4.2)$$

where X is a leaving group and Y is an entering group in the substitution reaction 4.2. Similarly, H_2O is the leaving group from the aquo-metal ion complex ($[M(H_2O)_6]^{2+}$), and the ligand, L, is the entering group in the complexation reaction 4.1. When X = Y = L = H_2O, equations 4.1 and 4.2 describe a water exchange reaction. Thus, in aqueous solutions, the rates of complexation reactions, mainly with monodentate ligands, frequently depend on the characteristic water exchange rates.[1,101,103] In the case of tetraaza macrocyclic ligands, particularly due to their configuration and the existence of various protonated species, the rates of

complexation of metal ions are much slower than the characteristic water exchange rates (see section 1.3).

However, *Hay et al.*[22] reported that due to the attachment of 2-hydroxyethyl pendant arms to cyclam the resulting metal complexes of THEC were more labile than those of cyclam. It was also reported by *Madeyski et al.*[23] that the pendant arm donor groups form a point of initial attachment for the metal ion followed by the insertion of the metal ion into the macrocyclic cavity, thus causing a rapid metalation reaction compared with those of cyclam or TMC. In fact, the rates of complexation of metal ions with THEC were not studied quantitatively and systematically by the above authors. Hence, the exact role of pendant arms on the rate of complexation was not clear. Thus the present studies on the complexation of $[Ni(H_2O)_6]^{2+}$ and $[Co(H_2O)_6]^{2+}$ ions with THEC are intended to give insight into the role of the 2-hydroxyethyl pendant arms in determining the rate of complexation and in the mechanistic pathway.

4.2 Results

4.2.1 Visible Spectra of Metal Complexes of THEC in Buffered Aqueous Solution

The visible spectra of metal complexes of THEC (with 1:1 molar ratio of metal to ligand) in aqueous solution in the presence of buffer (PIPES), at pH 6.8 and 7.4, 298.2 (±0.2) K, and ionic strength of 1.50 mol dm^{-3} adjusted with $NaNO_3$, are shown in Figures 4.1 and 4.2 for $[Ni(THEC)]^{2+}$ and $[Co(THEC)]^{2+}$ respectively. The visible spectra of

the respective aquo-metal ions, $[M(H_2O)_6]^{2+}$, at pH 6.8 under identical conditions are also shown. The values of maximum molar absorptivities, $\varepsilon_{max.}$ ($dm^3\ mol^{-1}\ cm^{-1}$), of these complexes are shown in Table 4.1. The wavelengths selected to monitor the formation of the $[Ni(THEC)]^{2+}$ and $[Co(THEC)]^{2+}$ in stopped-flow kinetic studies were 365 nm and 550 nm respectively, where the differences in molar absorptivities between $[M(THEC)]^{2+}$ and $[M(H_2O)_6]^{2+}$ have their maximum values.

$[M(THEC)]^{2+}$	pH	$\varepsilon_{max.}$ ($dm^3\ mol^{-1}\ cm^{-1}$)	λ (nm)
$[Ni(THEC)]^{2+}$	6.8	29.2	366
		12.9	588
	7.4	30.5	366
		13.4	588
$[Co(THEC)]^{2+}$	6.8	15.1	488
		14.9	538
	7.4	24.4	488
		23.7	538

Figure 4.1 The variation of molar absorptivity, ε ($dm^3\ mol^{-1}\ cm^{-1}$), as a function of wavelength, λ (nm), in aqueous solution in the presence of buffer (PIPES), at 298.2 (±0.2) K and ionic strength of 1.50 mol dm^{-3} $NaNO_3$:

(a) $[Ni(THEC)]^{2+}$ at pH 7.4,
(b) $[Ni(THEC)]^{2+}$ at pH 6.8, and
(c) $[Ni(H_2O)_6]^{2+}$ at pH 6.8.

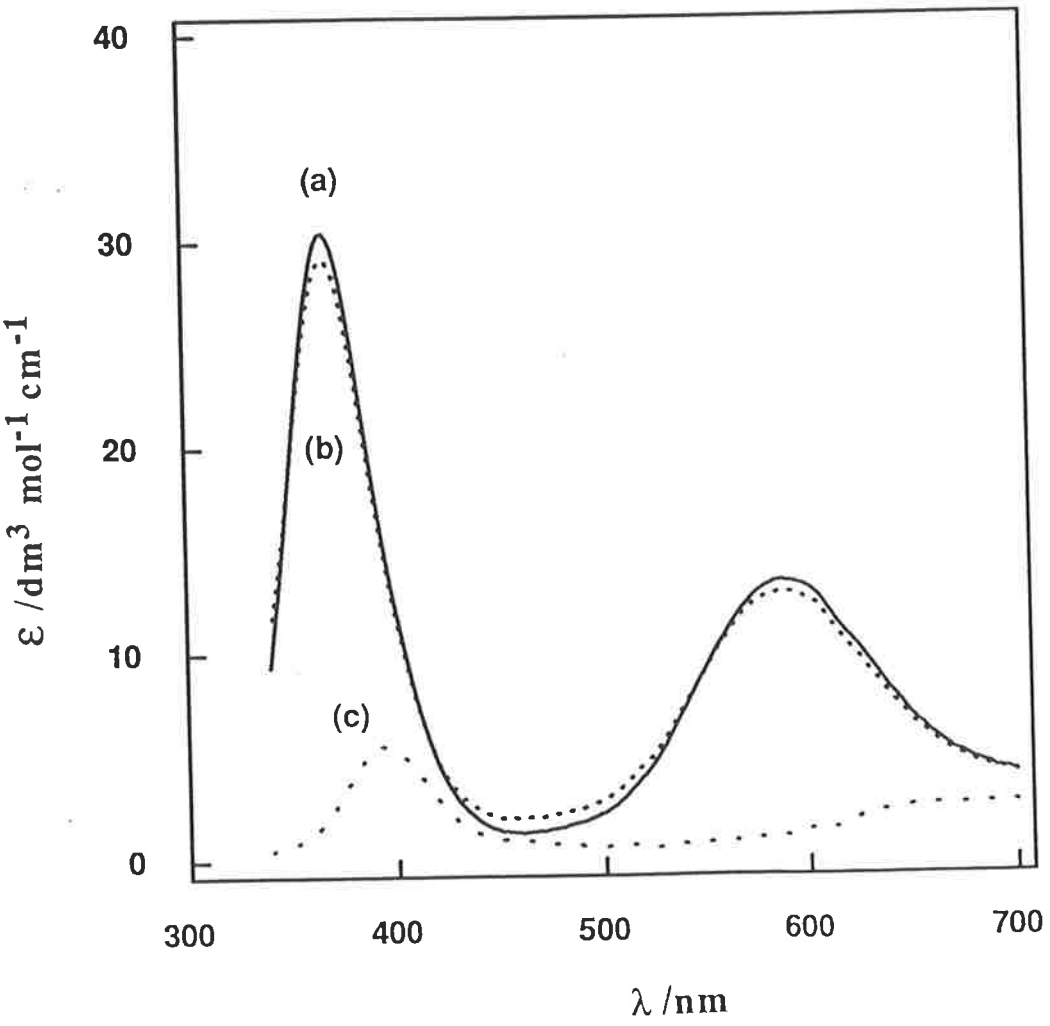

Figure 4.2 The variation of molar absorptivity, ε ($dm^3\ mol^{-1}\ cm^{-1}$), as a function of wavelength, λ (nm), in aqueous solution in the presence of buffer (PIPES), at 298.2 (±0.2) K and ionic strength of 1.50 mol dm^{-3} $NaNO_3$:

(a) $[Co(THEC)]^{2+}$ at pH 7.4,
(b) $[Co(THEC)]^{2+}$ at pH 6.8, and
(c) $[Co(H_2O)_6]^{2+}$ at pH 6.8.

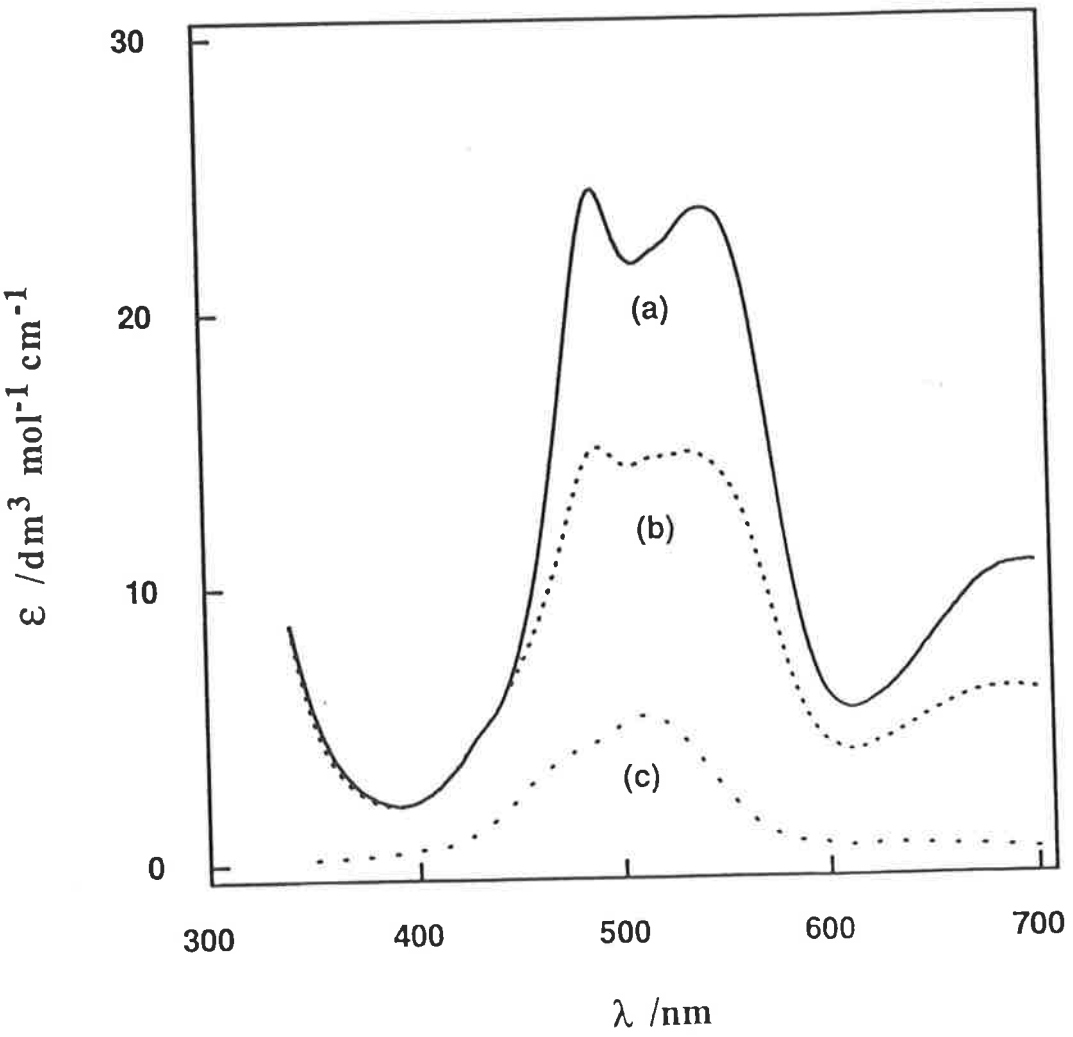

4.2.2 The Kinetics of Complexation

The rates of complexation of $[Ni(H_2O)_6]^{2+}$ and $[Co(H_2O)_6]^{2+}$ with THEC were studied under pseudo first-order conditions (more than 10 fold excess concentration of metal ions compared to the concentrations of THEC). The fixed concentrations of THEC used were 1.5×10^{-3} mol dm^{-3} and 2.5×10^{-3} mol dm^{-3} for the complexation of $[Ni(H_2O)_6]^{2+}$ and $[Co(H_2O)_6]^{2+}$ respectively. The observed values of the pseudo first-order rate constant, $k_{obs.}(s^{-1})$, for the complexation of $[Ni(H_2O)_6]^{2+}$ and $[Co(H_2O)_6]^{2+}$ in different concentrations of excess metal ions, $[M(H_2O)_6^{2+}]_{ex.}$ (mol dm^{-3}), at pH 6.8, 298.2 (±0.2) K and ionic strength of 1.50 mol dm^{-3} $NaNO_3$ are shown in Tables 4.2 and 4.3 respectively. It is to be noted that all magnitudes used for the concentrations of different components throughout this chapter represent the concentration of the respective component in the reaction chamber, i.e., after mixing.

The rates of complexation of $[Ni(H_2O)_6]^{2+}$ with THEC over a limited range of pH values were also studied under pseudo first-order conditions at 298.2 (±0.2) K and ionic strength of 1.50 mol dm^{-3} $NaNO_3$ while the concentrations of THEC and $[Ni(H_2O)_6]^{2+}$ were kept constant at 1.5×10^{-3} mol dm^{-3} and 7.5×10^{-2} mol dm^{-3} respectively. (The pH range was constrained at the low end by the decreased amount of complex formed and the resulting small absorbance change, and at the high end by precipitation of $Ni(OH)_2$.) The values of the pseudo first-order rate constant, $k_{obs.}(s^{-1})$, for these determinations are shown in Table 4.4.

Table 4.2 The observed values[a] of the pseudo first-order rate constant, $k_{obs.}$ (s^{-1}), for the complexation of $[Ni(H_2O)_6]^{2+}$ with THEC in various concentrations of excess metal ion, $[Ni(H_2O)_6{}^{2+}]_{ex.}$ (mol dm^{-3}), at 298.2 (±0.2) K, pH 6.8, ionic strength of 1.50 mol dm^{-3} $NaNO_3$, and wavelength 365 nm ([THEC] = 1.5 x 10^{-3} mol dm^{-3}).

$[Ni(H_2O)_6{}^{2+}]_{ex.}$ (mol dm^{-3})	$k_{obs.}$ (s^{-1})
0.0135	0.0100 (±0.0002)
0.0285	0.0230 (±0.0003)
0.0385	0.0310 (±0.0002)
0.0485	0.0430 (±0.0002)
0.0610	0.0510 (±0.0008)
0.0735	0.0700 (±0.0009)
0.0860	0.086 (±0.001)
0.0985	0.098 (±0.003)
0.1110	0.123 (±0.002)
0.1235	0.138 (±0.002)
0.1360	0.150 (±0.001)
0.1485	0.157 (±0.001)

[a] The values in parentheses represent one standard deviation for two or three sets of experimental traces of the same solution under identical conditions and there are between 8 and 12 computer averaged traces in each set.

Table 4.3 The observed values[a] of the pseudo first-order rate constant, $k_{obs.}(s^{-1})$, for the complexation of $[Co(H_2O)_6]^{2+}$ with THEC in various concentrations of excess metal ion, $[Co(H_2O)_6{}^{2+}]_{ex.}$ (mol dm^{-3}), at 298.2 (±0.2) K, pH 6.8, ionic strength of 1.50 mol dm^{-3} $NaNO_3$, and wavelength 550 nm ([THEC] = 2.5 x 10^{-3} mol dm^{-3}).

$[Co(H_2O)_6{}^{2+}]_{ex.}$ (mol dm^{-3})	$k_{obs.}$ (s^{-1})
0.0225	0.410 (±0.001)
0.0369	0.520 (±0.001)
0.0475	0.630 (±0.002)
0.0600	0.742 (±0.001)
0.0725	0.870 (±0.013)
0.0850	0.965 (±0.012)
0.0975	1.10 (±0.01)
0.1225	1.29 (±0.02)
0.1475	1.52 (±0.03)

[a] The values in parentheses represent one standard deviation for two or three sets of experimental traces of the same solution under identical conditions and there are between 8 and 12 computer averaged traces in each set.

Table 4.4 The observed values[a] of the pseudo first-order rate constant, $k_{obs.}$ (s^{-1}), for the complexation of $[Ni(H_2O)_6]^{2+}$ with THEC over a range of pH values, at 298.2 (±0.2) K, ionic strength of 1.50 mol dm^{-3} $NaNO_3$, and wavelength 365 nm (The concentrations of THEC and $[Ni(H_2O)_6]^{2+}$ are kept constant at 1.5 x 10^{-3} mol dm^{-3} and 7.5 x 10^{-2} mol dm^{-3} respectively).

pH	$k_{obs.}$ (s^{-1})
6.52	0.0297 (±0.0007)
6.67	0.0471 (±0.0014)
6.80	0.0700 (±0.0013)
6.94	0.123 (±0.0014)
7.12	0.204 (±0.004)

[a] The values in parentheses represent one standard deviation for two or three sets of experimental traces of same solution under identical conditions and there are between 8 and 12 computer averaged traces in each set.

It is to be noted that it was not possible to study the complexation of $[Cu(H_2O)_6]^{2+}$ at pH 6.8 due to the precipitation of $Cu(OH)_2$.

4.2.3 Data Analyses and Discussion

The rate law for the complexation of metal ions, $[M(H_2O)_6]^{2+}$, with THEC (at pH 6.8, 298.2 (±0.2) K, and ionic strength of 1.50 mol dm^{-3} $NaNO_3$) in presence of excess metal ions, is consistent with equation 4.3,

$$k_{obs.} = k_c [M(H_2O)_6^{2+}]_{ex.} + k_d \qquad (4.3)$$

where k_c (dm^3 mol^{-1} s^{-1}) and k_d (s^{-1}) are the rate constants for complexation and decomplexation respectively.

The variation of the observed pseudo first order rate constant, $k_{obs.}$(s^{-1}), with excess concentration of metal ion, $[M(H_2O)_6^{2+}]_{ex.}$ (mol dm^{-3}), fitted to equation 4.3 are shown in Figures 4.3 and 4.4 for $[[Ni(H_2O)_6]^{2+}$ and $[Co(H_2O)_6]^{2+}$ respectively. The values of k_c (dm^3 mol^{-1} s^{-1}) and k_d (s^{-1}) are evaluated respectively from the slope and intercept of the plots of $k_{obs.}$ against $[M(H_2O)_6^{2+}]_{ex.}$ (Figures 4.3 and 4.4), and are shown in Table 4.5.

The negative intercept of the plot for the complexation of $[Ni(H_2O)_6]^{2+}$ may be due to experimental errors. Moreover, in order to maintain pseudo first-order conditions and still have a significant THEC concentration giving rise to an experimentally measurable reaction trace, data points are not attainable at very low concentrations, but are needed for a more accurate determination of k_d. Therefore, this parameter is not further discussed, but is assumed to be small in magnitude. Only the complexation rate constant, k_c, has been analysed in detail.

Figure 4.3 The variation[a] of the observed pseudo first-order rate constant, $k_{obs.}(s^{-1})$, as a function of excess concentration of metal ion, $[Ni(H_2O)_6^{2+}]_{ex.}$(mol dm^{-3}), for the complexation of $[Ni(H_2O)_6]^{2+}$ with THEC at pH 6.8 and 298.2 (±0.2) K (I = 1.50 mol dm^{-3} $NaNO_3$, [THEC] = 1.5 x 10^{-3} mol dm^{-3}, and λ = 365 nm).

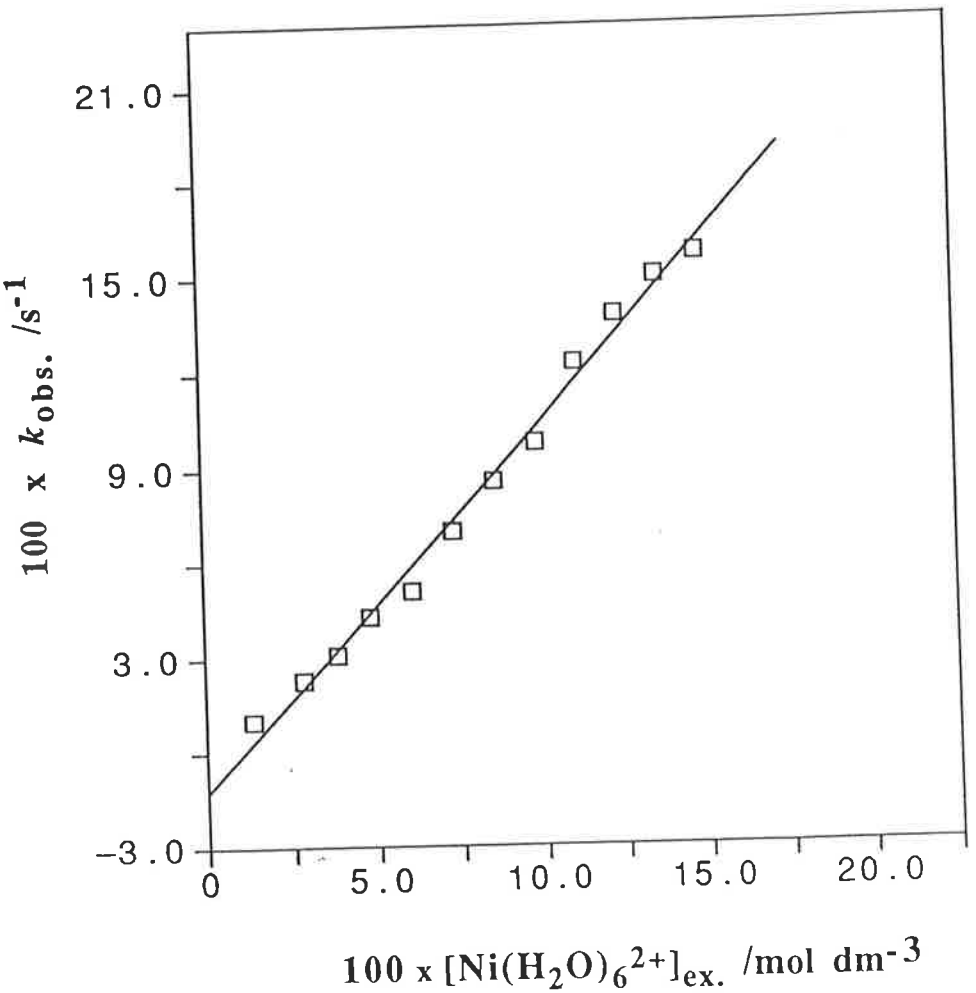

[a] The solid line represents the best fit of the experimental values of $k_{obs.}$ (s^{-1}) to the equation

$$k_{obs.} = k_c [Ni(H_2O)_6^{2+}]_{ex.} + k_d$$

Figure 4.4 The variation[a] of the observed pseudo first-order rate constant, $k_{obs.}(s^{-1})$, as a function of excess concentration of metal ion, $[Co(H_2O)_6^{2+}]_{ex.}$(mol dm^{-3}), for the complexation of $[Co(H_2O)_6]^{2+}$ with THEC at pH 6.8 and 298.2 (±0.2) K (I = 1.50 mol dm^{-3} $NaNO_3$, [THEC] = 2.5 x 10^{-3} mol dm^{-3}, and λ = 550 nm).

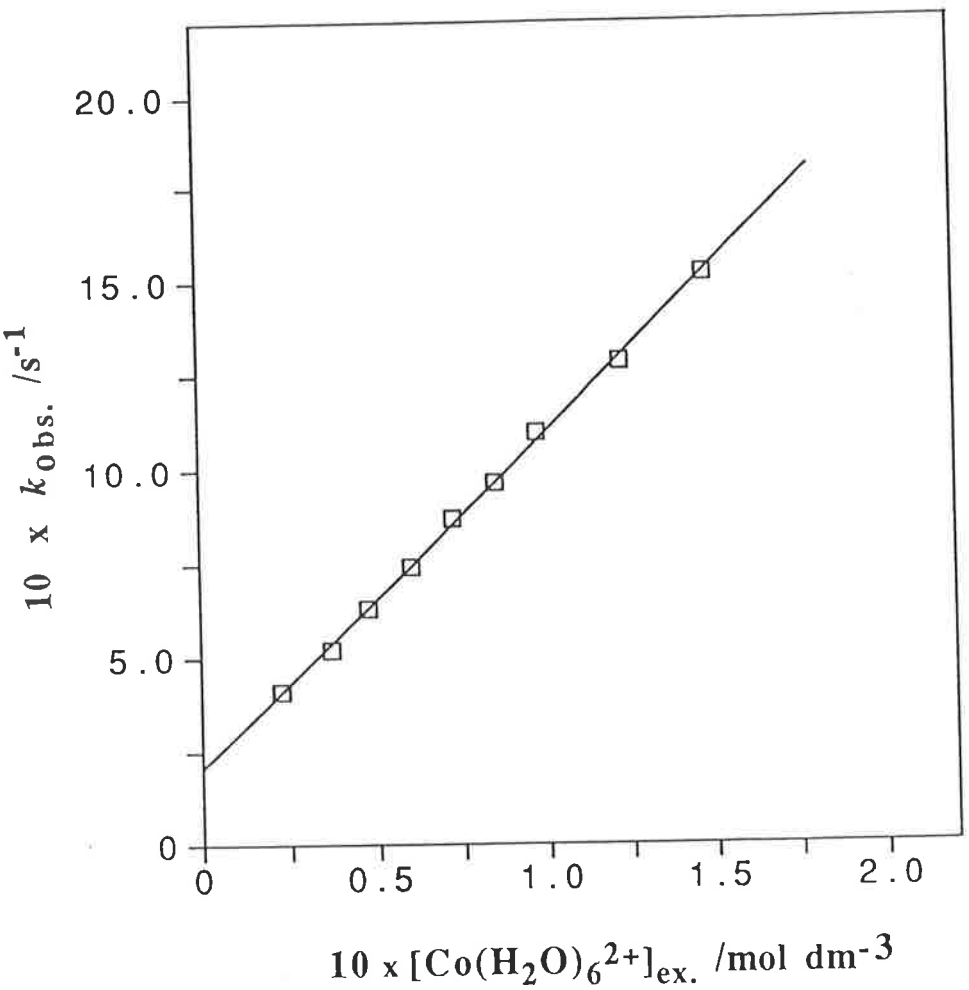

[a] The solid line represents the best fit of the experimental values of $k_{obs.}$ (s^{-1}) to the equation

$$k_{obs.} = k_c [Co(H_2O)_6^{2+}]_{ex.} + k_d$$

Table 4.5 The values[a] of k_c ($dm^3\ mol^{-1}\ s^{-1}$) and k_d (s^{-1}) for the complexation of $[Ni(H_2O)_6]^{2+}$ and $[Co(H_2O)_6]^{2+}$ evaluated from the plots (Figures 4.3 and 4.4) of $k_{obs.}$(s^{-1}) vs. $[M(H_2O)_6^{2+}]_{ex.}$ (mol dm^{-3}), for the best fit of the experimental data to equation 4.3.

$[M(H_2O)_6]^{2+}$	k_c ($dm^3\ mol^{-1}\ s^{-1}$)	k_d (s^{-1})
$[Ni(H_2O)_6]^{2+}$	1.17 (±0.03)	-0.012 (±0.003)
$[Co(H_2O)_6]^{2+}$	8.93 (±0.11)	0.21 (±0.01)

[a] The values in parentheses represent one standard deviation from the best fit of the experimental data (Tables 4.2 and 4.3) to equation 4.3.

In the present study, if it is assumed that an outer sphere complex is formed between $[M(H_2O)_6]^{2+}$ and LH^+ (since at pH 6.8 the mono-protonated species of THEC (L) is the reacting species, see the latter part of this section), in an interchange mechanism according to the scheme 4.3a,

$$[M(H_2O)_6]^{2+} + LH^+ \underset{\text{Rapid}}{\overset{K_{os}}{\rightleftharpoons}} \underset{\text{outer-sphere complex}}{[M(H_2O)_6]^{2+}\ldots LH^+} \quad \begin{matrix} k_{-i} \uparrow \\ \downarrow k_i \end{matrix} \quad [M(H_2O)_5L]^{2+} + H^+ \qquad (4.3a)$$

where subsequent fast steps in the postulated mechanism lead to the formation of $[M(THEC)]^{2+}$, then the rate expression for the scheme 4.3a, can be described by equation 4.3b (see section 1.5.4c),

$$k_{obs.} = \frac{k_i K_{os} [M(H_2O)_6^{2+}]_{ex.}}{1 + K_{os}[M(H_2O)_6^{2+}]_{ex.}} + k_{-i} \qquad (4.3b)$$

$k_{obs.}$ (s^{-1}) is the observed pseudo first-order rate constant. The parameter, K_{os} (dm^3 mol^{-1}), is the equilibrium constant characterising the rapid formation of an outer-sphere complex (encounter complex of ion-ion or ion-dipole nature) in which LH^+ resides in the second coordination sphere of the aquo-metal ion complex, $[M(H_2O)_6]^{2+}$. The second slower step is the rate determining interchange of LH^+ and coordinated H_2O characterised by forward rate constant k_i, and k_{-i} is the backward rate constant of the corresponding interchange. $[M(H_2O)_6^{2+}]_{ex.}$ represents the total concentration of excess metal ion.

Under limiting conditions, when K_{os} $[M(H_2O)_6]^{2+}]_{ex.} << 1$, then the equation 4.3b reduces to equation 4.3c,

$$k_{obs.} = k_i K_{os} [M(H_2O)_6^{2+}]_{ex.} + k_{-i} \qquad (4.3c)$$

a formulation that gives a linear relationship between $k_{obs.}$ and $[M(H_2O)_6^{2+}]_{ex.}$, which is consistent in form with equation 4.3, where $k_c = k_i K_{os}$, and $k_d = k_{-i}$.

Since, K_{os} can be measured by ultrasonic or temperature jump techniques, or can be estimated theoretically, the k_c value can be

separated into its K_{os} and k_i components.[103] In order to diagnose the reaction mechanism, in the case of metal ion complexation with a monodentate ligand, the values of k_i (s^{-1}) are compared with the values of the water exchange rate constant, $k_{ex.}$ (s^{-1}), for the respective metal ion. When the value of k_i is similar to the value of the water exchange rate constant, k_{ex}, for the corresponding metal ion then it indicates a dissociative interchange mechanism.

Thus, for the present study, the value of K_{os} can be approximately estimated in two separate ways.

(i) The values of water exchange rate constants, k_{ex} (s^{-1}) for the exchange of water on $[Ni(H_2O)_6]^{2+}$ and $[Co(H_2O)_6]^{2+}$ at 298.2 K are 3.16×10^4 s^{-1} and 1.78×10^6 s^{-1} respectively.[103] Thus, taking $k_{ex}=k_i$, the values of K_{os} (dm^3 mol^{-1}) are 3.7×10^{-5} and 5.0×10^{-6} for $[Ni(H_2O)_6]^{2+}$ and $[Co(H_2O)_6]^{2+}$ respectively. These low values of K_{os} indicates that the concentrations of outer-sphere complexes are very small indeed, such concentrations of complexes could represent simply the molecular collisions between the reactants, and obviously these values are in accord with K_{os} $[M(H_2O)_6^{2+}]_{ex.} << 1$.

(ii) The values of K_{os} for the formation of outer-sphere complexes between two oppositely charged ions and even between two positively charged ions[101] can also be estimated using the Fuoss equation (equation 4.3d),

$$K_{os} = \frac{4\pi Na^3}{3000} \exp - \frac{U(a)}{k_B T} \qquad (4.3d)$$

where the symbols have the usual significance (see section 1.5.4).

Taking a = 5Å arbitrarily, the value of K_{os} for the formation of an encounter complex between a doubly positively charged ion and a singly charged positive ion is calculated to be ~0.122 (dm^3 mol^{-1}), and thus the values of k_i are 9.6 (s^{-1}) and 73.2 (s^{-1}) respectively for the complexation of the metal ions, $[Ni(H_2O)_6]^{2+}$ and $[Co(H_2O)_6]^{2+}$, which are much lower than the water exchange rate constants for the respective ions. However, the K_{os} values calculated by both methods are only approximate. The very low values of k_i imply that dissociation of the first coordinated water molecule is not the rate determining step. Since, from the nmr studies[137] on the rates of water exchange on aquo-amine complexes of Ni^{2+}, it is evident that when one of the nitrogens coordinates to the metal ion after the dissociation of the first water molecule, the remaining water molecules appear to be labilised, i.e., desolvation of metal ion becomes faster, and thus the formation of coordination bonds between the metal ion and other nitrogen atoms of the ligand should be more favourable but the rate is still much slower than the water exchange rate. Thus some other factor is responsible for the slower rate determining step. This factor might be correlated to the various protonated species of the ligand. In aqueous solution the ligand exists in a variety of protonated forms, and hence the metal ion experiences electrostatic repulsion upon entering the macrocyclic ring prior to the formation of coordination bonds with the nitrogen atoms of the ligand.

This assumption of mutual ionic electrostatic repulsion leading to low values of k_c is also supported by the fact that the values of the rate constants, k_c (dm^3 mol^{-1} s^{-1}), for the complexation of Ni^{2+} ion with cyclam in DMF,[79] DMSO,[79] and in acetonitrile,[78] are 1.6 x 10^3,

1.8×10^3, and 7.6×10^2 respectively, which are similar to the values of the rate constant for the exchange of the corresponding solvent on the solvated Ni^{2+} ion, and thus it has been suggested that the dissocia-tion of the first coordinated solvent molecule is the rate determining step. In nonaqueous solution the ligand exists as the unprotonated species, and thus the metal ion does not experience the electrostatic repulsion that the protonated species does in aqueous solution. Hence, after the removal of the first coordinated solvent molecule, the formation of a coordination bond between the metal ion and the nitrogen atoms of the ligand, and consequent desolvation of the metal ion become more favourable and faster in nonaqueous solution.

Thus, to evaluate the role of differently protonated species of THEC on the complexation of metal ions, the rates of complexation of $[Ni(H_2O)_6]^{2+}$ at various pH values have been studied (see table 4.4). The values of pseudo first-order rate constant, $k_{obs.}(s^{-1})$, and their log values, $\log(k_{obs.})$, are plotted as a function of pH, and are shown in Figures 4.5 and 4.6 respectively.

From Figures 4.5 and 4.6, it is evident that the rate of complexation of $[Ni(H_2O)_6]^{2+}$ with THEC increases with the increase of pH. At higher pH, the concentrations of the less protonated species of the ligand are increased. The latter is probably more reactive compared to the more highly protonated species, because of lower electrostatic repulsion between the metal ion and the less protonated species of the ligand compared to that between the metal ion and the more protonated species of the ligand. Thus it is neccssary to consider the different species of the ligand which exist in the range of pH over which the complexation of $[Ni(H_2O)_6]^{2+}$ with THEC has been studied.

Figure 4.5 The variation[a] of the observed pseudo first-order rate constant, $k_{obs.}(s^{-1})$, as a function of pH, for the complexation of $[Ni(H_2O)_6]^{2+}$ with THEC at various pH values and at 298.2 (±0.2) K (the concentrations of THEC and $[Ni(H_2O)_6]^{2+}$ are kept constant at 1.5 x 10^{-3} mol dm^{-3} and 7.5 x 10^{-2} mol dm^{-3} respectively, I = 1.50 mol dm^{-3} $NaNO_3$, and λ = 365 nm).

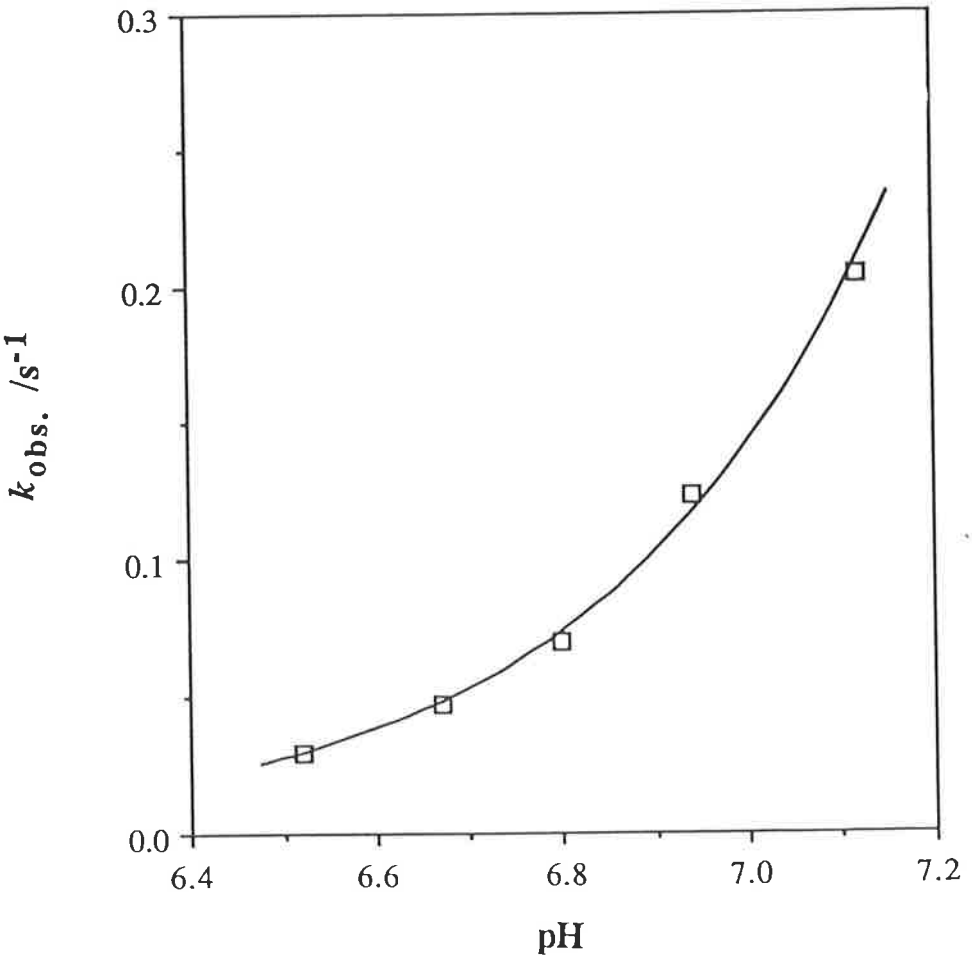

[a] The solid line is drawn by hand simply for graphical representation.

Figure 4.6 The variation[a] of log values of the observed pseudo first-order rate constant, $\log(k_{obs.})$, as a function of pH, for the complexation of $[Ni(H_2O)_6]^{2+}$ with THEC at various pH values and at 298.2 (±0.2) K (the concentrations of THEC and $[Ni(H_2O)_6]^{2+}$ are kept constant at 1.5×10^{-3} mol dm^{-3} and 7.5×10^{-2} mol dm^{-3} respectively, I = 1.50 mol dm^{-3} $NaNO_3$, and λ = 365 nm).

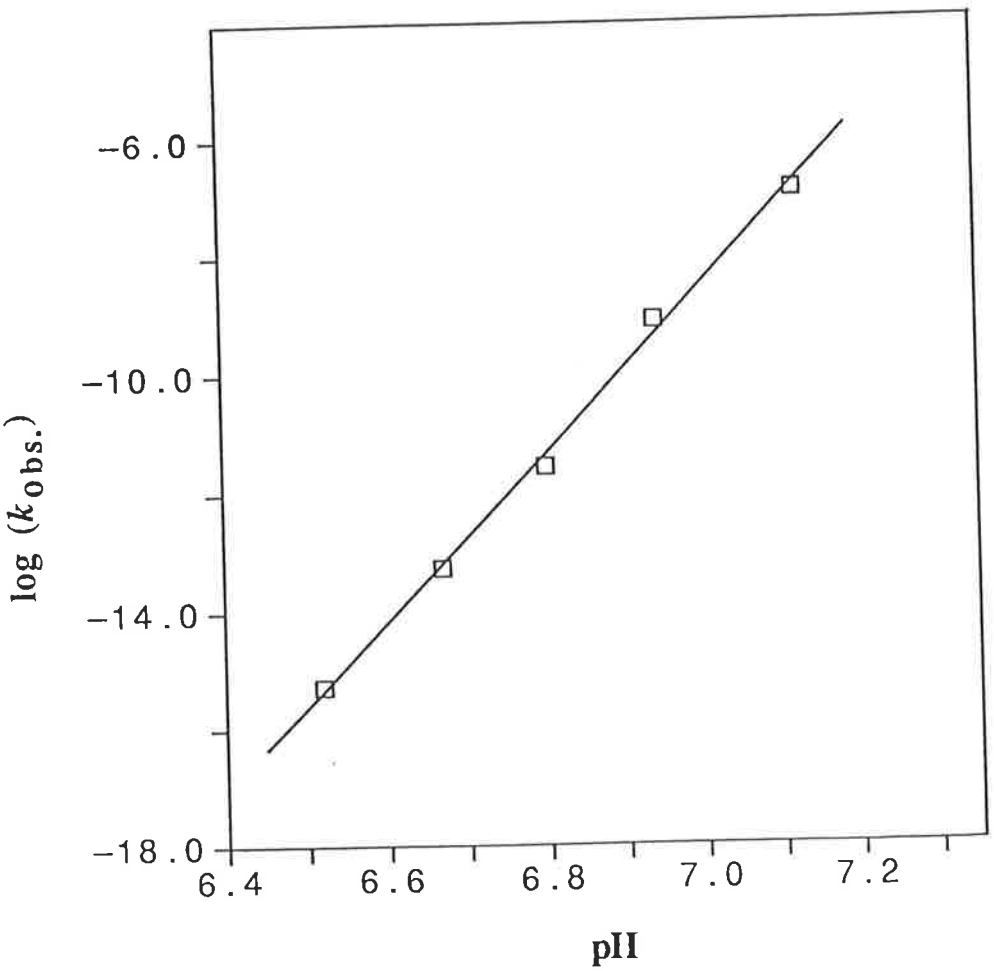

[a] The solid line is drawn by hand simply for graphical representation.

The complexation of a divalent metal ion, $[M(H_2O)_6]^{2+}$, with the various protonated species of THEC can be illustrated by a general equation 4.4 (M^{2+} = $[M(H_2O)_6]^{2+}$, and L = THEC, are used for simplicity).

$$M^{2+} + LH_n^{n+} \rightleftharpoons [ML]^{2+} + nH^+ \qquad (4.4)$$

At a constant pH, the rate of complexation is proportional to the total concentration of excess metal ion, $[M^{2+}]_{ex.}$, and total concentration of ligand, $[LH_n^{n+}]_T$. Thus the rate law for the reaction 4.4, at a given pH, can be expressed by equation 4.5.

$$\text{Rate} = k\ [M^{2+}]_{ex.}\ [LH_n^{n+}]_T \qquad (4.5)$$

where k ($dm^3\ mol^{-1}\ s^{-1}$) is a second order rate constant.

Depending on the pH, the ligand can exist as differently protonated species in addition to the free ligand (L). If all species are in equilibrium (see section 3.2.1), then the total concentration of ligand, $[LH_n^{n+}]_T$, can be expressed by equation 4.6.

$$[LH_n^{n+}]_T = [L] + [LH^+] + [LH_2^{2+}] + [LH_3^{3+}] + [LH_4^{4+}]$$

$$= [L] + \frac{[L]\,[H^+]}{K_{a1}} + \frac{[L]\,[H^+]^2}{K_{a1}\,K_{a2}} +$$

$$\frac{[L]\,[H^+]^3}{K_{a1}\,K_{a2}\,K_{a3}} + \frac{[L]\,[H^+]^4}{K_{a1}\,K_{a2}\,K_{a3}\,K_{a4}} \qquad (4.6)$$

$$= [L] \sum_{n=0}^{n=4} \frac{[H^+]^n}{\beta_n} \qquad (4.7)$$

where β_n = overall acid dissociation constant

$$= \prod_{n=1}^{n=4} K_{an} \qquad (4.8)$$

and $\beta_o = 1$

Therefore, equation 4.5 can be written as equation 4.9,

$$\text{Rate} = k\ [M^{2+}]_{ex.}\ [L] \sum_{n=0}^{n=4} \frac{[H^+]^n}{\beta_n} \qquad (4.9)$$

Under pseudo first order conditions (at least a 10 fold excess of metal ion concentration), $[M^{2+}]_{ex.}$ remains effectively constant. Hence, equation 4.9 reduces to equation 4.10.

$$\text{Rate} = k_{obs.}\ [L] \sum_{n=0}^{n=4} \frac{[H^+]^n}{\beta_n} \qquad (4.10)$$

where $k_{obs.}$ (s^{-1}) is the observed pseudo first-order rate constant.

The more protonated species reacts less rapidly with the metal ion mainly due to the greater electrostatic repulsion between the metal ion and the more positively charged species. Hence the reaction rate is

also a function of the pH and thus the following reactions (equation 4.11) must be considered.

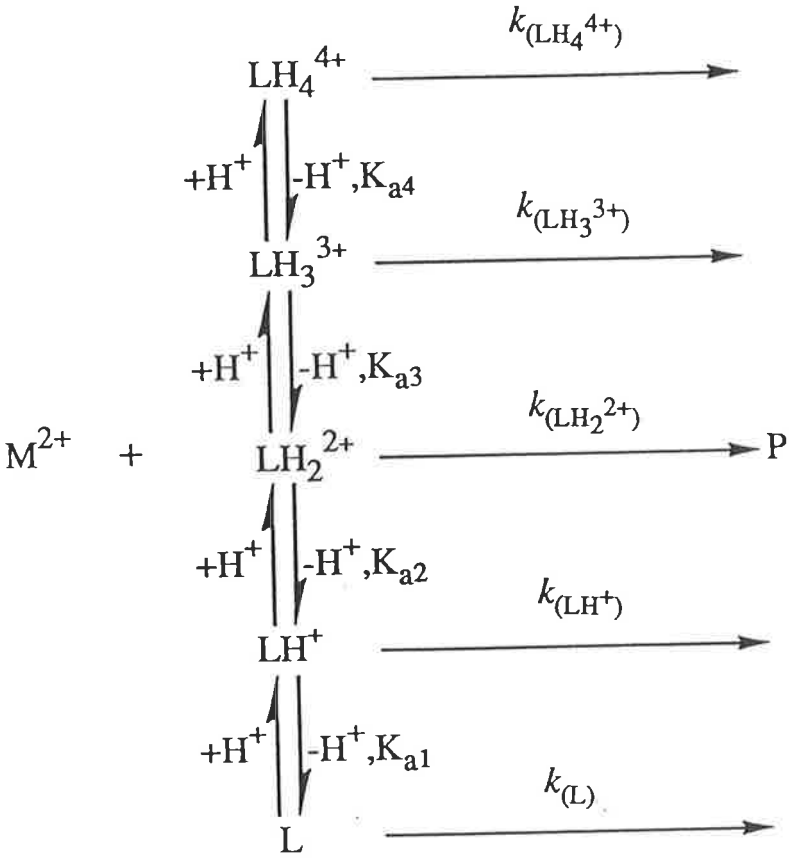

(4.11)

where K_{an} are the acid dissociation constants for the ligand (see section 3.2.1), and $k_{(LH_n^{n+})}$ are the second order rate constants ($dm^3\ mol^{-1}\ s^{-1}$) for the complexation of metal ion with the respective protonated species of the ligand, THEC (L). Considering all rate constants, the rate law for the reactions 4.11 can be expressed by equation 4.12.

$$\text{Rate} = [M^{2+}]_{ex.} \left(k_{(L)}\,[L] + k_{(LH^+)}\,[LH^+] + k_{(LH_2^{2+})}\,[LH_2^{2+}] + k_{(LH_3^{3+})}\,[LH_3^{3+}] + k_{(LH_4^{4+})}\,[LH_4^{4+}]\right) \quad (4.12)$$

Under pseudo first order conditions, $[M^{2+}]_{ex.}$ remains effectively constant, and thus equation 4.12 reduces to 4.13,

$$\text{Rate} = k'_{(L)}\,[L] + k'_{(LH^+)}\,[LH^+] + k'_{(LH_2^{2+})}\,[LH_2^{2+}] + k'_{(LH_3^{3+})}\,[LH_3^{3+}] + k'_{(LH_4^{4+})}\,[LH_4^{4+}] \qquad (4.13)$$

$$\text{or,} \qquad \text{Rate} = [L] \sum_{n=0}^{n=4} k'_{(LH_n^{n+})} \frac{[H^+]^n}{\beta_n} \qquad (4.14)$$

where $k'_{(LH_n^{n+})}(s^{-1})$ are the first-order rate constants for the complexation of metal ions with the respective species of THEC.

Thus, from equations 4.10 and 4.14, under pseudo first-order conditions, the rate law can be expressed by equation 4.15.

$$k_{obs.} = \frac{\sum_{n=0}^{n=4} k'_{(LH_n^{n+})} \frac{[H^+]^n}{\beta_n}}{\sum_{n=0}^{n=4} \frac{[H^+]^n}{\beta_n}} \qquad (4.15)$$

In the pH range of 6.52 to 7.12 over which the complexation of $[Ni(H_2O)_6]^{2+}$ was studied, the ligand, THEC (L), exists mainly as the di-protonated species (LH_2^{2+}) with a small amount of mono-protonated species (LH^+) and a very small amount of unprotonated species (L). The concentrations of tetra-protonated (LH_4^{4+}) and tri-protonated (LH_3^{3+})

species of the ligand are negligible (see section 3.2.3). Thus, considering the rate constants, $k'_{(L)}$, $k'_{(LH^+)}$, and $k'_{(LH_2{}^{2+})}$, for the complexation of metal ion under pseudo first-order conditions with the zero-, mono- and di- protonated species of the ligand respectively, the rate equation 4.15 reduces to 4.16.

$$k_{obs.} = \frac{k'_{(L)} K_{a1} K_{a2} + k'_{(LH^+)} K_{a2} [H^+] + k'_{(LH_2{}^{2+})} [H^+]^2}{K_{a1} K_{a2} + K_{a2} [H^+] + [H^+]^2} \quad (4.16)$$

The experimental values (Table 4.4) of pseudo first-order rate constant, $k_{obs.}(s^{-1})$, for the complexation of $[Ni(H_2O)_6]^{2+}$ with THEC at various pH values are fitted to equation 4.16, using the nonlinear least square regression program DATAFIT,[133-135] using the known values of K_{an} (acid dissociation constants of THEC, Table 3.1) and taking the rate constants as unknown parameters. The least squares best fit plot of $k_{obs.}(s^{-1})$ vs. $[H^+]$ (mol dm^{-3}) is shown in Figure 4.7, and the values of the unknown parameters obtained from this fitting are as follows:

$$k'_{(L)} = 340\ (\pm 288)\ s^{-1}$$
$$k'_{(LH^+)} = 8.23\ (\pm 2.75)\ s^{-1}$$
$$k'_{(LH_2{}^{2+})} = -0.023\ (\pm 0.016)\ s^{-1}$$

The values in parentheses represent one standard deviation. The uncertainty in the value of $k'_{(L)}$ is due to the very low concentration of unprotonated species of the ligand [L] in the pH range studied. However, the negative value of $k'_{(LH_2{}^{2+})}$ indicates that the di-protonated species of the ligand ($LH_2{}^{2+}$) does not react with the metal ion or its contribution is negligible.

Figure 4.7 The variation[a] of the observed pseudo first-order rate constant, $k_{obs.}(s^{-1})$, as a function of $[H^+]$ (mol dm^{-3}), for the complexation of $[Ni(H_2O)_6]^{2+}$ with THEC at various pH values and 298.2 (±0.2) K (the concentrations of THEC and $[Ni(H_2O)_6]^{2+}$ are kept constant at 1.5×10^{-3} mol dm^{-3} and 7.5×10^{-2} mol dm^{-3} respectively, I = 1.50 mol dm^{-3} $NaNO_3$, and λ = 365 nm).

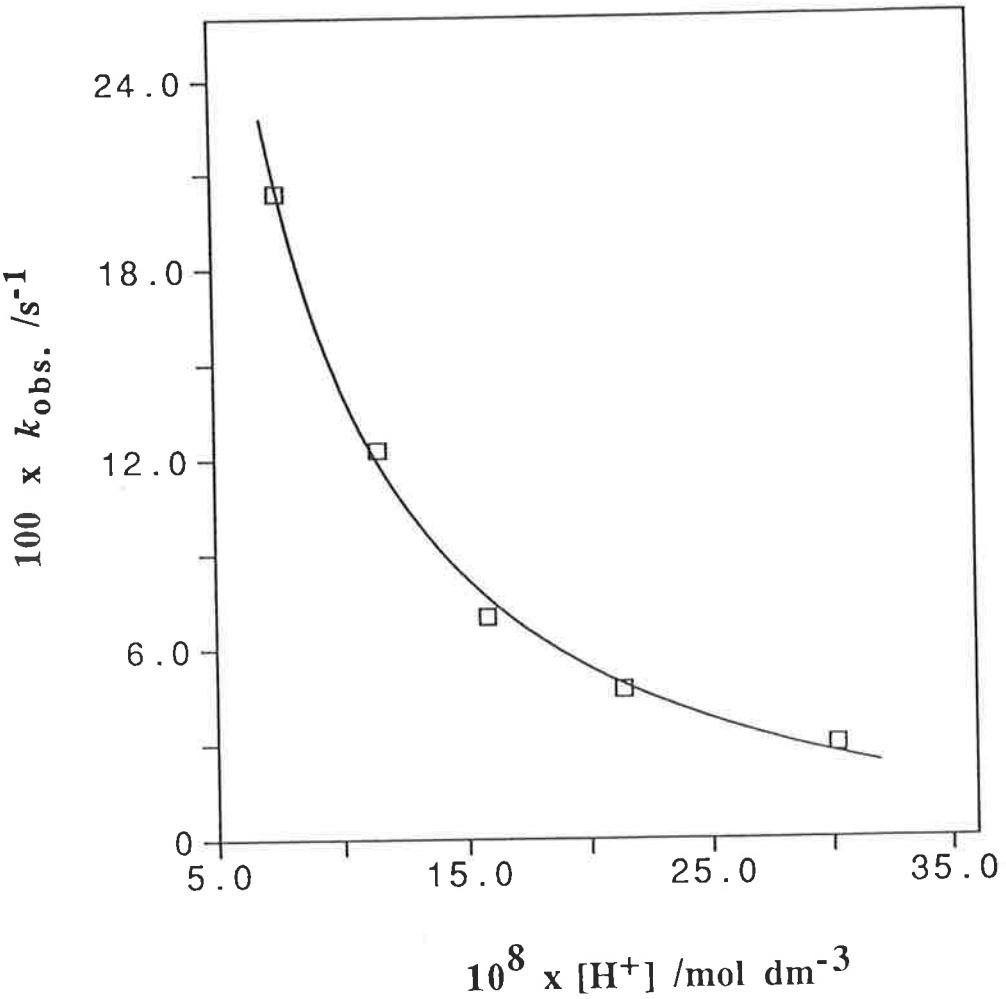

[a] The solid line represents the best fit of the experimental values of $k_{obs.}$ (s^{-1}) to the equation

$$k_{obs.} = \frac{k_{(L)} K_{a1} K_{a2} + k_{(LH^+)} K_{a2} [H^+] + k_{(LH_2^{2+})} [H^+]^2}{K_{a1} K_{a2} + K_{a2} [H^+] + [H^+]^2}$$

On the basis of the assumption that LH_2^{2+} does not react with the metal ion, the values of $k_{(LH^+)}$ for the complexation of $[Ni(H_2O)_6]^{2+}$ and $[Co(H_2O)_6]^{2+}$ at constant pH 6.8, can be evaluated from the variation of $k_{obs.}(s^{-1})$ against excess metal ion concentration, $[M(H_2O)_6^{2+}]_{ex.}$ (mol dm^{-3}), shown in Figures 4.3 and 4.4, as follows.

At a constant pH, the rate law (equation 4.5) can also be expressed by equation 4.17.

$$\text{Rate} = -\frac{d[LH_n^{n+}]_T}{dt} = k\ [M^{2+}]_{ex.}\ [LH_n^{n+}]_T \qquad (4.17)$$

$$\text{or,} \qquad -\frac{d[LH_n^{n+}]_T}{[LH_n^{n+}]_T} = k\ [M^{2+}]_{ex.}\ dt \qquad (4.18)$$

Under pseudo first-order conditions (at least a 10 fold excess of metal ion concentration), $[M^{2+}]_{ex.}$ remains effectively constant. Therefore, equation 4.18 reduces to equation 4.19.

$$-\frac{d[LH_n^{n+}]_T}{[LH_n^{n+}]_T} = k_{obs.}\ dt \qquad (4.19)$$

where $k_{obs.}(s^{-1})$ is the observed pseudo first-order rate constant. Thus, from equations 4.18 and 4.19 one can write,

$$k_{obs.} = k\ [M^{2+}]_{ex.}$$

$$\text{or,} \qquad k = \frac{k_{obs.}}{[M^{2+}]_{ex.}} = \text{slope} \qquad (4.20)$$

That is, the slope of the plot of $k_{obs..}$ vs. $([M(H_2O)_6^{2+}]_{ex.}$ represents the value of k ($dm^3\ mol^{-1}\ s^{-1}$).

At pH 6.8, from the speciation calculations for THEC (Figure 3.5), it is evident that the ligand mainly exists as di-protonated species (LH_2^{2+}) with a small amount of mono-protonated species (LH^+), and the unprotonated species (L) does not exist or its concentration is negligible. Moreover, as already mentioned LH_2^{2+} does not react with the metal ion, thus, LH^+ is the reacting species at pH 6.8. Therefore, rewriting the equation 4.17, the rate expression is,

$$\text{Rate} = -\frac{d[LH^+]}{dt} = k_{(LH^+)}\,[M^{2+}]_{ex.}\,[LH^+] \qquad (4.21)$$

where $k_{(LH^+)}$ ($dm^3\ mol^{-1}\ s^{-1}$) is the second order rate constant for the complexation of metal ion ($[M(H_2O)_6]^{2+}$) with the mono-protonated species of THEC (LH^+). Thus, from equations 4.17 and 4.21,

$$k\ [LH_n^{n+}]_T = k_{(LH^+)}\ [LH^+] \qquad (4.22)$$

or,
$$k_{(LH^+)} = k\,\frac{[LH_n^{n+}]_T}{[LH^+]}$$

$$= \text{slope}\ \frac{[LH_n^{n+}]_T}{[LH^+]} \qquad (4.23)$$

The values of the slopes are known (Tables 4.5), and the values of $[LH_n^{n+}]_T$ are also known from initial total concentrations of THEC

used (1.5×10^{-3} mol dm^{-3} and 2.5×10^{-3} mol dm^{-3} for the complexation of $[Ni(H_2O)_6]^{2+}$ and $[Co(H_2O)_6]^{2+}$ respectively). Since at pH 6.8, the concentrations of the LH_4^{4+}, LH_3^{3+}, and L species (L = THEC) are either zero or negligible, the equation 4.6 reduces to equation 4.24.

$$[LH_n^{n+}]_T = [LH_2^{2+}] + [LH^+] \qquad (4.24)$$

Again from equation 3.6, the second acid dissociation constant of the ligand can be written as equation 4.25,

$$K_{a2} = \frac{[LH^+]\,[H^+]}{[LH_2^{2+}]} \qquad (4.25)$$

Therefore, from equations 4.24 and 4.25, one can write,

$$[LH^+] = \frac{[LH_n^{n+}]_T\, K_{a2}}{K_{a2} + [H^+]} \qquad (4.26)$$

Hence, the values of $k_{(LH^+)}$, for the complexation of $[Ni(H_2O)_6]^{2+}$ and $[Co(H_2O)_6]^{2+}$ have been calculated from equation 4.23, and are shown in Table 4.6. For comparison, the values of $k_{(LH^+)}$, for the complexation of $[Ni(H_2O)_6]^{2+}$ and $[Co(H_2O)_6]^{2+}$, with various tetraaza macrocyclic ligands collected from the literature[20,68,71,72,74] are also shown in Table 4.6.

Table 4.6 The values of the rate constant, $k_{(LH^+)}$ ($dm^3\ mol^{-1}\ s^{-1}$), for the complexation of $[Ni(H_2O)_6]^{2+}$ and $[Co(H_2O)_6]^{2+}$ with the mono-protonated species (LH^+) of THEC and its cyclic analogues at 298.2 (±0.2) K and various ionic strengths.

M^{2+}	$k_{(LH^+)}$ ($dm^3\ mol^{-1}\ s^{-1}$)					
	cyclam	THEC[a]	Me-cyclam	Me_2-cyclam	TMC	TETA
Ni^{2+}	53[b]* 7.4[c]* 14[d]*	115.5 109.7[g]	55[c]	10[c]	1.4[c]	2.5×10^4[f]
Co^{2+}	15×10^2[b]	8.8×10^2			16[e]	

[a] I = 1.50 mol dm^{-3} $NaNO_3$. [present work] [b] I = 0.5 mol dm^{-3} KNO_3.[74]

[c] I = 0.5 mol dm^{-3} KNO_3.[72] [f] I = 0.25 mol dm^{-3} NaCl.[20]

[g] Obtained by dividing $k'_{(LH^+)} = 8.23\ s^{-1}$, obtained from the fitting of the data shown in Figure 4.7 to equation (4.16), by the appropriate total $[Zn^{2+}] = 7.5 \times 10^{-2}$ mol dm^{-3}.

*According to *Kaden et al.*,[74] the corrected value of $k_{(LH^+)}$ for the complexation of Ni^{2+} with cyclam is 53 ($dm^3\ mol^{-1}\ s^{-1}$), and in other two cases the pK_a values used in the calculation of $k_{(LH^+)}$ values were taken from other laboratories which were determined under different conditions. Thus in the present discussion for cyclam, $k_{(LH^+)} = 53$ ($dm^3\ mol^{-1}\ s^{-1}$) has been considered.

From the comparison of the values of $k_{(LH^+)}$ ($dm^3\ mol^{-1}\ s^{-1}$) in Table 4.6, if the effects of ionic strength are ignored, it is evident that the rates of complexation of the same metal ion with the kinetically

important LH^+ species of the tetraaza macrocyclic ligands, cyclam and THEC, are similar. This suggests that the N-functionalised 2-hydroxyethyl pendant arm has only a small role in determining the overall rate of metal ion complexation. Indeed it appears that the apparent very slow rate of metalation of cyclam compared to THEC is predominately due to the difference in pK_a values of cyclam and THEC (see Table 3.1). The reacting species for the complexation of metal ions are free ligand (L), and the mono-protonated species (LH^+) of the ligand. For cyclam these species exist only at very high pH. Hence the apparent complexation of metal ion with cyclam is very slow near pH 7. On the other hand, for THEC, a small amount of mono-protonated species and a very small amount of unprotonated ligand exist near pH 7. Consequently metalation with THEC appears to be faster than that with cyclam.

Thus, it is clear that if the similarly protonated species (LH^+) of both cyclam and THEC are considered their rates of complexation of the same metal ion are similar though not identical. This may be compared with the result reported by *Hay et al.*[78] that the rates of incorporation of Ni^{2+} into cyclam and its N-methylated derivatives in acetonitrile (where the ligands exist as unprotonated species) have identical values *ca* 900 ($dm^3\ mol^{-1}\ s^{-1}$) at 298.2K whereas the rate is markedly decreased as the solvent is changed. For example, the values of the rate constant, k_c ($dm^3\ mol^{-1}\ s^{-1}$), for the incorporation of Ni^{2+} into cyclam are 760, 54, and 0.5 ($dm^3\ mol^{-1}\ s^{-1}$) in CH_3CN, CH_3OH, and a CH_3OH-H_2O mixture (1:1 by volume) respectively. This decrease in rates of metalation is mainly due to the existence of different protonated

species of the ligand and also solvation of the ligand (due to hydrogen bonding) in hydrogen bonded solvents.

On the other hand, from Table 4.6, it is also evident that in the case of Ni^{2+} ion complexation with the mono-protonated species of N-methylated derivatives of cyclam, the values of the rate constant, $k_{(LH^+)}$ ($dm^3\ mol^{-1}\ s^{-1}$), decrease as the number of methyl groups is increased,that is, in the decreasing order of

$$\text{Me-cyclam} > \text{Me}_2\text{-cyclam} > \text{Me}_4\text{-cyclam (TMC)},$$

and the values of the rate constant, $k_{(LH^+)}$, for the complexation of Ni^{2+} and Co^{2+} ions with TMC are 38-94 times lower than those with cyclam. Such a decrease in rate constant is due to a steric effect associated with the introduction of N-methyl groups, and this effect is much more predominant in the case of alkyl substituted linear polyamines[138] where the rates of metal ion complexation are strongly decreased on going from secondary to tertiary amines. It has also been observed by *Hertly et al.*[79] that the rates of Ni^{2+} ion complexation with TMC in nonaqueous solvents (DMSO and DMF) are 20-250 times slower than those with cyclam in the same solvents. A significant steric effect has not been observed in CH_3CN[78] since the solvent molecules are linear, whereas it is strongly predominant in DMF and DMSO which are much bulkier solvents than CH_3CN. Similarly, it has been observed[80] that in an alkaline medium, the values of the rate constant, k_c ($dm^3\ mol^{-1}\ s^{-1}$), for the complexation of $Cu(OH)_3^-$ with cyclam and its N-methyl derivatives decrease with the increase in the number of Me-groups in the following order

cyclam (2.7×10^6) > Me_2-cyclam (5.6×10^5 > Me_4-cyclam (3.1×10^4).

Hence, significant steric effects of methyl groups on the rates of the metal ion complexation with N-functionalised derivatives of cyclam in water exist.

Thus, if a steric effect due to hydroxyethyl groups is considered in the case of THEC and the effect of ionic strength is ignored, then the rates of metal ion complexation with THEC should be similar to or less than those of TMC, whereas the observed values (Table 4.6) of the rate constants ($k_{(LH^+)}$) for the complexation of Co^{2+} and Ni^{2+} are 5.5-83 times greater than those with TMC. This implies that the steric effect in the case of THEC must be overcome or compensated by the pendant 2-hydroxyethyl arms which can cause an initial attachment of the metal ion outside the macrocyclic ring. Hence, the apparently rapid metal ion complexation with THEC is related to lower pK_a values (less protonated species exist near pH 7) as well as to the mode of entry of metal ion into the macrocyclic cavity. A similar argument has been made by *Hancock et al.*[23] that despite the lower pK_a value (pK_{a1} = 7.0) of TCEC, it equilibrates very slowly even with Cu^{2+} ion, and thus, it has been assumed that the 2-hydroxyethyl arms of THEC can attach the metal ion outside the macrocyclic ring.

In the case of the carboxylic derivative of THEC (TETA), where all hydroxy groups on the pendant arms in THEC are replaced by carboxylic groups, it has been found[20] that the rate of Ni^{2+} ion complexation with the mono-protonated species of TETA ($HTETA^{3-}$) is 10^3 times faster than that with the mono-protonated species of cyclam

(cyclamH$^+$). It has already been mentioned (see section 1.3) that the increased complexation rate might be due to the different charges of the ligands, TETA bearing a charge of 3-, and cyclam or THEC bearing a charge of 1+, and also the acetate groups could modify the mechanism through the formation of an adduct. Moreover, according to *Hancock et al.*[7] the carboxylic group is more efficient in coordination of metal ions compared to other donor groups present on the pendent arms.

However, although there would be an initial attachment of the metal ion with the 2-hydroxyethyl pendant arm of THEC, the rates of metal ion complexation with the similarly protonated species of THEC are still as slow as that with cyclam and much slower than the rate of water exchange on the corresponding aquo-metal ion ($[M(H_2O)_6]^{2+}$. This implies that the rate determining step for the complexation of metal ions with THEC in aqueous medium is not the dissociation of the first coordinated water molecule and the 2-hydroxyethyl pendant arms are not involved in the rate determining step either. The rate determining step must be the formation of a second or third metal nitrogen bond when the positively charged metal ion and the proton (of the mono-protonated species of the ligand) compete for the nitrogen atom in the macrocyclic ring.

CHAPTER 5

KINETIC STUDIES ON THE DECOMPLEXATION OF METAL COMPLEXES

1.1 Introduction

Due to the extremely slow decomplexation of the metal complexes of tetraaza macrocyclic ligands, considerable attention in the last three decades has been focused on the more labile macrocyclic systems including N-functionalised derivatives of tetraaza macrocyclic systems, N_2O_2, S_4, N_xS_{4-x}, N_3 and N_5 macrocyclic systems (see section 1.3), especially in the investigation of mechanistic pathways and the origin of the macrocyclic effect. Although the acid catalysed decomplexation of $[Cu(THEC)]^{2+}$ has been studied,[24] the decomplexation of other complexes, for example, $[Ni(THEC)]^{2+}$ and $[Co(THEC)]^{2+}$ has not been studied.

The acid catalysed decomplexation of divalent metal ion complexes ($[ML]^{2+}$) of polyaza macrocyclic ligands (L) in an aqueous medium can be described by reaction 5.1 (the aquation of metal complex, proton, and protonated ligand is not shown for simplicity).

$$[ML]^{2+} + nH^+ + 6H_2O \rightleftharpoons [M(H_2O)_6]^{2+} + H_nL^{n+} \qquad (5.1)$$

The rate laws associated with reaction 5.1 are more complicated than in the case of open chain polyamines,[1,12] particularly when considering such factors as the hydrogen ion dependence of reaction rates and the effects of the configuration of the ligand on reaction rates. Nonetheless, the rates of decomplexation measured under identical conditions can provide appropriate information about the various reaction mechanisms and relative labilities of different complexes. In particular the effect of the N-functionalised pendant arm on the rate of decomplexation can be studied.

Thus, in the present investigation, the acid catalysed decomplexation of metal complexes of THEC; ($[Cu(THEC)]^{2+}$, $[Ni(THEC)]^{2+}$, and $[Co(THEC)]^{2+}$) has been studied in excess HNO_3, at various temperatures and a constant ionic strength of 1.5 mol dm^{-3} adjusted with $NaNO_3$, using stopped-flow spectrophotometry.

5.2 Results

5.2.1 Visible Spectra of Metal Complexes of THEC in Unbuffered Aqueous Solution

The visible spectra of metal complexes of THEC, with 1:1 molar ratio of metal to ligand, in unbuffered aqueous solution at 298.2 (±0.2) K and ionic strength of 1.50 mol dm^{-3} $NaNO_3$, are shown in Figures 5.1, 5.2, and 5.3 for $[Cu(THEC)]^{2+}$, $[Ni(THEC)]^{2+}$, and $[Co(THEC)]^{2+}$ respectively. The visible spectra of the respective aquo-metal ion complexes, $[M(H_2O)_6]^{2+}$, under identical conditions, are also

shown. The maximum molar absorptivities of these complexes, $\varepsilon_{max.}$(dm^3 mol^{-1} cm^{-1}), are shown in Table 5.1.

Table 5.1 The values of the maximum molar absorptivities, $\varepsilon_{max.}$(dm^3 mol^{-1} cm^{-1}), of the metal complexes, $[Cu(THEC)]^{2+}$, $[Ni(THEC)]^{2+}$, and $[Co(THEC)]^{2+}$ (with a 1:1 molar ratio of metal to ligand) in unbuffered aqueous solution and the wavelengths, λ (nm), at which maximum absorption occurs, at 298.2 (±0.2) K and ionic strength of 1.50 mol dm^{-3} $NaNO_3$.

$[M(THEC)]^{2+}$	$\varepsilon_{max.}$ (dm^3 mol^{-1} cm^{-1})	λ (nm)
$[Cu(THEC)]^{2+}$	363	638
$[Ni(THEC)]^{2+}$	31.9	366
	14.4	588
$[Co(THEC)]^{2+}$	20.5	488
	20.0	538

The decomplexation reactions were studied by stopped-flow spectrophotometry and were monitored at 630 nm, 365 nm, and 550 nm for $[Cu(THEC)]^{2+}$, $[Ni(THEC)]^{2+}$, and $[Co(THEC)]^{2+}$, respectively.

Figure 5.1 The variation of molar absorptivity, ε (dm^3 mol^{-1} cm^{-1}), as a function of wavelength, λ (nm), in unbuffered aqueous solution at 298.2 (±0.2) K and ionic strength of 1.50 mol dm^{-3} $NaNO_3$:

(a) $[Cu(THEC)]^{2+}$ (pH ~6.2±0.15), and
(b) $[Cu(H_2O)_6]^{2+}$.

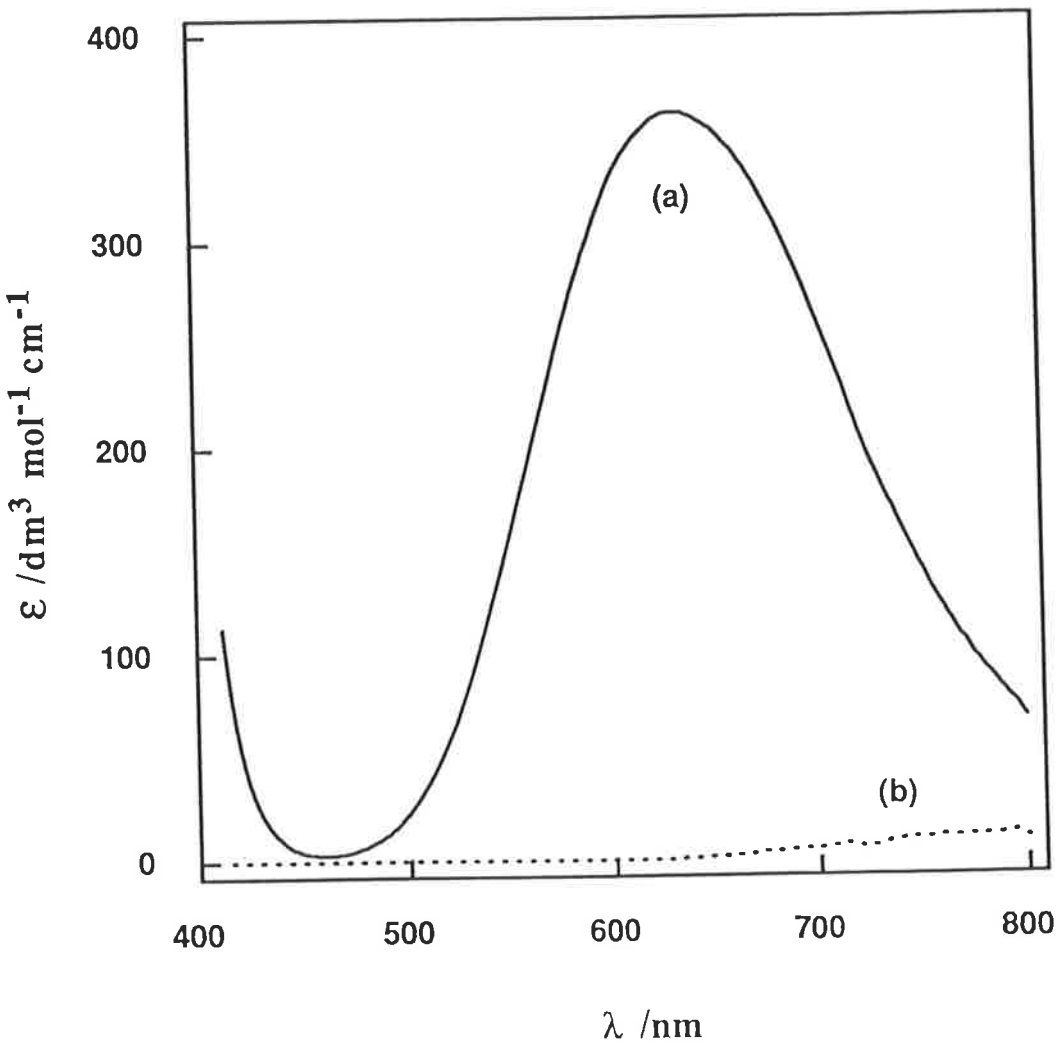

Figure 5.2 The variation of molar absorptivity, ε ($dm^3\ mol^{-1}\ cm^{-1}$), as a function of wavelength, λ (nm), in unbuffered aqueous solution at 298.2 (±0.2) K and ionic strength of 1.50 mol dm^{-3} $NaNO_3$:

(a) $[Ni(THEC)]^{2+}$(pH ~7.6±0.2), and
(b) $[Ni(H_2O)_6]^{2+}$.

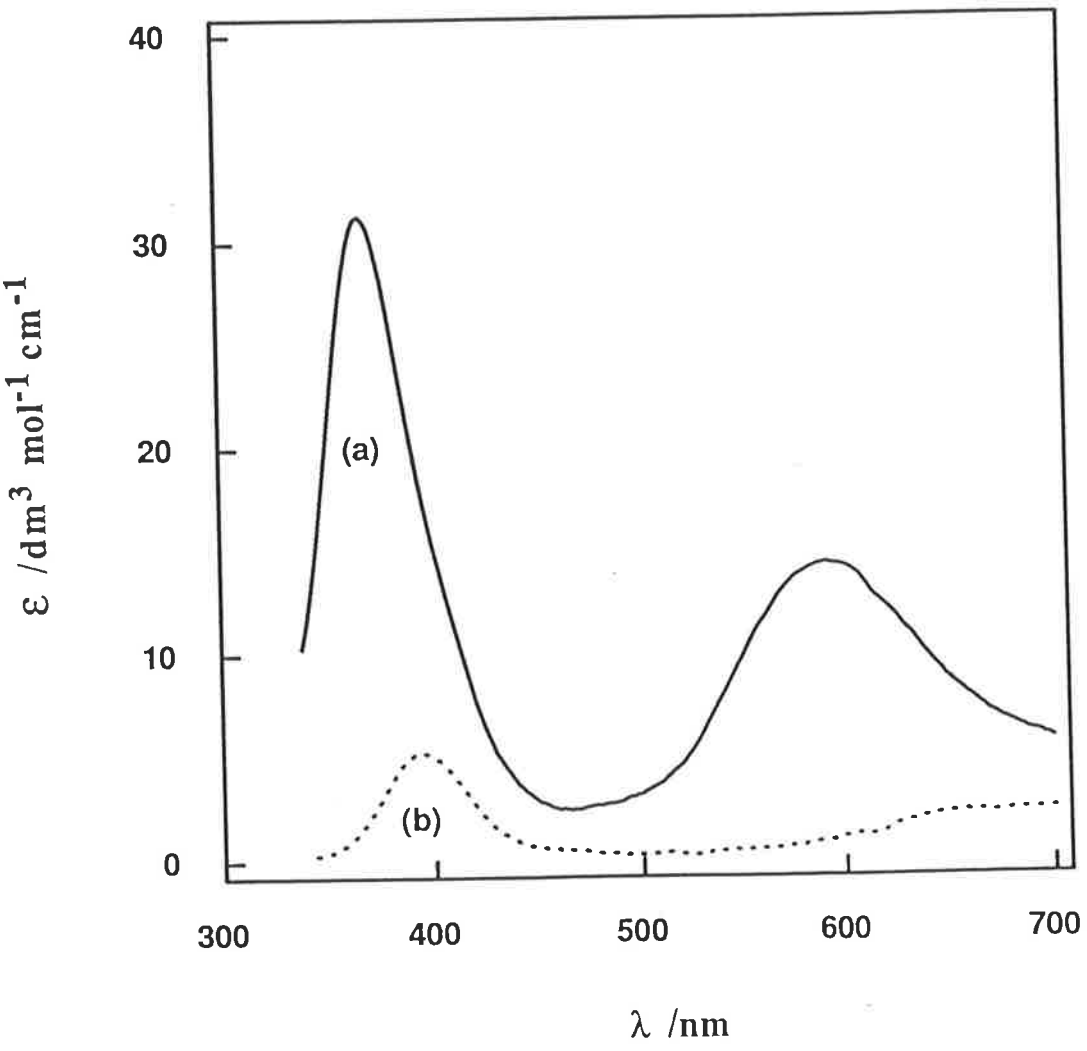

Figure 5.3 The variation of molar absorptivity, ε (dm^3 mol^{-1} cm^{-1}), as a function of wavelength, λ (nm), in unbuffered aqueous solution at 298.2 (±0.2) K and ionic strength of 1.50 mol dm^{-3} $NaNO_3$:

(a) $[Co(THEC)]^{2+}$(pH ~7.2±0.15), and
(b) $[Co(H_2O)_6]^{2+}$.

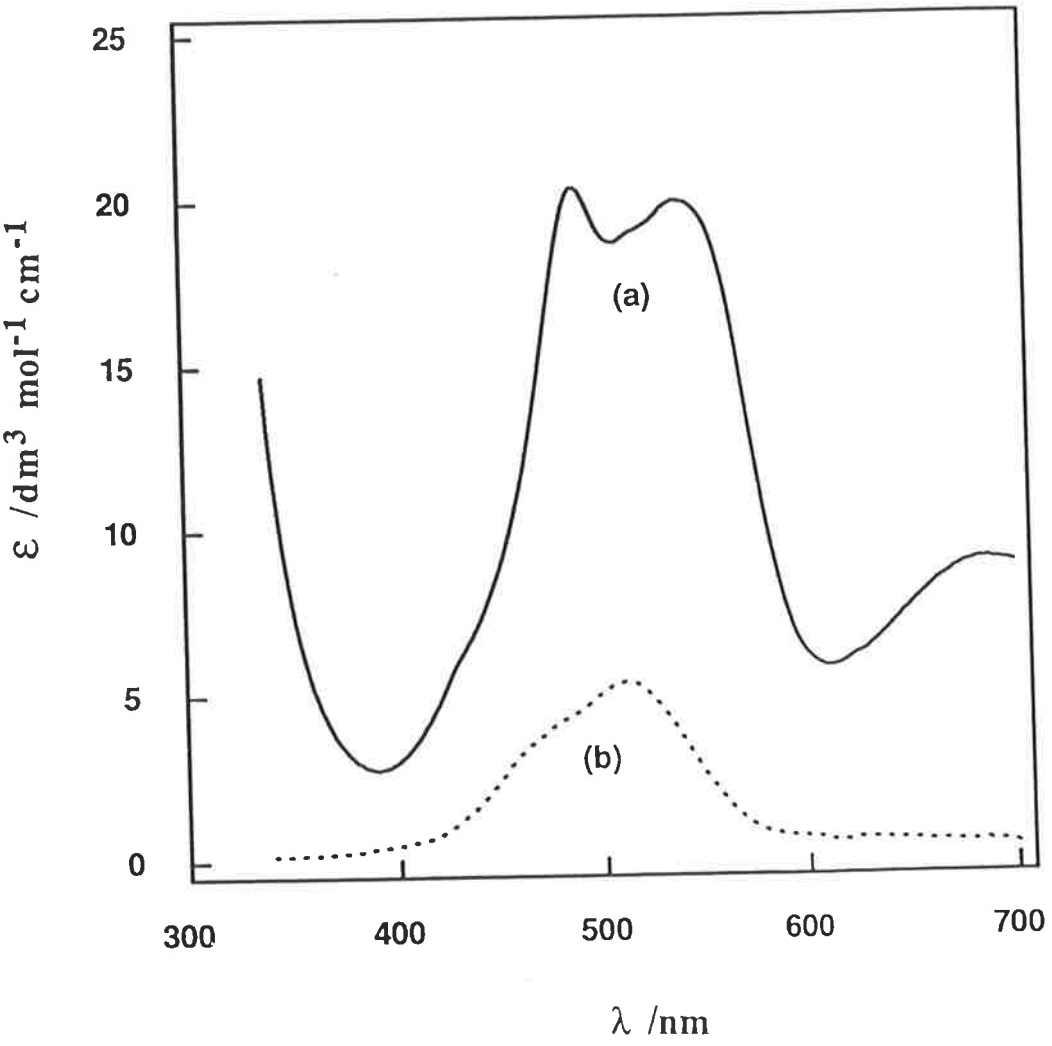

5.2.2 The Kinetics of Decomplexation

The decomplexation of the metal complexes of THEC, $[M(THEC)]^{2+}$, was studied in excess acid under pseudo first-order conditions (more than 10 fold excess concentration of acid compared to the concentration of the metal complexes). For $[Cu(THEC)]^{2+}$ and $[Ni(THEC)]^{2+}$, decomplexation was studied at 288.2, 298.2, 308.2, and 318.2 K. The decomplexation of $[Co(THEC)]^{2+}$ was found to be very fast and thus was studied at lower temperatures, namely, 283.2, 288.2, 293.2, and 298.2 K. In all cases the uncertainty in temperature was within the range of ±0.2 K and the ionic strength was kept constant at 1.50 mol dm^{-3} by adjustment with $NaNO_3$. The solutions of metal complexes of THEC contained an equimolar amount of the metal ion and the ligand. The concentrations of metal ions (and THEC) were 2.0×10^{-4} mol dm^{-3}, 7.5×10^{-4} mol dm^{-3}, and 2.5×10^{-3} mol dm^{-3} for Cu^{2+}, Ni^{2+}, and Co^{2+} respectively. The light path length of the reaction chamber was 2 cm. It should be noted that all magnitudes used for the concentrations of different components throughout this chapter represent the concentrations of the corresponding component in the reaction chamber, i.e., after mixing.

The observed values of the pseudo first-order rate constant, $k_{obs.}(s^{-1})$, for the decomplexation of $[Cu(THEC)]^{2+}$, $[Ni(THEC)]^{2+}$, and $[Co(THEC)]^{2+}$ in various concentrations of excess acid, $[H^+]_{ex.}$(mol dm^{-3}), at different temperatures and constant ionic strength of 1.50 mol dm^{-3} $NaNO_3$ are shown in Tables 5.2, 5.3, and 5.4 respectively.

Table 5.2 The observed values[a] of the pseudo first-order rate constant, $k_{obs.}(s^{-1})$, for the decomplexation of $[Cu(THEC)]^{2+}$ in various concentrations of excess acid, $[H^+]_{ex.}$(mol dm^{-3}), at 288.2, 298.2, 308.2, and 318.2 (± 0.2) K, ionic strength of 1.50 mol dm^{-3} $NaNO_3$, wavelength 630 nm ($[Cu^{2+}]$ = [THEC] = 2.0 x 10^{-4} mol dm^{-3}).

$[H^+]_{ex.}$ (mol dm^{-3})	$k_{obs.}$ (s^{-1})			
	288.2 K	298.2 K	308.2 K	318.2K
0.0078	0.014	0.027	0.049	0.083
0.0148	0.028	0.060	0.114	0.201
0.0248	0.048	0.110	0.220	0.411
0.0373	0.075	0.167	0.346	0.689
0.0498	0.096	0.224	0.480	0.949
0.0748	0.135	0.320	0.690	1.50
0.0998	0.170	0.402	0.900	1.98
0.1498	0.238	0.565	1.30	2.77
0.1998	0.305	0.724	1.67	3.45
0.2498	0.360	0.864	1.96	4.44
0.2998	0.415	0.989	2.32	4.92
0.3998	0.522	1.28	2.97	5.97
0.4998	0.625	1.51	3.45	7.29
0.6248	0.740	1.80	4.16	8.35
0.7498	0.837	2.05	4.73	9.60

[a] The experimental error in individual $k_{obs.}(s^{-1})$ values is within ±2%.

Table 5.3 The observed values[a] of the pseudo first-order rate constant, $k_{obs.}(s^{-1})$, for the decomplexation of $[Ni(THEC)]^{2+}$ in various concentrations of excess acid, $[H^+]_{ex.}$(mol dm^{-3}), at 288.2, 298.2, 308.2, and 318.2 (±0.2) K, ionic strength of 1.50 mol dm^{-3} $NaNO_3$, wavelength 365 nm ($[Ni^{2+}]$ = [THEC] = 7.5 x 10^{-4} mol dm^{-3}).

$[H^+]_{ex.}$ (mol dm^{-3})	$k_{obs.}$ (s^{-1})			
	288.2 K	298.2 K	308.2 K	318.2K
0.0199	0.0404	0.1090	0.2780	0.663
0.0314	0.0423	0.1170	0.3080	0.769
0.0404	0.0437	0.1220	0.3240	0.818
0.0507	0.0448	0.1260	0.3330	0.852
0.0743	0.0465	0.1285	0.3520	0.894
0.1022	0.0479	0.1360	0.3730	0.946
0.1536	0.0500	0.1440	0.3900	1.024
0.2051	0.0520	0.1460	0.4000	1.025
0.2493	0.0528	0.1510	0.4190	1.074
0.3080	0.0534	0.1540	0.4160	1.090
0.4109	0.0567	0.1630	0.4420	1.170
0.5138	0.0590	0.1700	0.4600	1.200

[a] The experimental error in individual $k_{obs.}(s^{-1})$ values is within ±2%.

Table 5.4 The observed values[a] of the pseudo first-order rate constant, $k_{obs.}(s^{-1})$, for the decomplexation of $[Co(THEC)]^{2+}$ in various concentrations of excess acid, $[H^+]_{ex.}$ (mol dm^{-3}), at 283.2, 288.2, 293.2, and 298.2 (± 0.2) K, ionic strength of 1.50 mol dm^{-3} $NaNO_3$, wavelength 550 nm ($[Co^{2+}]$ = [THEC] = 2.5 x 10^{-3} mol dm^{-3}).

$[H^+]_{ex.}$ (mol dm^{-3})	$k_{obs.}$ (s^{-1})			
	283.2 K	288.2 K	293.2 K	298.2 K
0.0493	10.3	15.6	22.7	32.1
0.0752	13.4	20.0	30.1	42.3
0.1011	16.5	24.6	35.3	50.7
0.1270	18.9	28.5	41.6	58.4
0.1529	22.0	33.4	48.0	68.3
0.2047	26.2	40.4	57.0	*b*
0.2565	29.3	44.6	64.0	*b*
0.3083	31.4	48.0	70.7	*b*
0.4119	36.0	55.7	*b*	*b*
0.5155	39.8	62.3	*b*	*b*
0.6191	43.8	*b*	*b*	*b*
0.7227	45.2	*b*	*b*	*b*

[a] The experimental error in individual $k_{obs.}(s^{-1})$ values is within ±5%.

[b] Data at these concentration of excess acid could not be collected because the rates of decomplexation were too fast.

5.2.3 Data Analyses and Discussion

The rate law for the decomplexation of metal complexes of THEC, $[M(THEC)]^{2+}$, can be expressed by the general equation 5.2

$$k_{obs.} = \frac{k_0 + k_1 K_1 [H^+]_{ex.} + k_2 K_1 K_2 ([H^+]_{ex.})^2}{1 + K_1 [H^+]_{ex.} + K_1 K_2 ([H^+]_{ex.})^2} \qquad (5.2)$$

where k_o, k_1, k_2 are the rate constants characterising decomplexation of zero-, mono-, and di- protonated species of metal complexes of THEC ($[M(THECH_n)]^{(n+2)+}$) respectively, and K_1 and K_2 are the corresponding protonation constants as expressed by equation 5.3.

$$K_n = \frac{[MLH_{(n+1)}{}^{(n+3)+}]}{[MLH_n{}^{(n+2)+}]\,[H^+]} \qquad (5.3)$$

The rate law (equation 5.2), is consistent with the following reaction scheme (equation 5.4, where L = THEC and the aquation of different species is not shown for simplicity) :

$$\begin{array}{ccccc} & \overset{+H^+,\,K_1}{\rightleftharpoons} & & \overset{+H^+,\,K_2}{\rightleftharpoons} & \\ [ML]^{2+} & \underset{-H^+}{} & [MLH]^{3+} & \underset{-H^+}{} & [MLH_2]^{4+} \\ \Big\downarrow (1)\ k_0 & & \Big\downarrow (2a)\ k_1 & & \Big\downarrow (2b)\ k_2 \\ M^{2+} + L & & M^{2+} + LH^+ & & M^{2+} + LH_2{}^{2+} \end{array} \qquad (5.4)$$

Inspection of the kinetic plots for each metal complex of THEC reveals that the free solvolytic decomplexation rate constant, k_o (s^{-1}), reflected in the y-axis intercept of each curve is too small to be distinguishable from the experimental error in $k_{obs.}$. Moreover, in order to maintain pseudo first-order conditions and still have a significant concentration of metal complex of THEC ([$M(THEC)^{2+}$]) to have an experimentally measurable reaction trace, data points are not attainable at very low concentrations, but are needed for a more accurate determination of k_o. Therefore, this parameter is not further discussed, although its existence is recognised.

In the case of $[Cu(THEC)]^{2+}$ decomplexation, path 2a of reaction scheme 5.4 is predominant, and the observed values (Table 5.2) of the rate constant, $k_{obs.}$(s^{-1}), were fitted to equation 5.5, using the nonlinear least square best fit program DATAFIT.[133-135]

$$k_{obs.} = \frac{k_1 K_1 [H^+]_{ex.}}{1 + K_1 [H^+]_{ex.}} \qquad (5.5)$$

The variation of $k_{obs.}$ as a function of $[H^+]_{ex.}$ fitted to equation 5.5 for the decomplexation of $[Cu(THEC)]^{2+}$ at various temperatures is shown in Figure 5.4, and the values of the parameters, k_1 (s^{-1}), and K_1 (dm^3 mol^{-1}), evaluated from the best fit are shown in Table 5.5.

Figure 5.4 The variation[a] of the observed pseudo first-order rate constant, $k_{obs.}(s^{-1})$, as a function of concentration of excess acid, $[H^+]_{ex.}$ (mol dm^{-3}), for the decomplexation of $[Cu(THEC)]^{2+}$ in excess acid, at 288.2, 298.2, 308.2, and 318.2 (± 0.2) K, ionic strength of 1.50 mol dm^{-3} $NaNO_3$, and wavelength 630 nm.

($[Cu^{2+}] = [THEC] = 2.0 \times 10^{-4}$ mol dm^{-3}).

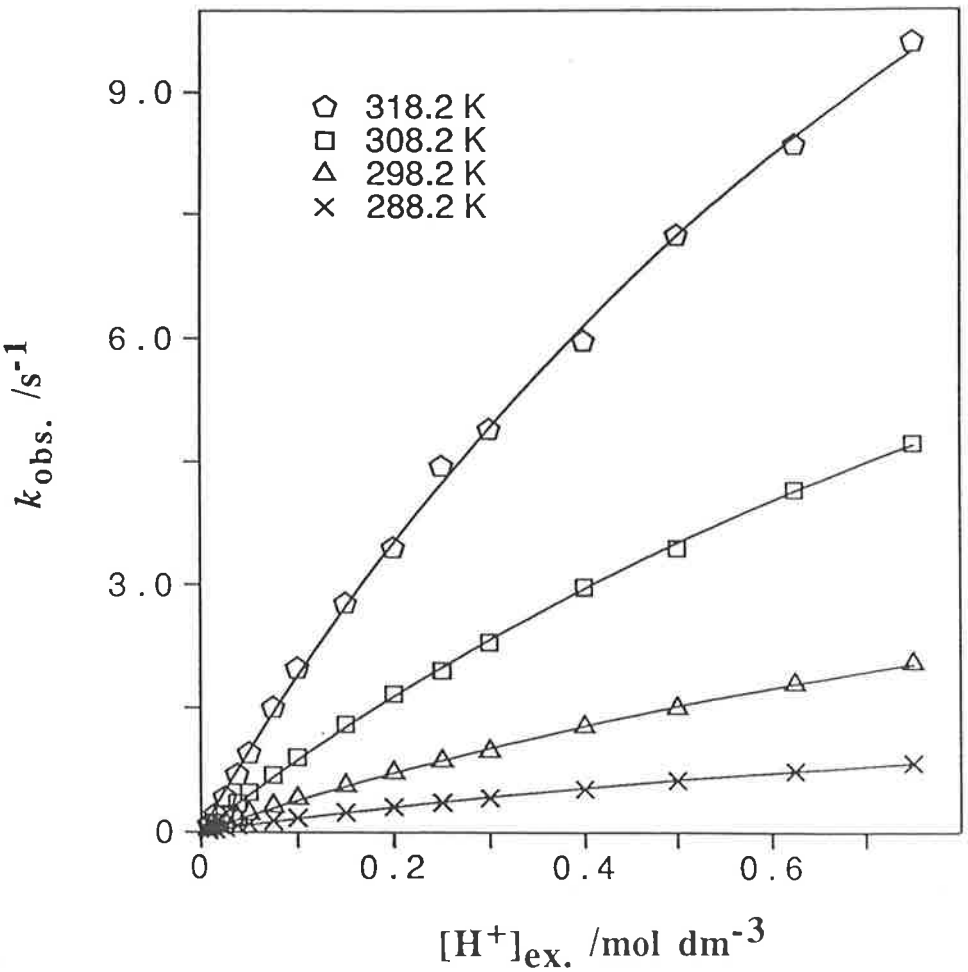

[a] The solid line represents the best fit of the experimental values of $k_{obs.}(s^{-1})$ to the equation

$$k_{obs.} = \frac{k_1 K_1 [H^+]_{ex.}}{1 + K_1 [H^+]_{ex.}}$$

308.2, and 318.2 K, and ionic strength of 1.50 mol dm^{-3} $NaNO_3$, evaluated from the best fit of the experimental values (Table 5.2) of $k_{obs.}(s^{-1})$ to equation 5.5 ($[Cu^{2+}] = [THEC] = 2.0 \times 10^{-4}$ mol dm^{-3}).

T (K)	k_1 (s^{-1})	K_1 (dm^3 mol^{-1})
288.2	2.29 (±0.11)	0.76 (±0.05)
298.2	6.07 (±0.29)[b]	0.67 (±0.04)[b]
308.2	14.5 (±0.6)	0.64 (±0.03)
318.2	24.9 (±1.2)	0.82 (±0.06)

[a] All errors (in parentheses) represent one standard deviation from the best fit of the experimental data (Table 5.2) to equation 5.5.

[b] The values of the parameters k_1 and K_1, evaluated from the best fit of the data (from the literature[24]) for the decomplexation of $[Cu(THEC)]^{2+}$ at 298.2 K and ionic strength of 1.0 mol dm^{-3} $NaClO_4$ to equation 5.5, are 7.79 (±0.86) s^{-1} and 0.565 (±0.076) dm^3 mol^{-1} respectively.

For the decomplexation of $[Ni(THEC)]^{2+}$, path 2a of reaction scheme 5.4 is predominant, but path 2b also has a minor contribution. The observed values (Table 5.3) of the rate constant, $k_{obs.}(s^{-1})$, are fitted to equation 5.6, using the same program DATAFIT.

$$k_{obs.} = \frac{k_1 K_1 [H^+]_{ex.} + k_2 K_1 K_2 ([H^+]_{ex.})^2}{1 + K_1 [H^+]_{ex.} + K_1 K_2 ([H^+]_{ex.})^2} \qquad (5.6)$$

The variation of $k_{obs.}$ (s^{-1}) as a function of $[H^+]_{ex.}$ (mol dm^{-3}) fitted to equation 5.6 for the decomplexation of $[Ni(THEC)]^{2+}$ at various temperatures is shown in Figure 5.5, and the values of the

parameters, k_1 (s^{-1}), k_2 (s^{-1}), K_1 (dm^3 mol^{-1}), and K_2 (dm^3 mol^{-1}) evaluated from the best fit are shown in Table 5.6.

Table 5.6 The values[a] of the kinetic parameters, k_1 (s^{-1}), k_2 (s^{-1}), K_1 (dm^3 mol^{-1}), and K_2 (dm^3 mol^{-1}) for the decomplexation of $[Ni(THEC)]^{2+}$ at 288.2, 298.2, 308.2, and 318.2 K, and ionic strength of 1.50 mol dm^{-3} $NaNO_3$, evaluated from the best fit of the experimental values (Table 5.3) of $k_{obs.}$(s^{-1}) to equation 5.6, considering double protonation steps, i.e., both paths 2a and 2b of reaction scheme 5.4 ($[Ni^{2+}]$ = [THEC] = 7.5 x 10^{-4} mol dm^{-3}).

T (K)	k_1 (s^{-1})	k_2 (s^{-1})	K_1 (dm^3mol^{-1})	K_2 (dm^3mol^{-1})
288.2	0.0460 (±0.0008)	0.098 (±0.027)	301 (±53)	0.659 (±0.479)
298.2	0.132 (±0.004)	0.311 (±0.127)	216 (±35)	0.546 (±0.518)
308.2	0.370 (±0.015)	0.727 (±0.287)	139 (±21)	0.685 (±0.798)
318.2	0.991 (±0.03)	4.1 (±12.9)	101 (±14)	0.16 (±0.74)

[a] All errors (in parentheses) represent one standard deviation from the best fit of the experimental data (Table 5.3) to equation 5.6.

Figure 5.5 The variation[a] of the observed pseudo first-order rate constant, $k_{obs.}$(s^{-1}), as a function of concentration of excess acid, $[H^+]_{ex.}$ (mol dm^{-3}), for the decomplexation of $[Ni(THEC)]^{2+}$ in excess acid, at

Figure 5.5 The variation[a] of the observed pseudo first-order rate constant, $k_{obs.}(s^{-1})$, as a function of concentration of excess acid, $[H^+]_{ex.}$ (mol dm^{-3}), for the decomplexation of $[Ni(THEC)]^{2+}$ in excess acid, at 288.2, 298.2, 308.2, and 318.2 (± 0.2) K, I = 1.50 mol dm^{-3} $NaNO_3$, λ = 365 nm. ($[Ni^{2+}]$ = [THEC] = 7.5 x 10^{-4} mol dm^{-3}).

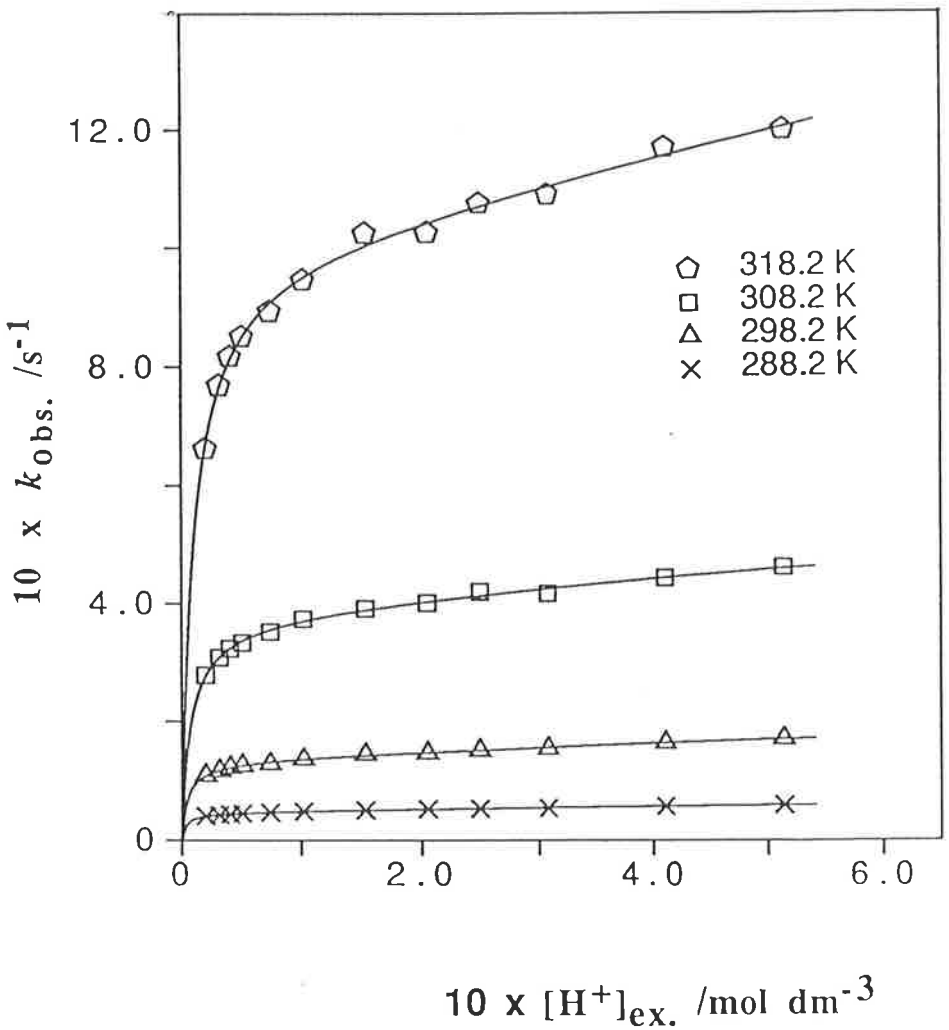

[a] The solid line represents the best fit of the experimental values of $k_{obs.}(s^{-1})$ to the equation

$$k_{obs.} = \frac{k_1 K_1 [H^+]_{ex.} + k_2 K_1 K_2 ([H^+]_{ex.})^2}{1 + K_1 [H^+]_{ex.} + K_1 K_2 ([H^+]_{ex.})^2}$$

The sums of the squares of the residuals divided by the number of degrees of freedom (8) for the fitting of the data were: 1.7433 x 10^{-7}, 1.9249 x 10^{-6}, 2.0148 x $10^{-5}$and 1.7388 x 10^{-4} in increasing magnitude of temperature.

Figure 5.6 The variation[a] of the observed pseudo first-order rate constant, $k_{obs.}(s^{-1})$, as a function of concentration of excess acid, $[H^+]_{ex.}$ (mol dm^{-3}), for the decomplexation of $[Ni(THEC)]^{2+}$ in excess acid, at 288.2, 298.2, 308.2, and 318.2 (± 0.2) K, I = 1.50 mol dm^{-3} $NaNO_3$, λ = 365 nm. ($[Ni^{2+}]$ = [THEC] = 7.5 x 10^{-4} mol dm^{-3}).

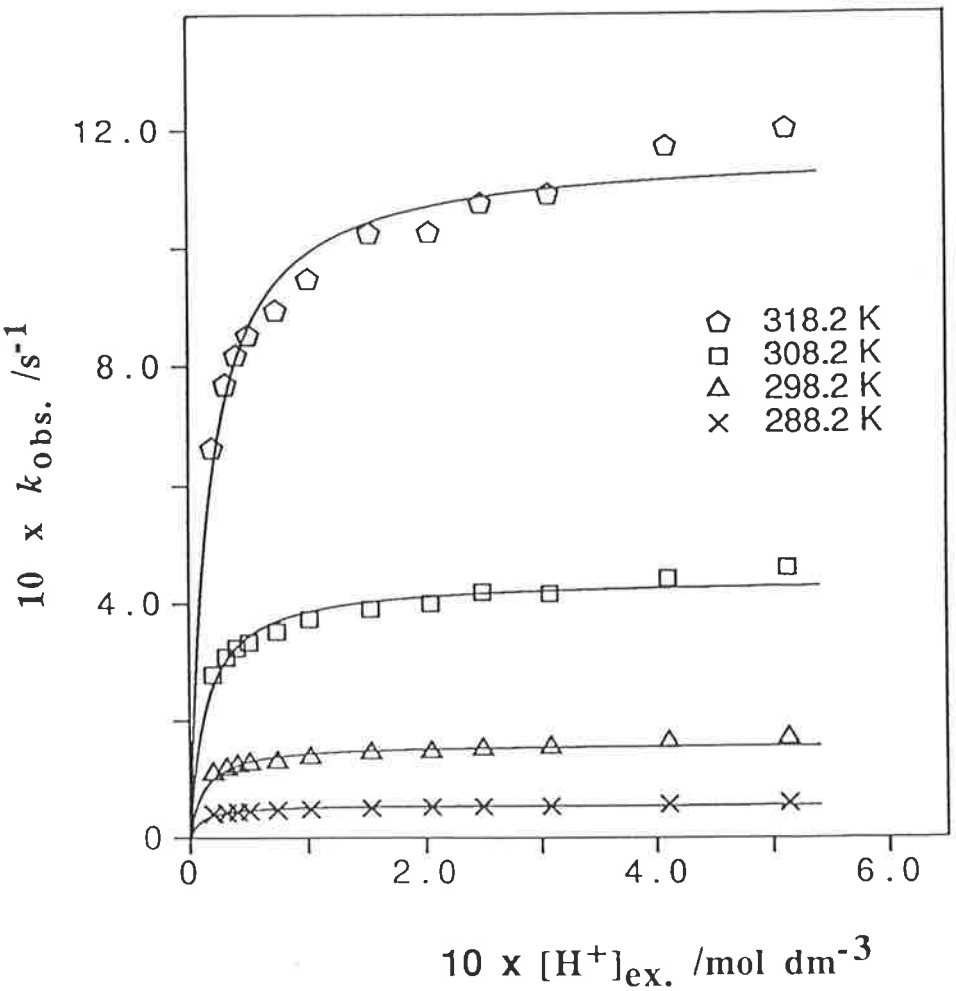

[a] The solid line represents the best fit of the experimental values of $k_{obs.}(s^{-1})$ to the equation

$$k_{obs.} = \frac{k_1 K_1 [H^+]_{ex.}}{1 + K_1 [H^+]_{ex.}}$$

The sums of squares of the residuals divided by the number of degrees of freedom (10) for fitting of the data were: 6.1107 x 10^{-6}, 5.3125 x 10^{-5}, 2.7098 x 10^{-4} and 1,8697 x 10^{-2} in increasing magnitude of temperature.

first-order rate constant, $k_{obs.}(s^{-1})$, were also fitted to equation 5.5, using the same DATAFIT program, and the variations of $k_{obs.}$ as a function of $[H^+]_{ex.}$ is shown in Figure 5.6, and the values of parameters k_1 and K_1 evaluated from the best fit are shown in Table 5.7.

Table 5.7 The values[a] of the kinetic parameters, k_1 (s^{-1}), and K_1 (dm^3 mol^{-1}), for the decomplexation of $[Ni(THEC)]^{2+}$ at 288.2, 298.2, 308.2, and 318.2 K, and ionic strength of 1.50 mol dm^{-3} $NaNO_3$, evaluated from the best fit of the experimental values (Table 5.3) of $k_{obs.}(s^{-1})$ to equation 5.5, considering only one protonation step, i.e., path 2a of reaction scheme 5.4 ($[Ni^{2+}] = [THEC] = 7.5 \times 10^{-4}$ mol dm^{-3}).

T (K)	k_1 (s^{-1})	K_1 (dm^3 mol^{-1})
288.2	0.0554 (±0.0012)	101.(±17)
298.2	0.160 (±0.004)	83 (±13)
308.2	0.441 (±0.008)	69.8 (±8.5)
318.2	1.16 (±0.02)	57.3 (±6.5)

[a] All errors (in parentheses) represent one standard deviation from the best fit of the experimental data (Table 5.3) to equation 5.5.

Comparison between Figures 5.5 and 5.6, reveals that the experimental data for the decomplexation of $[Ni(THEC)]^{2+}$ in excess acid is better fitted to equation 5.6. However, activation parameters have been evaluated corresponding to the kinetic parameter k_1 for both models (see the latter part of this section).

In the case of $[Co(THEC)]^{2+}$ decomplexation at various temperatures, path 2a (of equation 5.4) is predominant. The observed values (Table 5.4) of the pseudo first-order rate constant, $k_{obs.}(s^{-1})$, were fitted to equation 5.5 using the program DATAFIT. The variation of $k_{obs.}$ as a function of $[H^+]_{ex.}$ are shown in Figure 5.7, and the values of the parameters k_1 and K_1 evaluated from the best fit are shown in Table 5.8.

Table 5.8 The values[a] of the kinetic parameters, k_1 (s^{-1}), and K_1 (dm^3 mol^{-1}) for the decomplexation of $[Co(THEC)]^{2+}$ at 283.2, 288.2, 293.2, and 298.2, and ionic strength of 1.50 mol dm^{-3} $NaNO_3$, evaluated from the best fit of the experimental values (Table 5.4) of $k_{obs.}(s^{-1})$ to equation 5.5 ($[Co^{2+}] = [THEC] = 2.5 \times 10^{-3}$ mol dm^{-3}).

T (K)	k_1 (s^{-1})	K_1 (dm^3 mol^{-1})
283.2	62.7 (±1.4)	3.47 (±0.17)
288.2	95.0 (±2.9)	3.50 (±0.21)
293.2	127 (±6)	3.98 (±0.30)
298.2	151 (±19)	5.2 (±1.0)

[a] All errors (in parentheses) represent one standard deviation from the best fit of the experimental data (Table 5.4) to equation 5.5.

Figure 5.7 The variation[a] of the observed pseudo first-order rate constant, $k_{obs.}(s^{-1})$, as a function of concentration of excess acid, $[H^+]_{ex.}$ (mol dm^{-3}), for the decomplexation of $[Co(THEC)]^{2+}$ in excess acid, at

Figure 5.7 The variation[a] of the observed pseudo first-order rate constant, $k_{obs.}(s^{-1})$, as a function of concentration of excess acid, $[H^+]_{ex.}$ (mol dm^{-3}), for the decomplexation of $[Co(THEC)]^{2+}$ in excess acid, at 283.2, 288.2, 293.2, and 298.2 (± 0.2) K, ionic strength of 1.50 mol dm^{-3} $NaNO_3$, and wavelength 550 nm.

($[Co^{2+}] = [THEC] = 2.5 \times 10^{-3}$ mol dm^{-3}).

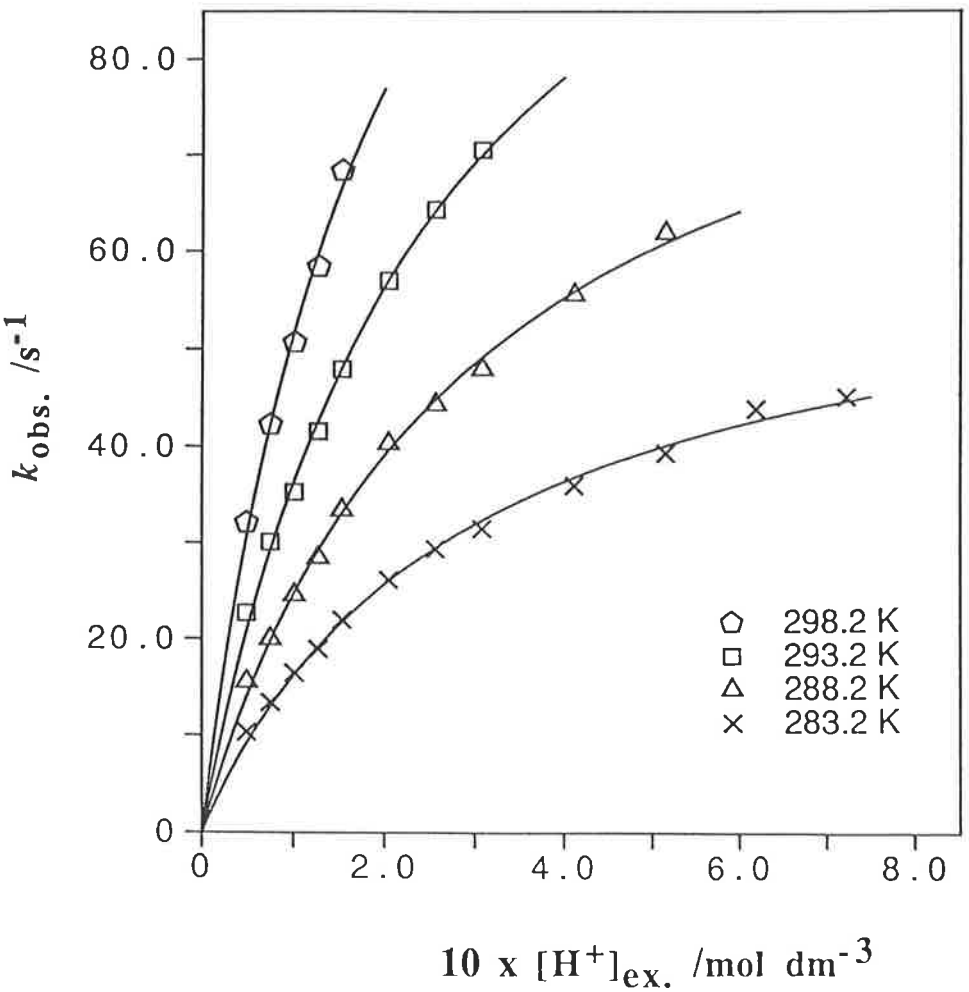

[a] The solid line represents the best fit of the experimental values of $k_{obs.}(s^{-1})$ to the equation

$$k_{obs.} = \frac{k_1 K_1 [H^+]_{ex.}}{1 + K_1 [H^+]_{ex.}}$$

protonated species ($[M(THECH)]^{3+}$), and (ii) $[Ni(THEC)]^{2+}$ occurs via mono-protonated species ($[Ni(THECH)]^{3+}$) and a very small amount of di-protonated species ($[Ni(THECH_2)]^{4+}$).

The observed half lives, $t_{(1/2)}$ (s) for the decomplexation of metal complexes of THEC ($[M(THEC)]^{2+}$) found in the present studies in aqueous solution of 0.1 mol dm^{-3} acid at 298.2 K and ionic strength of 1.50 mol dm^{-3} $NaNO_3$ are as follows :

$[M(THEC)]^{2+}$	$[Cu(THEC)]^{2+}$	$[Ni(THEC)]^{2+}$	$[Co(THEC)]^{2+}$
$t_{(1/2)}$ (s)	1.8	5.1	0.013

These values may be compared to the half-life observed by *Hay et al.*[21] for the decomplexation of $[Cu(TCEC)]^{2+}$ at 298.2 K, in ~0.5 mol dm^{-3} $[H^+]$ (I = 0.98 mol dm^{-3}) of ~0.03 s. The half-life for the decomplexation of $[Cu(TCEC)]^{2+}$ is shorter than that of $[Cu(THEC)]^{2+}$ which is consistent, since the -CN group is an electron withdrawing group, and thus Cu-N bonds in the macrocyclic ring of TCEC are much weaker than those in THEC. On the other hand, the decomplexation of metal complexes of cyclam is very slow. For example, the decomplexation of $[Ni(cyclam)]^{2+}$ in 1.0 mol dm^{-3} $HClO_4$ is estimated to have a half life of 30 years,[93] and $[Cu(cyclam)]^{2+}$ dissolved in 6 mol dm^{-3} HCl is not decomplexed over a period of several weeks.[69] This indicates the significant effect of coordinating pendant arms on the lability of metal complexes of THEC.

Figure 5.8 The variation[a] of the observed pseudo first-order rate constant, $k_{obs.}$(s^{-1}), as a function of excess acid concentration, $[H^+]_{ex.}$ (mol dm^{-3}), for the decomplexation of $[Cu(THEC)]^{2+}$ in excess acid, at

Figure 5.8 The variation[a] of the observed pseudo first-order rate constant, $k_{obs.}(s^{-1})$, as a function of excess acid concentration, $[H^+]_{ex.}$ (mol dm^{-3}), for the decomplexation of $[Cu(THEC)]^{2+}$ in excess acid, at 298.2K, ionic strength of 1.0 mol dm^{-3} adjusted with $NaClO_4$, and wavelength 627 nm (data collected from the literature,[24] Table 5.9; in the literature, the experimental data were fitted to the linear form of equation 5.5, assuming the limiting conditions, $K_1 [H^+]_{ex.} << 1$).

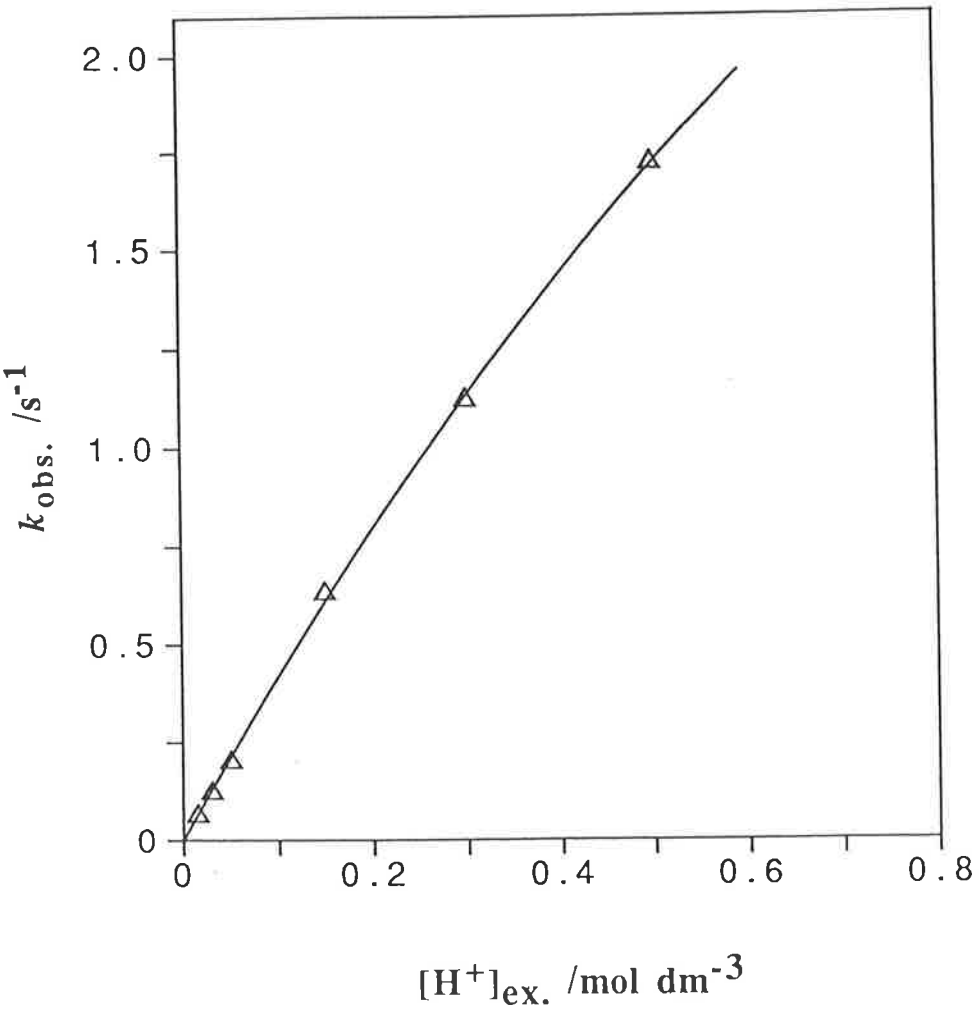

[a] The solid line represents the best fit of the experimental values of $k_{obs.}(s^{-1})$ to the equation

$$k_{obs.} = \frac{k_1 K_1 [H^+]_{ex.}}{1 + K_1 [H^+]_{ex.}}$$

Figure 5.9 The variation[a] of the observed pseudo first-order rate constant, $k_{obs.}(s^{-1})$, as a function of concentration of excess acid, $[H^+]_{ex.}$ (mol dm^{-3}), for the decomplexation of $[Cu(THEC)]^{2+}$ in excess acid, at 298.2K :

△ data from the literature (I = 1.0 mol dm^{-3} $NaClO_4$),[24] and

□ present work (I = 1.50 mol dm^{-3} $NaNO_3$).

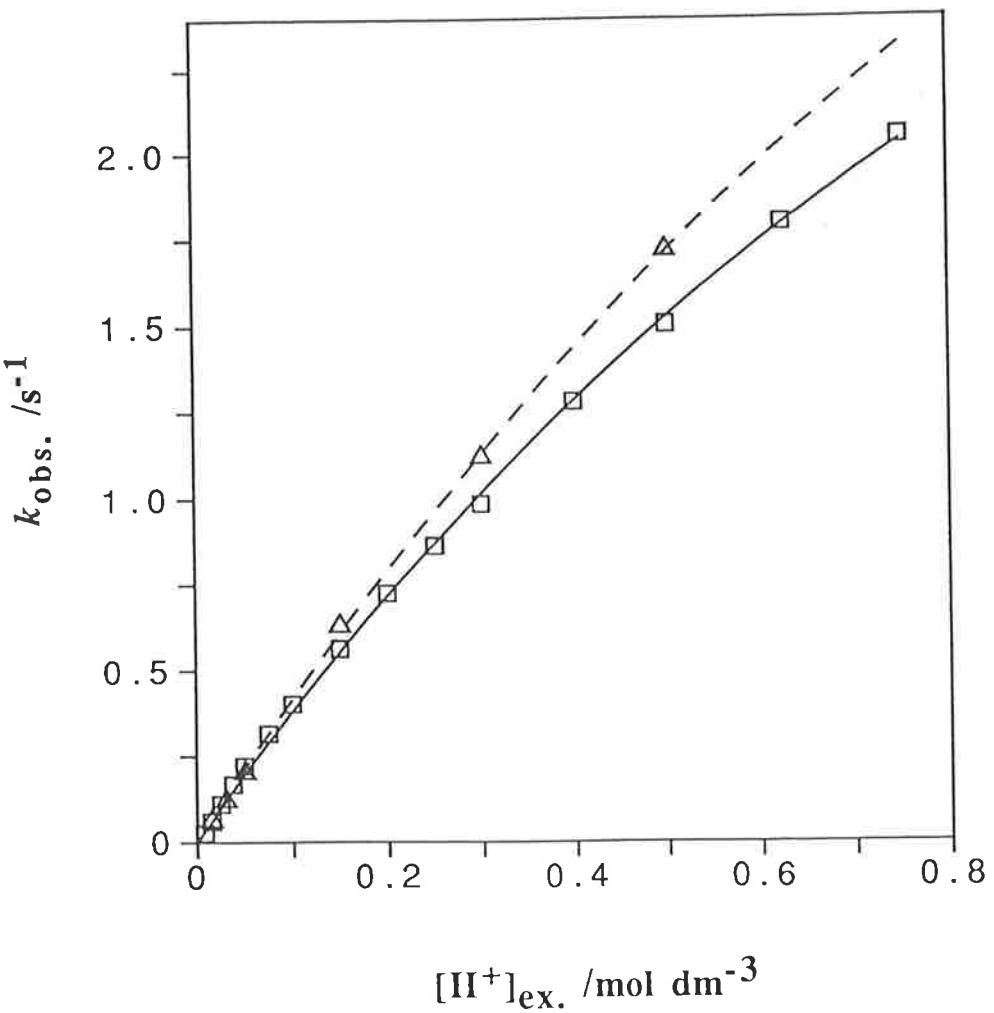

[a] The solid line represents the best fit of the values of $k_{obs.}(s^{-1})$ to the equation

$$k_{obs.} = \frac{k_1 K_1 [H^+]_{ex.}}{1 + K_1 [H^+]_{ex.}}$$

298.2 K and ionic strength of 1.0 mol dm^{-3} of $NaClO_4$ in various concentrations of $HClO_4$ acid carried out by *Hay et al.*, are collected from the literature,[24] and are fitted to equation 5.5 using the DATAFIT program, and the best fit plot of $k_{obs.}(s^{-1})$ vs. $[H^+]_{ex.}$ (mol dm^{-3}) are shown in Figure 5.8 (and together with that of the present work are shown in Figure 5.9), and the values of the parameters k_1 and K_1 evaluated from the best fit are shown at the bottom of Table 5.5 (In the literature, the experimental data were fitted to the linear equation 5.5 assuming the limiting conditions, $K_1\ [H^+]_{ex.} << 1$) which are comparable to the values evaluated from the present work (see Table 5.5). The higher value of the equilibrium constant (K_1) for the formation of mono-protonated complex species and the lower values of rate constant (k_1) observed in the present study may be due to higher ionic strength, since at higher ionic strength the higher charged species are more stable.

At a given temperature, the order of lability exhibited for the decomplexation of $[M(THEC)]^{2+}$ ($Co^{2+} > Cu^{2+} > Ni^{2+}$) contrasts with that observed in six coordinate systems ($Cu^{2+} > Co^{2+} > Ni^{2+}$).[88,140,141] Thus for mechanistic investigation, it is necessary to consider the activation parameters, $\Delta H^{\#}$ (enthalpy of activation), and $\Delta S^{\#}$ (entropy of activation). These parameters can be evaluated from transition state theory.[142] According to this theory, using the Eyring equation, the temperature dependence of the kinetic parameter, k_1, can be expressed by equation 5.7,

$$k_1 = \frac{T k_B}{h} \left(\exp - \frac{\Delta H^{\#}}{R T} \right) \left(\exp \frac{\Delta S^{\#}}{R} \right) \qquad (5.7)$$

where k_B = Boltzmann's constant,
T = absolute temperature,

h = Planck's constant, and
R = Gas constant.

Thus, the values of $\Delta H^{\#}$ and $\Delta S^{\#}$ for the decomplexation of $[M(THEC)]^{2+}$ have been evaluated by fitting the experimental values of kinetic parameter, k_1, at different temperatures (Tables 5.5, 5.6 and 5.8) to equation 5.7 using the same nonlinear least square best fit program DATAFIT. The variation of $\ln(\frac{k_1}{T})$ as a function of $\frac{1}{T}$ are shown in Figures 5.10, 5.11, and 5.12, for the decomplexation of $[Cu(THEC)]^{2+}$, $[Ni(THEC)]^{2+}$, and $[Co(THEC)]^{2+}$, respectively, and the values of $\Delta H^{\#}$ (kJ mol^{-1}) and $\Delta S^{\#}$ ($JK^{-1}mol^{-1}$) are shown in Table 5.9.

Table 5.9 reveals that $\Delta H^{\#}$ is the main contributor to the lability of the metal complexes, $[M(THEC)]^{2+}$, and the order of the lability of metal complexes ($Co^{2+} > Cu^{2+} > Ni^{2+}$) is consistent with the order of $\Delta H^{\#}$ ($Co^{2+} < Cu^{2+} < Ni^{2+}$). Thus the decomplexation of $[Co(THEC)]^{2+}$ is very rapid, and the higher rate is due to a lower positive $\Delta H^{\#}$ value.

From the negative $\Delta S^{\#}$ values, it is not possible to conclude whether the decomplexation occurs through an I_a or an I_d mechanism, since the negative sign (the decrease in entropy value) may arise from the electrostriction effect and solvation effect.

Table 5.9 The values[a] of enthalpy of activation, $\Delta H^{\#}$ (k J mol^{-1}), and entropy of activation, $\Delta S^{\#}$ (J K^{-1} mol^{-1}), for the acid catalysed decomplexation of $[M(THEC)]^{2+}$, at various temperatures and ionic strength of 1.50 mol dm^{-3} $NaNO_3$, where the experimental values (Tables 5.5, 5.6, 5.7, and 5.8) of the kinetic parameter, k_1 (s^{-1}), are fitted to equation 5.7.

$[M(THEC)]^{2+}$	$\Delta H^{\#}$ (k J mol^{-1})	$\Delta S^{\#}$ (J K^{-1} mol^{-1})
$[Cu(THEC)]^{2+}$	58.9 (±4.2)	-32.9(±13.9)
$[Ni(THEC)]^{2+}$	75.5(±0.8)[b] 74.8(±0.4)[c]	-8.3 (±2.7)[b] -9.1(±1.6)[c]
$[Co(THEC)]^{2+}$	38.8 (±5.0)	-73 (±17)

[a] All errors (in parentheses) represent one standard deviation from the best fit of the experimental data to equation 5.12.

[b] These values of $\Delta H^{\#}$ and $\Delta S^{\#}$ for the decomplexation of $[Ni(THEC)]^{2+}$ are evaluated on the basis of a two step model, equation 5.6 (considering both the paths 2a and 2b of reaction scheme 5.4).

[c] These values of $\Delta H^{\#}$ and $\Delta S^{\#}$ for the decomplexation of $[Ni(THEC)]^{2+}$ are evaluated on the basis of a one step model, equation 5.5 (considering the path 2a of reaction scheme 5.4).

(i) The electrostriction effect

The rate laws for the decomplexation of $[M(THEC)]^{2+}$ indicate that at least one proton is involved in the transition state of the decomplexation reactions. That is, the activated complex, $[M(THECH)]^{3+}$, is formed from two ions of like charge, $[M(THEC)]^{2+}$ and H^+. Thus the water molecules around the activated complex are more ordered causing a decrease in entropy of activation.[105]

(ii) The solvation effect

A fully coordinated N-atom can not be protonated. Thus to form the mono-protonated complex, $[M(THECH)]^{3+}$ in the transition state one M-N bond must be broken or partly broken.[82] According to the mechanism proposed in Figure 6.1, in the transition state the metal ion is less coordinated to the ligand and is potentially susceptible to increased solvation . Since the rate determining step is very slow compared to water exchange rates, there is some probability of increased solvation of the metal ion in the transition state which may cause a decrease in entropy of activation values.

However, the reasons for a large decrease in the values of $\Delta H^{\#}$ and $\Delta S^{\#}$ for the decomplexation of $[Co(THEC)]2^+$ is not clear. The size effect of metal ion (octahedral ionic radii),[143]

$$Co^{2+}\ (75\ pm) > Cu^{2+}\ (73\ pm) > Ni^{2+}\ (69\ pm)$$

is not sufficient enough to account for so large a difference.

Figure 5.10 The variation[a] of $\ln(\frac{k_1}{T})$ as a function of $\frac{1}{T}$ (K^{-1}) for the acid catalysed decomplexation of $[Cu(THEC)]^{2+}$ at various temperatures and at an ionic strength of 1.50 mol dm^{-3} $NaNO_3$.

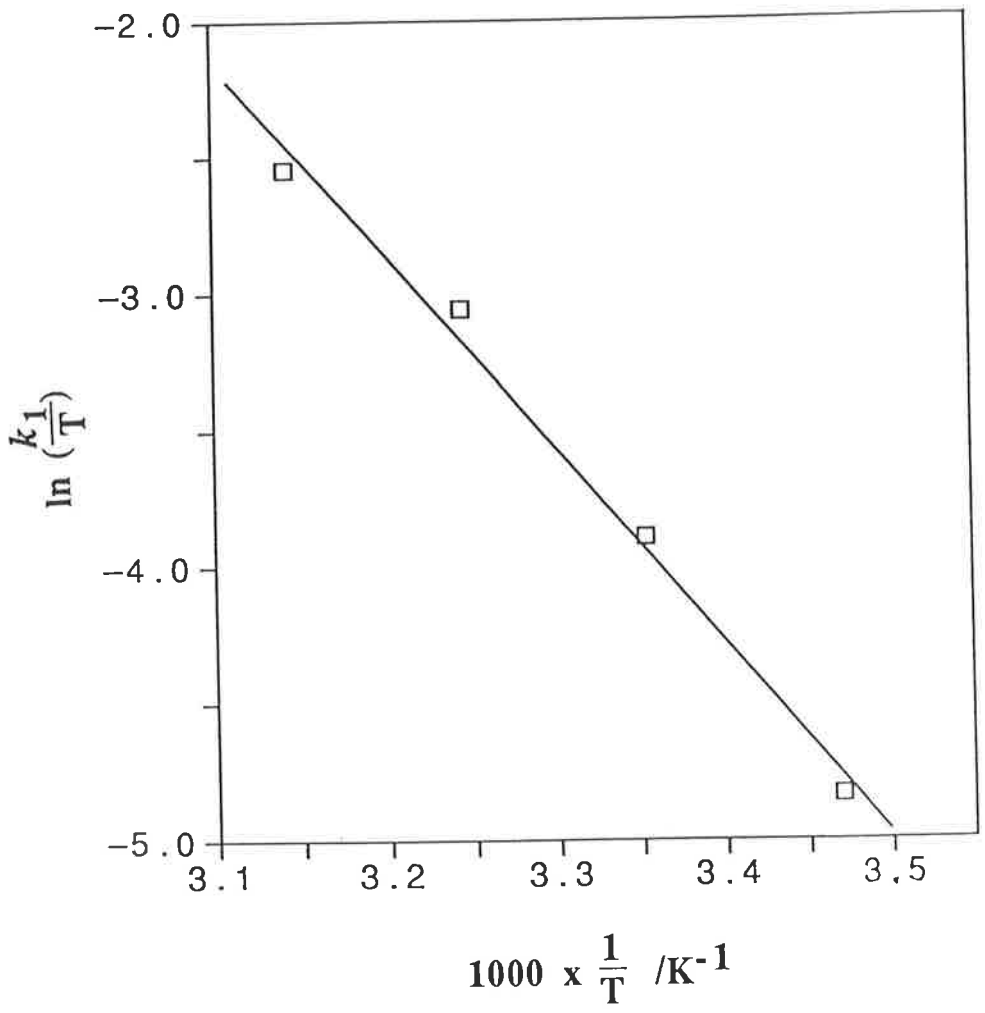

[a] The solid line represents the best fit of the experimental values of the kinetic parameter, k_1 (s^{-1}), to the equation

$$k_1 = \frac{Tk_B}{h} \left(\exp - \frac{\Delta H^{\#}}{RT} \right) \left(\exp \frac{\Delta S^{\#}}{R} \right)$$

Figure 5.11 The variation[a] of $\ln(\frac{k_1}{T})$ as a function of $\frac{1}{T}$ (K^{-1}) for the acid catalysed decomplexation of $[Ni(THEC)]^{2+}$ at various temperatures and at an ionic strength of 1.50 mol dm^{-3} $NaNO_3$ (data from the two step model, Table 5.6).

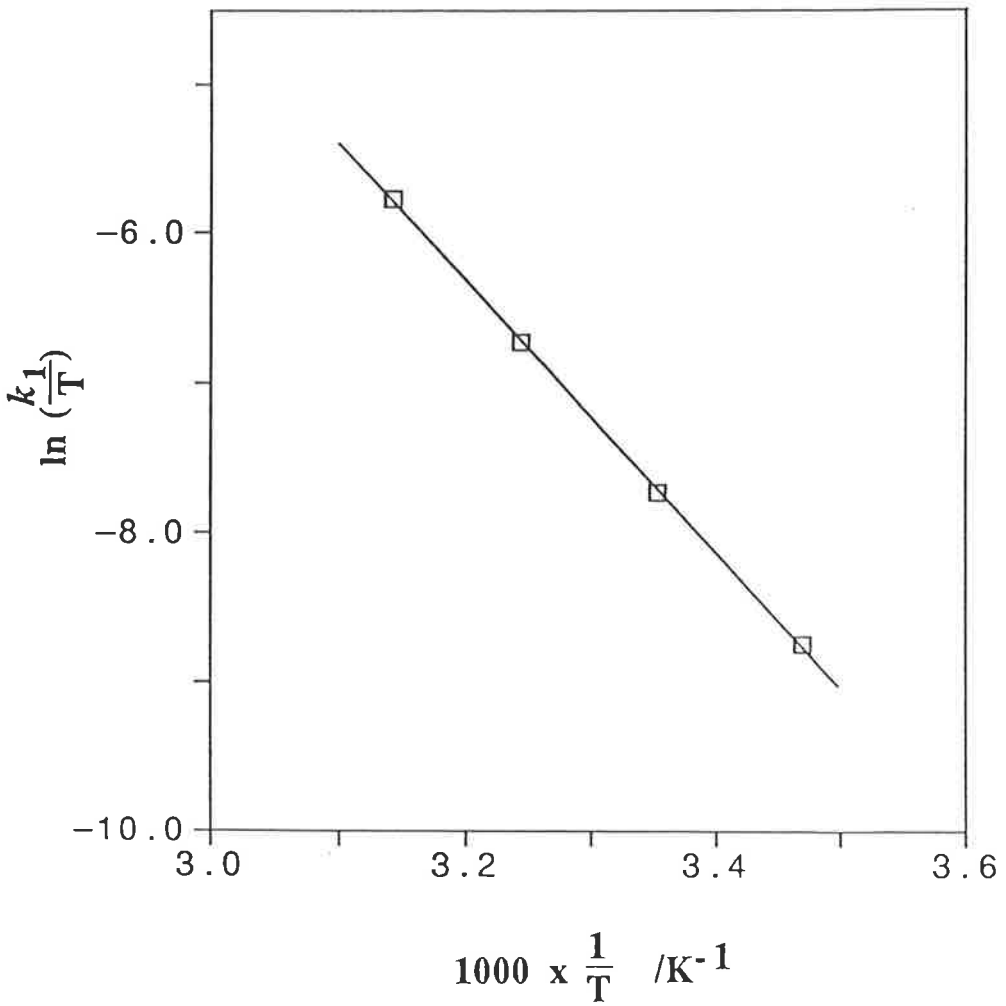

[a] The solid line represents the best fit of the experimental values of the kinetic parameter, k_1 (s^{-1}), to the equation

$$k_1 = \frac{Tk_B}{h} \left(\exp - \frac{\Delta H^{\#}}{RT}\right) \left(\exp \frac{\Delta S^{\#}}{R}\right)$$

Figure 5.11a The variation[a] of $\ln(\frac{k_1}{T})$ as a function of $\frac{1}{T}$ (K^{-1}) for the acid catalysed decomplexation of $[Ni(THEC)]^{2+}$ at various temperatures and at an ionic strength of 1.50 mol dm^{-3} $NaNO_3$ (data from the one step model, Table 5.7).

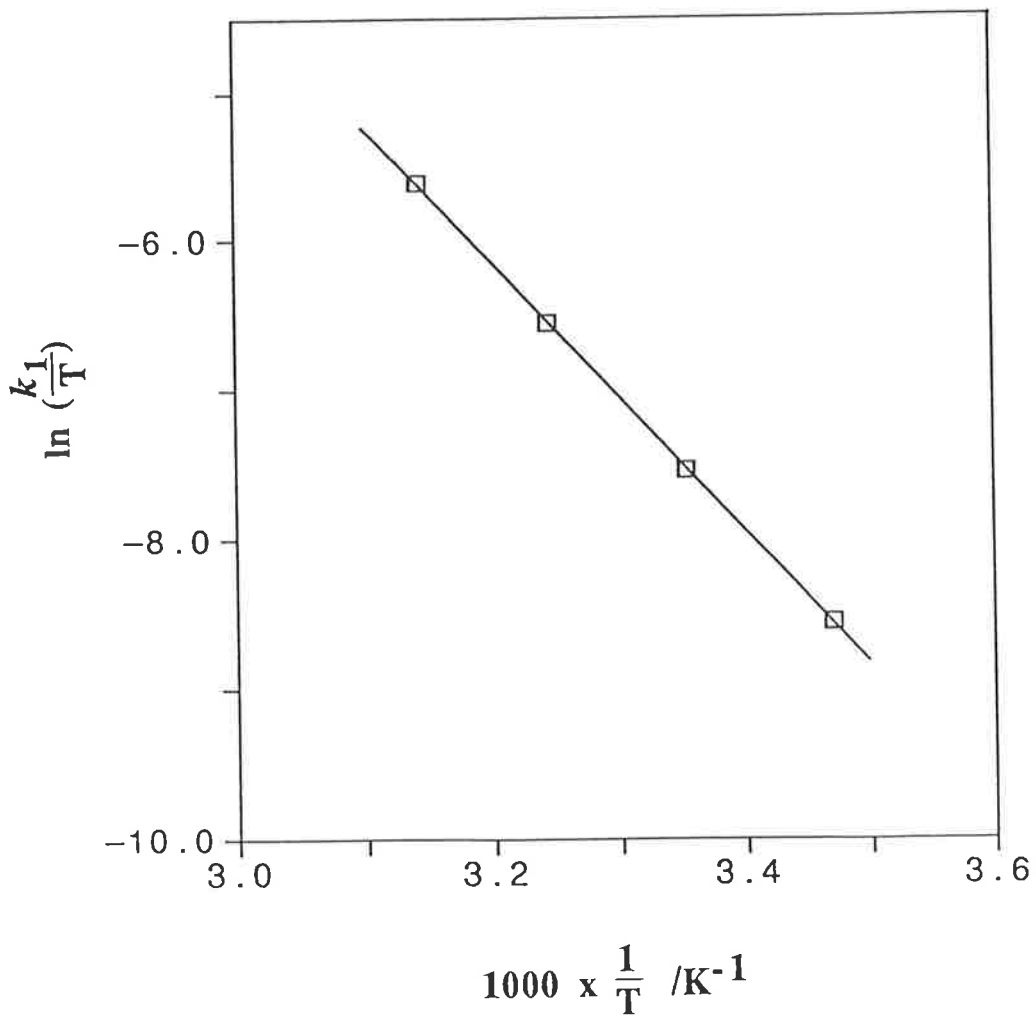

[a] The solid line represents the best fit of the experimental values of the kinetic parameter, k_1 (s^{-1}), to the equation

$$k_1 = \frac{Tk_B}{h} \left(\exp - \frac{\Delta H^{\#}}{RT}\right) \left(\exp \frac{\Delta S^{\#}}{R}\right)$$

Figure 5.12 The variation[a] of $\ln(\frac{k_1}{T})$ as a function of $\frac{1}{T}$ (K^{-1}) for the acid catalysed decomplexation of $[Co(THEC)]^{2+}$ at various temperatures and at an ionic strength of 1.50 mol dm^{-3} $NaNO_3$.

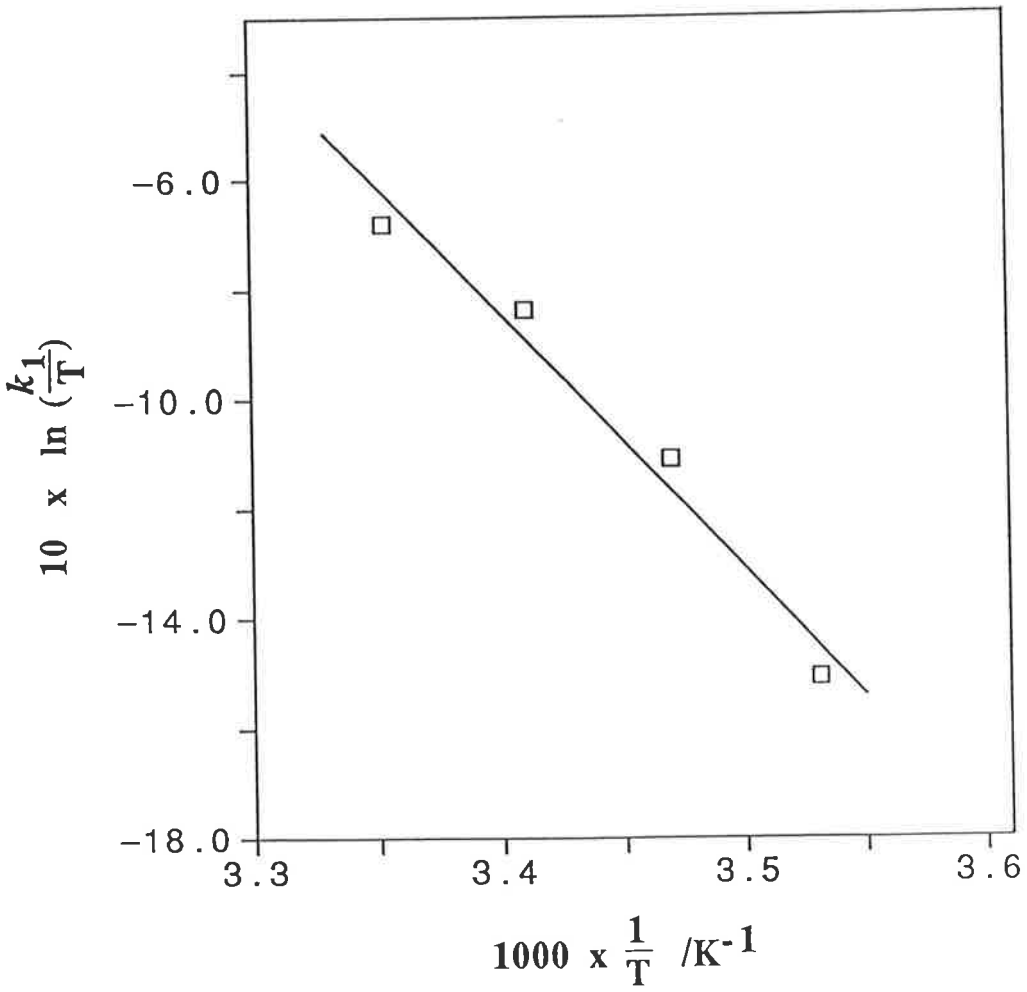

[a] The solid line represents the best fit of the experimental values (Table 5.8) of the kinetic parameter, k_1 (s^{-1}), to the equation

$$k_1 = \frac{Tk_B}{h} \left(\exp - \frac{\Delta H^{\#}}{RT} \right) \left(\exp \frac{\Delta S^{\#}}{R} \right)$$

The rate law (equation 5.2) for the reaction scheme (equation 5.3) can also be expressed by equations 5.9 to 5.11

$$\text{Rate} = k_o\,[ML] + k_1\,[MLH^+] + k_2\,[MLH_2^{2+}] \qquad (5.9)$$

$$= k_o\,[ML] + k_1 K_1\,[ML]\,[H^+] + k_2 K_1 K_2\,[ML]\,[H]^2 \qquad (5.10)$$

$$= k^{ML}\,[ML] + k_H^{ML}\,[ML]\,[H^+] + k_{H2}^{ML}\,[ML]\,[H]^2 \qquad (5.11)$$

where $k^{ML} = k_o$, (s^{-1})

$k_H^{ML} = k_1 K_1$, $(dm^3\ mol^{-1}s^{-1})$

$k_{H2}^{ML} = k_2 K_1 K_2$, $(dm^6\ mol^{-2}\ s^{-1})$

For comparison, the values of k_H^{ML} for the decomplexation of $[M(TMC)]^{2+}$ carried out by *Hertli et al.*,[72] are collected and shown in Table 5.10 including the present values ($k_H^{ML} = k_1 K_1$) for the decomplexation of $[M(THEC)]^{2+}$.

From Table 5.10, it is evident that the 2-hydroxyethyl pendant arm has a significant effect on the rates of decomplexation of $[M(THEC)]^{2+}$ in excess acid. In Chapter 4, it has been observed that the rates (see Table 4.6) of complexation of $[Co(H_2O)_6]^{2+}$ and $[Ni(H_2O)_6]^{2+}$ with THEC are 5-83 times faster than those with TMC whereas the rates of decomplexation (see Table 5.10) of metal complexes of THEC, $[M(THEC]^{2+}$, are 300-800 times faster than those of TMC, $[M(TMC)]^{2+}$. Thus the enhanced stabilities of metal complexes of TMC, $[M(TMC)]^{2+}$, are due to their slower decomplexation compared to those of THEC. Similarly, it can be concluded that the extremely high stability

(the macrocyclic effect) observed in the case of metal complexes of cyclam is due to the very slow decomplexation of its complexes.

Table 5.10 The values of k_H^{ML} (dm^3 mol^{-1} s^{-1}) for the acid catalysed decomplexation of $[M(TMC)]^{2+}$ carried out by *Hertli et al.*,[72] at 298.2 K and ionic strength of 0.5 mol dm^{-3} KNO_3, and for the acid catalysed decomplexation of $[M(THEC)]^{2+}$ carried out in the present investigation (at 298.2 ±0.2 K and ionic strength of 1.50 mol dm^{-3} $NaNO_3$).

Ligand	k_H^{ML} (dm^3 mol^{-1} s^{-1})		
	Cu^{2+}	Ni^{2+}	Co^{2+}
TMC	6.7×10^{-3}	2.9×10^{-2} *a*	2.5
THEC	4.07	28.5*b*	785.2

a The half life for the decomplexation of $[Ni(cyclam)]^{2+}$ in acid solution is 30 years.[93]

b This value calculated from the two step model and for the one step model the corresponding value is 13.2 dm^3 mol^{-1} s^{-1}.

CHAPTER 6

GENERAL CONCLUSIONS

6.1 INTRODUCTION

The interpretation of the observed kinetic data and the deduction of a mechanism from the interpreted rate law is based on previous experience[99] and is a product of the intellectual imagination.[101] Sometimes the interpreted rate law or proposed mechanism is incorrect or controversial. For example, from the observed kinetic data for the acid catalysed decomplexation of the Ni^{2+} complex of cis,cis-1,3,5-triaminocyclohexane (c-tach), *Childers et al.*[144] proposed a mechanism which was strongly criticised by *Margerum et al.*,[82] and the latter group of authors postulated an alternative mechanism. Subsequently, in a kinetic study of acid catalysed decomplexation of Ni^{2+} complexes of some triaza macrocyclic ligands, *Murphy et al.*[114] observed some marked similarities between their results and those observed by *Childers et al.* Thus *Murphy et al.* proposed a mechanism which was a combination of both the mechanisms proposed by *Childers et al.* and *Margerum et al.* Similarly the mechanism proposed by *Chock*[145] for a crown ether system was rejected by *Cox et al.*[146]

The main conclusions of the present study and the incidental measured parameters are outlined briefly in the following sections, and where appropriate are compared with the literature.

6.2 The pK_a values of THEC

The apparent pK_a values (Table 3.1) for THEC evaluated in this study are found to be greater than the literature values[23, 24] probably due to the higher ionic strength. The difference between the present values and the literature values,[23] that is, ΔpK_a, increase in the following order:

$$\Delta pK_{a1}\ (0.45) < \Delta pK_{a2}\ (0.55) < \Delta pK_{a3}\ (0.62) < \Delta pK_{a4}\ (1.86).$$

This trend implies that the presence of ions of inert electrolyte stabilises the higher charged species to a greater extent than the lower charged ones.

6.3 The Stabilities of Complex Species in Solution

The determination of the concentration stability constants of the various complex species by potentiometric titration indicates that mainly two complex species exist in aqueous solution for each metal-THEC system studied. The $[M(THEC)]^{2+}$ species is predominant at lower pH (6-8) and the mono-deprotonated species $[M(THEC-H)]^{+}$ is predominant at higher pH (>8). The di-deprotonated species, $[M(THEC-H_2)]$, was not observed in the pH range over which the titration was carried out.

Thc log values of the stability constants, $\log\beta_{110}$ and $\log\beta_{11-1}$, respectively for $[M(THEC)]^{2+}$ and $[M(THEC-H)]^{+}$ evaluated in this study (Table 3.2) may be compared to the literature values.[23,24] For example, the values of $\log\beta_{110}$ for $[Cu(THEC)]^{2+}$ and $[Ni(THEC)]^{2+}$ are larger than the literature values[24] by 0.5 whereas that for $[Co(THEC)]^{2+}$ is less

than the literature value[23] by 0.21. Such discrepancies may arise either (i) from the effect of higher ionic strength, since the effects of ionic strength on different systems or even on the same system are not always linear,[147] or (ii) from experimental errors, for example, the difference in $\log\beta_{110}$ values for $[Cu(THEC)]^{2+}$ at the same ionic strength and temperature determined by *Hay et al.*[24] and *Madeyski et al.*[23] is 0.5.

6.4 The Macrocyclic Effect

From the comparison of the rates of complexation and rates of decomplexation, if the effects of ionic strength are ignored, it has been observed that the rates of metal ion (Co^{2+} and Ni^{2+}) complexation with THEC are only 5-83 times faster than those with TMC (Table 4.6) whereas the rates of acid catalysed decomplexation of the metal complexes of THEC are 300-980 times faster than those of TMC (see Table 5.10). This indicates that the larger stability constants for the metal complexes of TMC are due to the much slower rates of decomplexation compared to those of THEC. From this fact, it can be concluded that the enhanced stability (the macrocyclic effect) observed in the case of metal complexes of tetraaza macrocyclic ligands is related to their rates of decomplexation rather than in their rates of formation. A similar conclusion has also been drawn by other authors, namely that the stability of metal complexes of tetraaza macrocyclic ligands is reflected mostly in the decomplexation rate constant.[26,28,40]

6.5 The Kinetics of Complexation of Metal Ions with THEC

The kinetic studies of complexation of metal ions with THEC indicate that although the di-protonated form of the ligand, LH_2^{2+}, is the predominant species over the pH range studied, the mono-protonated species is the predominant reacting species. *Kaden et al.*[68,70,71,74] and *Kodama et al.*[31] have also reported that the mono-protonated form of the tetraaza macrocyclic ligands is the reacting species in addition to the unprotonated species.

The similar values (Table 4.6) of the resolved rate constant, $k_{(LH^+)}$ ($dm^3\ mol^{-1}\ s^{-1}$), for the complexation of the same metal ion (Ni^{2+} and Co^{2+}) with the mono-protonated species (LH^+) of the ligands THEC and cyclam indicate that their different pK_a values are responsible for the apparently slower reaction of cyclam compared to THEC near pH 7. It is due to the fact that near pH 7 the concentrations of reacting species (less protonated species) of cyclam are much less compared to THEC, since the first two pK_a values of cyclam are much higher than those of THEC (see Table 3.1).

It has been shown in Table 4.6 that for Ni^{2+}, increasing methyl substitution on cyclam at N decreases $k_{(LH^+)}$, whereas hydroxyethyl substitution causes a 2 fold increase in $k_{(LH^+)}$which is moderate compared with the *ca.* 500 fold increase caused by acetato substitution. If the increased stiffness caused by the hydroxyethyl groups of THEC has a similar substitution rate decreasing effect to that of the methyl groups of TMC [71], the *ca.* 80 fold increased complexation rate of THEC over TMC is attributable to the coordinating ability of the hydroxo groups.

This suggests that a prior coordination of Ni^{2+} involving one or more hydroxyl groups of $THECH^{+}$ before coordination of $Ni^{2+}$by all four amine nitrogens is achieved. (Although it is thought that the acetato pendant groups of TETA coordinate Ni^{2+} in the initial stages of complexation, the large value of $k_{(LH^{+})}$ cannot be solely attributable to this as the negative charge of $TETAH^{3-}$ should greatly increase the magnitude of K_{os} in equation 4.3b for this system [20]). The $k_{(LH^{+})}$ data for the analogous Co^{2+} systems are consistent with this interpretation also.

There are probably several conformers of $THECH^{+}$ in solution which need not correspond to the conformer in $[M(THEC)]^{2+}$, as exemplified by the observation of the *trans* IV (*RSSR*) conformer of THEC in the solid state [151]. To convert this conformation to the *trans* III (*RRSS*) conformation observed in $[Ni(THECH)]^{3+}$, $[Cd(THEC)]^{2+}$, $[Hg(THEC)]^{2+}$and $[Pb(THEC)]^{2+}$[24,149,150], two nitrogen inversions are required which may represent major activation barriers in the formation of $[M(THEC)]^{2+}$. Similar considerations arise for the *trans* I (*RSRS*) and *trans* V (*RRRR*) conformers of $THECH^{+}$ and also the *cis* conformers. Evidence for a rate determining role for conformational change is presented in a study of the substitution of cyclam , Me-cyclam, Me_2-cyclam, Me_3-cyclam and TMC by Ni^{2+} in DMF where a second order substitution step was followed by first order intramolecular process[152]. The rate determining step for the second order process is assigned to the formation of the second Ni-N bond and the rate of the slower first order process is thought to be controlled by ligand conformational change.

6.6 The Decomplexation Kinetics

The reactions of metal complexes of THEC, $[M(THEC)]^{2+}$, in excess strong acid, in most cases, involve a rapid pre-equilibrium protonation step followed by a slow loss of the metal ion from the mono-protonated complex, $[M(THECH)]^{3+}$. This is consistent with the involvement of the mono-protonated species of the ligand in the complex formation reaction. The decomplexation of $[Ni(THEC)]^{2+}$ also shows very little second order dependence on the acid concentration, with a high uncertainty. Thus, only the kinetic parameters k_1 (s^{-1}) and K_1 (dm^3 mol^{-1}) of the reaction scheme 5.4 (rate law, equation 5.2) have been considered in detail for all the metal-THEC systems studied and other kinetic parameters have been ignored for simplicity, although their existence may be recognised but with a very high degree of uncertainty.

6.7 The Proposed Mechanism

The form of equation 5.2 which describes the acid catalysed decomplexation of $[M(THEC)]^{2+}$ requires the rapid breaking of an M-N bond prior to the rate determining step which is acid catalysed by protonation of the amine group no longer bonded to M^{2+}. Ground state $[M(THEC)]^{2+}$ may be in the *trans* III (*RRSS*) configuration with M^{2+} octahedrally coordinated by four coplanar nitrogens and two oxygens of hydroxyethyl arms diagonally opposed across the macrocyclic ring in *trans* related sites (as observed for $[Ni(THEC\text{-}H)]^{+}$) [24] , or with two oxygens of adjacent hydroxyethyl arms bound to the 4,8 nitrogens to give trigonal prismatic coordination (as observed for $[Cd(THEC)]^{2+}$, $[Hg(THEC)]^{2+}$and $[Pb(THEC)]^{2+}$) [149,150]. In the mechanistic scheme of

Fig. 6.1, these two alternative ground states are shown in equilibrium prior to the rapid breaking of a M-N bond to produce an intermediate in which M^{2+} is coordinated by two hydroxo and three amine groups of THEC and a water (not shown). The rate determining steps characterized by k_0 and k_1 in equation 5.2 then occur through this unprotonated intermediate and its monoprotonated analogue.

Figure 6.1 The proposed Mechanism for the Complexation of metal ion, M^{2+}, with the mono-protonated species of the ligand, $THECH^{+}$.

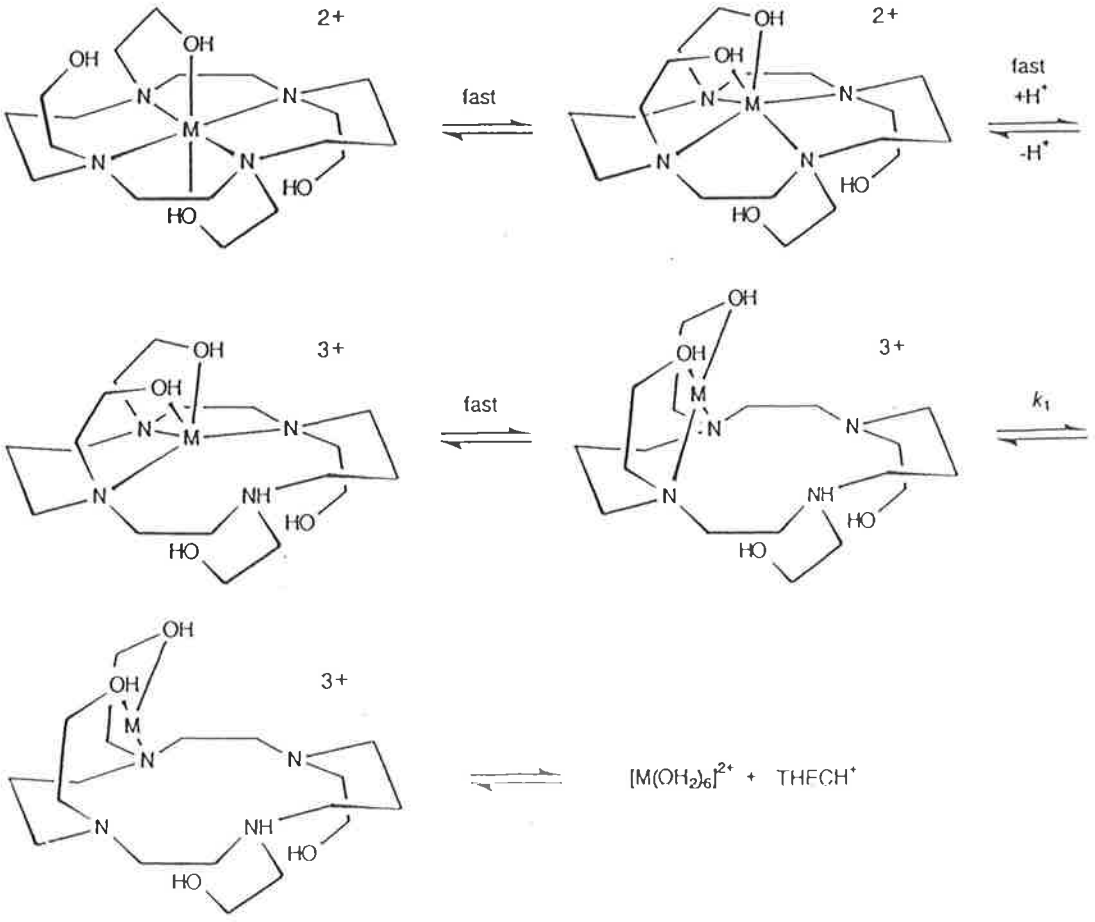

Consideration of the sequential decomplexation steps subsequent to the breaking of the first M-N bond is speculative, but a species in which M^{2+} is bound to THEC through two hydroxy groups is in accord with the expectation that the initial complexation of M^{2+} should also proceed through such an intermediate. The reverse of this sequence is the mechanism of complexation.

When the alternative acid decomplexation mechanism involving $[M(THECH_2)]^{4+}$ is operative, the rapid breaking of two M-N bonds would be required prior to the rate determining decomplexation step characterized by k_2.

The decrease in lability towards complexation at 298.2 K through the k_1 path ($[Co(THECH)]^{3+}$ > $[Cu(THECH)]^{3+}$ > $[Ni(THECH)]^{3+}$) coincides with an increase in $\Delta H_1^{\#}$ in the order $[CoTHECH]^{3+}$< $[Cu(THECH)]^{3+}$ < $[Ni(THECH)]^{3+}$, and $\Delta S_1^{\#}$ becoming less negative in the order: $[Co(THECH)]^{3+}$ > $[Cu(THECH)]^{3+}$ > $[Ni(THECH)]^{3+}$ (Table 5.9). The lability towards ligand substitution on the hexaaqua metal ions decreases in the sequence Cu^{2+}> Co^{2+}> Ni^{2+} and is explicable in terms of the larger ligand field activation energy (LFAE) of Ni^{2+} and and the labilisation of Cu^{2+} through a dynamic Jahn-Teller effect [153]. That this order of lability is not observed for $[M(THECH)]^{3+}$ indicates the superimposition of effects emanating from LH^+ on lability. Possibly a departure from octahedral stereochemistry and the dissimilarity of the tetraaza and hydroxo donor sets makes the lability relationships between the complexed metal ions quite different from those observed for the hexaaqua metal ions. The decrease in K_{1a} in the sequence: $[Ni(THECH)]^{3+}$> $[Co(THECH)]^{3+}$> $[Cu(THECH)]^{3+}$ shows the greater effective basicity of the amine group of the first complex,

which is a measure of the competition between the metal centre and the proton for the lone pair of electrons of the amine nitrogen. This variation in basicity is related to the lability of $[M(THECH)]^{3+}$ to acid catalysed decomplexation but further discussion of the trends, in the absence of knowledge of the stereochemistries of these species, would be speculative.

The half life for the decomplexation of $[Ni(CyclamH)]^{3+}$ in acid solution has been estimated to be *ca.* 30 years[93] which emphasises the role of the hydroxyethyl pendant arms of THEC in the labilisation of $[Ni(THEC)]^{2+}$ towards decomplexation by the hydroxyethyl pendant arms of THEC. A more quantitative comparison may be made with $[M(TMCH)]^{3+}$ where k_1K_{1a} = 2.5, 29 x 10^{-2} and 6.7 x 10^{-3} dm^3 mol^{-1} s^{-1}, respectively, when M^{2+}= Co^{2+}, $Ni^{2+}$and Cu^{2+},[73] which compare with k_1K_{1a} = 785, 28.5 and 4.07 dm^3 mol^{-1} s^{-1}, respectively, for $[M(THECH)]^{3+}$, when M^{2+}= Co^{2+}, $Ni^{2+}$and Cu^{2+} at 298.2 K[This work]. As $THECH^+$ is of similar acidity to $TMCH^+$ Table 3.1 it is probable that K_{1a} for $[M(THECH)]^{3+}$ is similar to K_{1a} for $[M(TMCH)]^{3+}$ and thus that k_1 for $[M(THECH)]^{3+}$ is several orders of magnitude greater than that for $[M(TMCH)]^{3+}$. Thus its hydroxyethyl arms labilise $[M(THECH)]^{3+}$ towards decomplexation compared with $[M(CyclamH)]^{3+}$ and $[M(TMCH)]^{3+}$ which is consistent with the coordinating hydroxyethyl groups stabilising a structure with M^{2+} out of the plane of the tetraaza ring as described in the mechanism shown in Figure 6.1. When considered in conjunction with the complexation data, it can be seen that the hydroxyethyl arms of THEC cause $[M(THECH)]^{3+}$to be less stable than its analogues $[M(CyclamH)]^{3+}$ and $[M(TMCH)]^{3+}$ largely because they labilise $[M(THECH)]^{3+}$ towards decomplexation.

References

[1] Lindoy, L.F. *"The Chemistry of Macrocyclic Ligand Complexes"*, Cambridge University Press, Cambridge, **1989**.

[2] *"Coordination Chemistry of Macrocyclic Compounds"*, edited by Melson, G.A., Plenum Press, New York, **1979**.

[3] *"Synthetic Multidentate Macrocyclic Compounds"*, edited by Izatt, R.M. and Christensen, J.J., Academic Press, Inc., New York, **1978**.

[4] Bernhardt, P.V.; Lawrance, G.A. *Coord. Chem. Rev.*, **1990**, 104, 297-343.

[5] Reid, G.; Schröder, M. *Chem. Soc. Rev.*, **1990**, 19, 239-269.

[6] Parker, D. *Chem. Soc. Rev.*, **1990**, 19, 271-291.

[7] Hancock, R.D.; Martell, A.E. *Chem. Rev.*, **1989**, 89, 1875-1914.

[8] Lindoy, L.F. *Pure and Appl. Chem.*, **1989**, 61, 1575-1580.

[9] Kaden, T.A. *Pure and Appl. Chem.*, **1988**, 60, 1117-1122.

[10] Izatt, R.M.; Bradshaw, J.S.; Nielsen, S.A.; Lamb, J.D.; Christensen, J.J.; Sen, D. *Chem. Rev.*, **1985**, 85, 271-339.

[11] Kaden, T.A. *Top. Curr. Chem.*, **1984**, 121, 157-179.

[12] Busch, D.H. *Acc. Chem. Res.*, **1978**, 11, 392-400.

[13] Lehn, J.M. *Pure and Appl. Chem.*, **1977**, 49, 857-870.

[14] Lindoy, L.F. *Chem. Soc. Rev.*, **1975**, 4, 421-441.

[15] Christensen, J.J.; Eatough, D.J.; Izatt, R.M.
Chem. Rev., **1974**, 74, 351-384.

[16] Poon, C.K. *Coord. Chem. Rev.*, **1973**, 10, 1-35.

[17] Hambright, P. *Coord. Chem. Rev.*, **1971**, 6, 247-268.

[18] Curtis, N.F. *Coord. Chem. Rev.*, **1968**, 3, 3-47.

[19] Louvet, V.; Appriou, P.; Handel, H.
Tetrahedron Lett., **1982**, 23, 2445-2448.

[19a] Thöm, V.J.; Hosken, G.D.; Hancock, R.D.
Inorg. Chem., **1985**, 24, 3378-3381.

[20] Kasprzyk, S.P.; Wilkins, R.G. *Inorg. Chem.*, **1982**, 21, 3349-3352.

[21] Hay, R.W.; Bembi, R. *Inorg. Chim. Acta*, **1982**, 65, L227-L230.

[22] Hay, R.W.; Clark, M.S.D. *Inorg. Chim. Acta*, **1984**, 83, L23-L24.

[23] Madeyski, C.M.; Michael, J.P.; Hancock, R.D.
Inorg. Chem., **1984**, 23, 1487-1489.

[24] Hay, R.W.; Pujari, M.P.; Moodie, W.T.; Craig, S.; Richens, D.T.;
Perotti, A.; Ungaretti, L. *J. Chem. Soc., Dalton Trans.*, **1987**, 2605-2613.

[25] Cabbiness, D.K.; Marjerum, D.W.
J. Am. Chem. Soc., **1969**, 91, 6540-6541.

[26] Kodama, M.; Kimura, E. *J. Chem. Soc., Chem. Commun.*, **1975**, 326-327.

[27] Kodama, M.; Kimura, E. *J. Chem. Soc., Chem. Commun.*, **1975**, 891-892.

[28] Kodama, M.; Kimura, E. *J. Chem. Soc., Dalton Trans.*, **1976**, 116-121.

[29] Kodama, M.; Kimura, E. *J. Chem. Soc., Dalton Trans.*, **1976**, 1720-1724.

[30] Kodama, M.; Kimura, E. *J. Chem. Soc., Dalton Trans.*, **1976**, 2341-2345.

[31] Kodama, M.; Kimura, E. *J. Chem. Soc., Dalton Trans.*, **1977**, 2269-2276.

[32] Micheloni, M.; Sabatini, A.; Paoletti, P.
J. Chem. Soc., PerkinTrans.II, **1978**, 828 - 830.

[33] Hinz, F.P.; Margerum, D.W. *J. Am. Chem. Soc.*, **1974**, 96, 4993-4994.

[34] Hinz, F.P.; Margerum, D.W. *Inorg. Chem.*, **1974**, 13, 2941-2949.

[35] Micheloni, M.; Paoletti, P. *Inorg. Chim. Acta,*, **1980**, 43, 109-112.

[36] Bianchi, A.; Bologni, L.; Dapporto, P.; Micheloni, M.; Paoletti, P.
Inorg. Chem., **1984**, 23, 1201-1205.

[37] Thöm, V.J.; Hancock, R.D.
J. Chem. Soc., Dalton Trans., **1985**, 1877-1885.

[38] Evers, A.; Hancock, R.D. *Inorg. Chim. Acta,* **1989**, 160, 245-248.

[39] Smith, G.F.; Margerum, D.W.
J. Chem. Soc., Chem. Commun., **1975**, 807-808.

[40] Jones, T.E.; Zimmer, L.L.; Diaddario, L.L.; Rorabacher, D.B.
Ochrymowycz, L.A. *J. Am. Chem. Soc.*, **1975**, 97, 7163-7165.

[41] Diaddario, L.L.; Zimmer, L.L.; Jones, T.E.; Sokol, L.S.W.L.; Cruz, R.B.;
Yee, E.L.; Ochrymowycz, L.A.; Rorabacher, D.B.
J. Am. Chem. Soc., **1979**, 101, 3511-3520.

[42] Sokol, L.S.W.L.; Ochrymowycz, L.A.; Rorabacher, D.B.
Inorg. Chem., **1981**, 20, 3189-3195.

[43] Frensdorff, H.K. *J. Am. Chem. Soc.*, **1971**, 93, 600-606.

[44] Izatt, R.M.; Nelson, D.P.; Rytting, J.H.; Haymore, B.L.; Christensen, J.J. *J. Am. Chem. Soc.*, **1971**, 93, 1619-1623.

[45] Haymore, B.L.; Lamb, J.D.; Izatt, R.M.; Christensen, J.J. *Inorg. Chem.*, **1982**, 21, 1598-1602.

[46] Bünzli, J.C.G.; Pilloud, F. *Inorg. Chem.*, **1989**, 28, 2638-2642.

[47] Anderegg, G. *Helv. Chim. Acta*, **1975**, 58, 1218-1225.

[48] Lehn, J.M.; Sauvage, J.P. *J. Am. Chem. Soc.*, **1975**, 97, 6700-6707.

[49] Kauffmann, E.; Lehn, J.M.; Sauvage, J.P. *J. Am. chem. Soc.*, **1976**, 59, 1099-1111.

[50] Arnaud-Neu, F.; Schwing-Weill, M.J.; Juillard, J.; Louis, R.; Weiss, R. *Inorg. Nucl. Chem. Lett.*, **1978**, 14, 367-373.

[51] Arnaud-Neu, F.; Schwing-Weill, M.J.; Louis, R.; Weiss, R. *Inorg. Chem.*, **1979**, 18, 2956-2961.

[52] Micheloni, M.; Paoletti, P.; Hertli, L.S.; Kaden, T.A. *J. Chem. Soc., Dalton Trans.*, **1985**, 1169-1172.

[53] Westerby, B.C.; Juntunen, K.L.; Leggett, G.H.; Pett, V.B.; Koenigbauer, M.J.; Purgett, M.D.; Taschner, M.J.; Ochrymowycz, L.A.; Rorabacher, D.B. *Inorg. Chem.*, **1991**, 30, 2109-2120.

[54] Fabbrizzi, L.; Paoletti, P.; Lever, A.B.P. *Inorg. Chem.*, **1976**, 15, 1502-1506.

[55] Delgado, R.; Frausto Da Silva, J.J.R.; Vaz, M.C.T.A. *Inorg. Chim. Acta*, **1984**, 90, 185-190.

[56] Dei, A.; Gori, R. *Inorg. Chim. Acta*, **1975**, 14, 157-160.

[57] Anichini, A.; Fabbrizzi, L.; Paoletti, P.
J. Chem. Soc., Chem. Commun., **1977**, 244-245.

[58] Clay, R.M.; Micheloni, M.; Paoletti, P.; Steele, W.V.
J. Am. Chem. Soc., **1979**, 101, 4119-4122.

[59] Paoletti, P.; Fabbrizzi, L.; Barbucci, R.
Inorg. Chim. Acta Rev., **1973**, 7, 43-68.

[60] Paoletti, P.; Fabbrizzi, L.; Barbucci, R.
Inorg. Chem., **1973**, 12, 1961-1962.

[61] Anichini, A.; Fabbrizzi, L.; Paoletti, P.; Clay, R.M.
Inorg. Chim. Acta, **1977**, 22, L25-L27.

[61a] Fabbrizzi, L.; Paoletti, P.; Clay, R.M. *Inorg. Chem.*, **1978**, 17, 1042-1046.

[62] Anichini, A.; Fabbrizzi, L.; Paoletti, P.; Clay, R.M.
J. Chem. Soc., Dalton Trans., **1978**, 577-583.

[63] Pedersen, C.J. *J. Am. Chem. Soc.*, **1967**, 89, 7017-7036.

[63a] Pedersen, C.J. *J. Am. Chem. Soc.*, **1970**, 92, 391-394.

[64] Munro, D. *Chem. Br.*, **1977**, 13, 100-105.

[64a] Andregg, G. in *"Coordination Chemistry"*., Vol. 1, edited by
Martell, A.E. Van Nostrand Reinhold, N.Y., **1971.**

[65] Sinmons, E.L. *J. Chem. Educ.*, **1979**, 56, 578-579.

[66] Busch, D.H.; Farmery, K.; Goedken, V.; Kalovic, V.; Melnyk, A.C.;
Sperati, C.R.; Tokel, N. in *"Bioinorganic Chemistry"*, edited by
Gould, R.F., A.C.S., Washington, D.C. **1971**.

[66a] Hancock, R.D; McDougall, J.G.
J. Am. Chem. Soc., **1980**, 102, 6551-6553.

[67] Rorabacher, D.B. *Inorg. Chem.*, **1966**, 5, 1891-1899.

[67a] Taylor, R.W.; Stepien, H.K.; Rorabacher, D.B. *Inorg. Chem.*, **1974**, 13, 1282-1289.

[68] Kaden, T.A. *Helv. Chim. Acta*, **1970**, 53, 617-622.

[69] Cabbiness, D.K; Margerum, D.W. *J. Am.Chem. Soc.*, **1970**, 92, 2151-2153.

[70] Kaden, Th.A. *Helv. Chim. Acta*, **1971**, 54, 2307-2312.

[71] Buxtorf, R.; Kaden, T.A. *Helv. Chim. Acta*, **1974**, 57, 1035-1042.

[72] Hertli, L.; Kaden, T.A. *Helv. Chim. Acta*, **1974**, 57, 1328-1333.

[73] Steinmann, W.; Kaden, T.A. *Helv. Chim. Acta*, **1975**, 58, 1358-1366.

[74] Leugger, P.A.; Hertli, L.; Kaden, T.A. *Helv. Chim. Acta*, **1978**, 61, 2296-2306.

[75] Margerum, D.W.; Rorabacher, D.B.; Clarke, P.G. *Inorg. Chem.*, **1963**, 2, 667-677.

[76] Barefield, E.K.; Wagner, F. *Inorg. Chem.*, **1973**, 12, 2435-2439.

[77] Lin, C.; Rorabacher, D.B.; Cayley, G.R.; Margerum, D.W. *Inorg. Chem.*, **1975**, 14, 919-925.

[78] Hay, R.W.; Norman, P.R. *Inorg. Chim. Acta*, **1980**, 45, L139-L141.

[79] Hertli, L.; Kaden, T.A. *Helv. Chim. Acta*, **1981**, 64, 33-37.

[80] Drumhiller, J.A.; Montavon, F.; Lehn, J.M.; Taylor, R.W. *Inorg. Chem.*, **1986**, 25, 3751-3757.

[81] McLaren, F.; Moore, P.; Wynn, A.M.
J. Chem. Soc., Chem. Commun., **1989**, 798-800.

[82] Margerum, D.W.; Cayley, G.R.; Weatherburn, D.C.; Pagenkopf, G.K. in *"Coordination Chemistry"*, Vol. 2, edited by Martell, A.E.
A.C.S., Washington D.C., **1978**.

[83] Popplewell, D.S.; Wilkins, R.G. *J. Chem. Soc.*, **1955**, 4098-4103.

[84] Wilkins, R.G. *J. Chem. Soc.*, **1957**, 4521-4527.

[85] Ahmed, A.K.S.; Wilkins, R.G. *J. Chem. Soc.*, **1959**, 3700-3708.

[86] Ahmed, A.K.S.; Wilkins, R.G. *J. Chem. Soc.*, **1960**, 2895-2900.

[87] Ahmed, A.K.S.; Wilkins, R.G. *J. Chem. Soc.*, **1960**, 2901-2906.

[88] Wilkins, R.G. *J. Chem. Soc.*, **1962**, 4475-4478.

[89] Melson, G.A.; Wilkins, R.G. *J. Chem. Soc.*, **1963**, 2662-2672.

[90] Weatherburn, D.C. *Aust. J. Chem.*, **1983**, 36, 433-439.

[91] Curtis, N.F. *J. Chem. Soc.*, **1964**, 2644-2650.

[92] Bosnich, B.; Tobe, M.L.; Webb, G.A. *Inorg. Chem.*, **1965**, 4, 1109-1112.

[93] Billo, E.J. *Inorg. Chem.*, **1984**, 23, 236-238.

[94] Graham, P.G.; Weatherburn, D.C. *Aust. J. Chem.*, **1981**, 34, 291-300.

[95] Reido, T.J.; Kaden, T.A. *Helv. Chim. Acta*, **1979**, 62, 1089-1097.

[96] Hay, R.W.; Bembi, R.; Moodie, W.T.; Norman, P.R.
J. Chem. Soc., Dalton Trans., **1982**, 2131-2136.

[97] Hay, R.W.; Bembi, R.; Mclaren, F.; Moodie, W.T.

Inorg. Chim. Acta, **1984**, 85, 23-31.

[98] Atkins, P.W. *"Physical Chemistry"*, Oxford University Press, Oxford, **1990**.

[99] Edwards, J.O.; Greene, E.F.; Ross, J. *J. Chem. Educ.*, **1968**, 45, 381-385.

[100] Bunnett, J.F. *"From Kinetic Data to Reaction Mechanism"*, Chapter VII, in *"Investigation of Rates and Mechanisms of reactions"*, Part 1, edited by Lewis, E.S., in *"Techniques of Chemistry"*, Vol. VI, edited by Weissberger, A. John Wiley and Sons, Inc., U.S.A., **1974.**

[101] Wilkins, R.G. *"The Study of Kinetics and Mechanism of Reactions of Transition Metal Complexes"*, Allyn and Bacon, Inc., Boston, **1974**.

[102] Lincoln, S.F. *Coord. Chem. Rev.*, **1971**, 6, 309-329.

[103] Burgess, J. *"Metal ions in Solution"*, Ellis Horwood Ltd., Sussex, **1978**.

[104] Wilkins, R.G. *Acc. Chem. Res.*, **1970**, 3, 408-416.

[105] Shriver, D.F.; Atkins, P.W.; Langford, C.H. *"Inorganic Chemistry"*, Oxford University Press, Oxford, **1990**.

[106] Langford, C.H.; Gray, H.B. *"Ligand Substitution Processes"*, W.A. Benjamin, N.Y., **1965**.

[107] Fuoss, R.M. *J. Amer. Chem. Soc.*, **1958**, 80, 5059-5061.

[108] Rorabacher, D.B. *Inorg. Chem.*, **1966**, 5, 1891-1899.

[109] Prue, J.E. *J. Chem. Soc.*, **1965**, 7534-7535.

[110] Pearson, R.G.; Ellgen, P. *Inorg. Chem.*, **1967**, 6, 1379-1385.

[111] Kruse, W.; Thusius, D. *Inorg. Chem.*, **1968**, 7, 464-468.

[112] Wendt, H. *Inorg. Chem.*, **1969**, 8, 1527-1528.

[113] Hammes, G.G.; Steinfeld, J.I.
J. Am. Chem. Soc., **1962**, 84, 4639-4643.

[114] Murphy, L.J.(Jr); Zompa, L.J.
Inorg. Chem., **1979**, 18, 3278-3281.

[115] Graham, P.G.; Weatherburn, D.C.
Aust. J. Chem., **1981**, 34, 291-300.

[116] Wainwright, K. P. School of Physical Science,
The Flinders University of South Australia,
Bedford Park, South Australia 5042, Australia.

[117] Flaschka , H.A. *"EDTA Titrations"*, Pergamon Press, London,**1964.**

[118] Vogel, A.I. *"A Text-book of Quantitative Inorganic Analysis Including Elementary Instrumental Analysis"*, Longmans, **1961**.

[119] Perrin, D.D.; Dempsey, B. *"Buffers for pH and metal ion control"*, Chapman and Hall, London, **1974**.

[120] *"Buffers. A Guide for the Preparation and Use of Buffers in Biological Systems"*, edited by Gueffroy, D.E., Calbiochem, **1975.**

[121] Sabatini, A.; Vacca, A.; Gans, P. *Talanta*, **1974**, 21, 53-77

[122] Bernasconi, C.F. *"Relaxation Kinetics"*, Academic press, N.Y., **1976**.

[123] Caldin, E.F. *"Fast Reactions in Solution"*,
Blackwell Scientific, London, **1964**.

[124] *"Investigation of Rates and Mechanisms of Reactions"*, Part II, " *Techniques of Chemistry"*, Vol. VI, edited by Hammes, G.G., Wiley(Interscience), N.Y., **1974**.

[125] Eigen, M. *Pure and Applied Chem.*, **1963**, 6, 97-115.

[126] Moore, P. *"Stopped-flow. An Experimental Manual"*,
University of Warwick, **1972**.

[127] Laurence, G.S. *"An Experimental Manual for stopped-flow Apparatus"*, University of Adelaide, **1976.**

[128] Doddridge, B.G. *"Ph.D. Thesis"*, University of Adelaide, **1986.**

[129] Faeder, E.J. *"Ph.D. Thesis "*, Cornell University, Ithaca, N.Y., **1970.**

[130] Collins, P.R. *"Ph.D. Thesis"*, University of Adelaide, **1979.**

[131] Coates, J.H.; Plush, B.G. Programme *"NLFITS"*, University of Adelaide, **1982.**

[132] Brown, S. Programme *"Kinfits"*, University of Adelaide, **1988.**

[133] Pitha, P.; Jones, R.N. *Can. J. Chem.*,**1966**, 4, 3030-3050.

[134] Flanagan, P.D.; Vitale, P.A.; Mendelsohn, J. *Technometrics*, **1969**, 11, 265-284.

[135] Kurucsev, T. Program *"DATAFIT""*, University of Adelaide, **1982.**

[136] Martel, A.E.; Motekaitis, R.J. *"The Determination and Use of Stability Constants"*, VCH Publishers, **1988.**

[137] Desai, A.G.; Dodgen, H.W.; Hunt, J.P. *J. Am. Chem. Soc.*, **1970**, 92, 798-801.

[138] Turan, T.S.; Rorabacher, D.B. *Inorg. Chem.*, **1972**, 11, 288-295.

[139] Desreux, J.F.; Merciny, E; Loncin, M.F. *Inorg. Chem.*, **1981**, 20, 987-991.

[140] Basolo, F.; Pearson, R.G. *"Mechanisms of Inorganic Reactions"*, Wiley, New York, **1967**.

[141] Hewkin, D.J.; Prince, R.H. *Coord. Chem. Rev.*, **1970**, 5, 45-73.

[142] Glasstone, S.; Laidler, K.J.; Eyring, H. *"The Theory of Rate Processes"*, McGraw-Hill Book Company, INC., U.S.A., **1941**.

[143] Shannon, R.D. *Acta Cryst*, **1976**, A32, 751-767.

[144] Childers, R.F.; Wentworth, A.D. *Inorg. Chem.*, **1969**, 8, 2218-2220.

[145] Chock, P.B. *Proc. Nat. Acad. Sci., U.S.A.*, **1972**, 69, 1939-1942.

[146] Cox, B.G.; Firman, P.; Schneider, H.
Inorg. Chim. Acta, **1982**, 64, L263-L265.

[147] Hefter, G.; May, P.M. *Chem. Br.*, **1991**, 27, 620.

[148] Burwell, R.L.(Jr.); Pearson, R.G. *J. Phys. Chem.*, **1966**, 70, 300-302.

[149] Clarke, P.; Hounslow, A.M.; Keough, R.A.; Lincoln, S.F.;
Wainwright, K.P. *Inorg. Chem.*, **1990**, 29, 1793-1797.

[150] Clarke, P.; Lincoln, S.F.; Wainwright, K.P.
Inorg. Chem., **1991**, 30, 134-139.

[151] Soldini, M.I., Taylor, M.R. and Wainwright, K.P.
Acta Cryst., **1991**, C47, 2239-2240.

[152] Röper, J.R.and Elias, H. *Inorg. Chem.*, **1992**, 31, 1202- 1210.

[153] Helm, L., Lincoln, S.F., Merbach, A..E. and Zbiden, D., *Inorg. Chem.*, **1986**, 25, 2550- 2552.